Příloha: Publikace **I-VI**

Available online at www.sciencedirect.com
SCIENCE DIRECT®
Journal of Chromatography B, 808 (2004) 75–82
JOURNAL OF CHROMATOGRAPHY B
www.elsevier.com/locate/chromb

Analysis of synthetic derivatives of peptide hormones by capillary zone electrophoresis and micellar electrokinetic chromatography with ultraviolet-absorption and laser-induced fluorescence detection

Veronika Šolínová, Václav Kašička*, Dušan Koval, Tomislav Barth, Alice Ciencialová, Lenka Žáková

Institute of Organic Chemistry and Biochemistry, Academy of Sciences of the Czech Republic, Flemingovo 2, 166 10 Prague 6, Czech Republic

Available online 27 February 2004

Abstract

Capillary zone electrophoresis (CZE) and micellar electrokinetic chromatography (MEKC) were used for the analysis of new synthetic derivatives of hypophysis neurohormones—vasopressin and oxytocin, and pancreatic hormone—human insulin (HI) and its octapeptide fragment, derivatized by fluorescent probe, 4-chloro-7-nitrobenzo[1,2,5]oxadiazol (NBD). The suitable composition of background electrolytes (BGEs) was selected on the basis of calculated pH dependence of effective charge of analyzed peptides. Basic ionogenic peptides were analyzed by CZE in the acidic BGE composed of 100 mM H_3PO_4, 50 mM Tris, pH 2.25. The ionogenic peptides with fluorescent label, NBD, were analyzed in 0.5 M acetic acid, pH 2.5. The best MEKC separation of non-ionogenic peptides was achieved in alkaline BGE, 20 mM Tris, 5 mM H_3PO_4, with micellar pseudophase formed by 50 mM sodium dodecylsulfate (SDS), pH 8.8. Selected characteristics (noise, detectability of substance, sensitivity of detector) of the UV-absorption detectors (single wavelength detector, multiple-wavelength photodiode array detector (PDA), both of them operating at constant wavelength 206 nm) and laser-induced fluorescence (LIF) detector (excitation/emission wavelength 488/520 nm) were determined. The detectability of peptides in the single wavelength detector was 1.3–6.0 μmol dm^{-3} and in the PDA detector 1.6–3.1 μmol dm^{-3}. The LIF detection was more sensitive, the applied concentration of NBD derivative of insulin fragment in CZE analysis with LIF detection was three orders lower than in CZE with UV-absorption detector, and the detectability of this peptide was improved to 15.8 nmol dm^{-3}.

Keywords: Derivatization, CE; Derivatization, MEKC; Insulin; Peptides

1. Introduction

High-performance capillary electromigration methods, capillary zone electrophoresis (CZE) and micellar electrokinetic chromatography (MEKC), providing fast (few minutes) and high-efficient separation (10^5–10^6 theoretical plates per meter) of picomole to attomole quantities of analytes in the nanolitre sample volume, have a high application potential in the field of chemistry of peptides: they are broadly utilized for separation, analysis, preparation and characterization of peptides in chemistry, biochemistry, biomedicine, biotechnology, pharmacy and agriculture, as documented in several recent reviews [1–7].

Peptides and their analogs, fragments and derivatives are either isolated from the natural material or synthesized from amino acid building blocks. Sometimes they are prepared semisynthetically; i.e. synthetic peptide is attached to the isolated peptide or its fragment. In all cases it is important to check the success of the whole isolation or synthesis, eventually single steps of the process, because the obtained products can contain various admixtures, e.g. by-products of peptide synthesis. This is a suitable task for capillary electrophoresis (CE), since determination of purity degree is the most common application of CE in peptide chemistry [2].

One group of biopeptides analyzed in this work are represented by synthetic derivatives of neurohormones, oxytocin and vasopressin, produced by the pituitary gland (hypophysis) [8]. Oxytocin is responsible for contraction of the uterus in labor and ejection of milk from mammary glands during breast-feeding. Vasopressin and its analogs

* Corresponding author. Tel.: +420-220-183-239; fax: +420-220-183-592.
E-mail address: kasicka@uochb.cas.cz (V. Kašička).

1570-0232/$ – see front matter © 2004 Elsevier B.V. All rights reserved.
doi:10.1016/j.jchromb.2004.01.062

are also known as hormones with anti-diuretic activity [9]; they stimulate the retention of water by kidneys [10].

Structurally similar analogues of vasopressin and other biopeptides, enkephalins and dalargins, have been separated by CZE in acidic background electrolyte (BGE), 150 mM phosphoric acid, pH 1.8 [11,12]. Analogues of dalargin were analyzed by CZE in 0.5 M acetic acid, pH 2.5, and then separated in preparative scale by free-flow zone electrophoresis [13]. These peptides were also separated by MEKC in 20 mM tetraborate BGE with micellar pseudophase formed by sodium dodecylsulfate (SDS), pH 9.2 [11,12]. Oxytocin, vasopressin and other neurohypophyseal nonapeptides were determined by MEKC in four different micellar systems—with cationic, anionic, zwitterionic and neutral micellar constituents [14]. Chiral separations of dalargin analogs with D- and L-isomers of phenylalanine in the fourth position in peptide chain were performed in 50 mM phosphate buffer, pH 2.5 with 10 mM β-cyclodextrin [12]. Peptide neurohormones, derivatives of vasopressin, enkephalins and dalargin, and human insulin (HI) were analyzed also by different variants of HPLC, reverse-phase [11,12] and ion-exchange [15,16] HPLC.

Insulin is the peptide hormone produced by pancreatic β-cells that regulates the metabolism of carbohydrates, proteins and fatty acids [17]. Insulin molecule consists of 2 polypeptide chains, A and B, containing 21 and 30 amino acid residues, respectively. The two chains of insulin are connected by two disulfide bonds and the third disulfide bond is intra-chain bond in chain A. Its relative molar mass is $M_r = 5808$, the isoelectric point, pI, is 5.4–5.5.

CZE and HPLC have been frequently used for analysis of human insulin and its derivatives. Stable derivative of insulin with exo-3,6-epoxy-1,2,3,6-tetrahydrophtalic anhydride (ETPA) were identified by ion-exchange HPLC and CE [18]. CZE with UV detection was utilized for analysis of HI in CHES-acetate-acetonitrile BGE, pH 7–8 [19]. CE was also used to validate the HPLC assay of insulin as an analytical method [20]. Human insulin, proinsulin and intermediate forms were simultaneously quantified by CE in TAPS (*N*-[tris(hydroxymethyl)-methyl]-3-aminopropanesulfonic acid), DETA (diethylenetriamine) and methanol [21]. CZE with fluorescence detection was used mainly for immunoassay of insulin. In some cases the native fluorescence of insulin was detected (excitation 275 nm, emission 305 nm) [22]. The analysis was performed in acidic BGE—50 mM citric acid, pH 2.3, or in alkaline BGE 20 mM Tricine, pH 8.5. Insulin with bonded fluorescent dye NN 382 was analyzed in 50 mM phosphate and 25 mM potassium sulfate, pH 7.0 with laser-induced fluorescence (LIF) detection in near infrared range [23].

The aim of this work was to analyze synthetic derivatives and analogs of hypophyseal neurohormones, oxytocin and vasopressin, and of pancreatic hormone, human insulin, and its octapeptide fragment, B23-30-HI, derivatized by fluorescent label, 4-chloro-7-nitrobenzo[1,2,5]oxadiazol (NBD), by CZE and MEKC, in the home-made CE device with single wavelength UV-absorption detector and in commercial Beckman–Coulter CE-MDQ apparatus with multiple-wavelength UV-absorption detector and LIF detector. The rational approach, based on the calculated pH dependence of effective charge of peptides, is used for selection of suitable separation conditions. The sensitivity of UV and LIF detectors and detectability of non-labeled and labeled peptides as well as other characteristics of detectors are compared and discussed.

2. Experimental

2.1. Chemicals

All chemicals used were of analytical reagent grade. Tris (tris(hydroxymethyl)aminomethane) was obtained from Serva (Heidelberg, Germany), phosphoric acid, acetic acid and dimethyl sulfoxide (DMSO) were supplied by Lachema (Brno, Czech Republic) and sodium dodecylsulfate was from Fluka (Buchs, Switzerland).

2.2. Peptides

The sequences of analyzed peptides and their abbreviations are presented in Table 1. Analogs of oxytocin, vasopressin and octapeptide B23-B30 of the C-terminal part of the B-chain of human insulin (HI) were synthesized in our institute (IOCB) by the solid phase method described elsewhere [24]. 4-Chloro-7-nitrobenzo[1,2,5]oxadiazol (NBD) was used as fluorescent probe for B23-B30 octapeptide of HI. NBD reacted with free ε-amino group of lysine B29 in octapeptide of HI. The α-amino group of lysine was protected by the Fmoc protecting group [25]. Fluorescent-labeled human insulin was prepared semisynthetically by the trypsin-catalyzed peptide bond formation between C-terminal arginine B22 of desoctapeptide of insulin and N-terminal glycine residue of NBD-labeled octapeptide B23-B30 of HI [26].

2.3. Instrumentation

The electrophoretic experiments were carried out in two apparatuses. The first one was home made CE device developed in our institute, IOCB, further indicated as CE-IOCB [27]. It is equipped with single wavelength UV-absorption photometric detector operating at 206 nm; the light source is electrodeless, high-frequency excited iodine discharge lamp (LKB-Pharmacia, Uppsala, Sweden), and UV-sensitive Si-photodiode with built-in preamplifier (Hamamatsu Photonics Deutschland, Herrsching, Germany) is used as light detector. The bare fused silica capillary with outer polyimide coating, 50 μm i.d. × 200 μm O.D., total length 30 cm and effective length 19 cm, was supplied by the Institute of Glass and Ceramics Materials, Czech Academy of Sciences (Prague, Czech Republic). The separations were

Table 1
Sequences of analyzed peptides

Peptide	Abbreviation	Sequence in three-letters code	Sequence in single-letter code
Oxytocin	OT	Cys-Tyr-Ile-Gln-Asn-Cys-Pro-Leu-GlyNH_2	CYIQNCPLG-NH_2
Deamino-oxytocin	dOT	Mpa-Tyr-Ile-Gln-Asn-Cys-Pro-Leu-GlyNH_2	MpaYIQNCPLG-NH_2
Arg^8-vasopressin	AVP	Cys-Tyr-Phe-Gln-Asn-Cys-Pro-Arg-GlyNH_2	CYFQNCPRG-NH_2
(Deamino-D-Arg^8)-vasopressin	dDAVP	Mpa-Tyr-Phe-Gln-Asn-Cys-Pro-D-Arg-GlyNH_2	MpaYFQNCPrG-NH_2
Insect diuretic hormone	IDH	Cys-Leu-Ile-Thr-Asn-Cys-Pro-Arg-GlyNH_2	CLITNCPRG-NH_2
(Deamino-D-Arg^8)-IDH	dDA-IDH	Mpa-Leu-Ile-Thr-Asn-Cys-Pro-D-Arg-GlyNH_2	MpaLITNCPrG-NH_2
(D-Arg^8)-IDH	DA-IDH	Cys-Leu-Ile-Thr-Asn-Cys-Pro-D-Arg-GlyNH_2	CLITNCPrG-NH_2
(Deamino-Arg^8)-vasopressin	dAVP	Mpa-Tyr-Phe-Gln-Asn-Cys-Pro-Arg-GlyNH_2	MpaYFQNCPRG-NH_2
NBD-derivative of B23-B30-human insulin fragment	NBD-B23-30-HI	Gly-Phe-Phe-Tyr-Thr-Pro-Lys-(NBD)-Thr	GFFYTPK(NBD)T

NBD: 4-chloro-7-nitrobenzo[1,2,5]oxadiazol.

performed at ambient temperature 22–24 °C without active cooling of the capillary.

The second apparatus was commercial P/ACE MDQ System (Beckman–Coulter, Fullerton, CA, USA), further indicated as CE-MDQ, with multiwavelength spectrophotometric photodiode array (PDA) detector (190–600 nm) and Ar-ion laser-induced fluorescence (LIF) detector (excitation wavelength 488 nm, emission wavelength 520 nm). The fused silica capillary with outer polyimide coating as well as in IOCB device was internally uncoated, total length was 40 cm and effective length was 30.2 cm, with diameters 75 μm I.D. × 360 μm O.D. The temperature was set at 25 °C with liquid coolant continuously circulating around the capillary.

The new capillary was gradually flushed with water, 0.1 M NaOH, water and BGE, each wash for 5 min. Finally, the capillary was conditioned by a 20 min application of the high voltage to equilibrate the inner surface and to stabilize electroosmotic flow. Between runs under the same conditions, the capillary was rinsed with the BGE for 2 min. Prior to any change of the BGE the capillary was rinsed with 0.1 M NaOH for 5 min and then repeatedly stabilized. The separation voltage was in the range 10–20 kV. The samples were injected with pressure 5–10 mBar for 5–15 s. The samples were dissolved in deionized water or in BGE and their concentrations were in the range 0.005–1.3 mg/ml for UV-absorption detection and 10–1000× lower for CE with LIF detection. The BGEs were filtered through a 0.45 μm syringe filter (Millipore, Bedford, MA, USA) before use.

3. Results and discussion

3.1. Selection of separation conditions

The strategy of the rational selection of conditions in CE separation of peptides follows the general rules of selection of suitable CE separation conditions [28,29] and takes into account the specific peptide properties. The specific properties of peptides result from their primary structure—number and sequence of the linked amino acid residues. The structure determines the electric charge, size (relative molecular mass), shape (conformation), hydrophobicity and specific binding capability. From the structure of peptides also their ionogenicity is deduced, which determines whether CZE or MEKC can be used for analysis of given peptide sample. CZE is used for analysis of ionogenic peptides and the separation is based on differences in electrophoretic mobilities, which are determined by charge, size and shape of peptide molecules. MEKC is used for analysis of non-ionogenic peptides; the separation is based on their different hydrophobicity.

The selection of the composition of the BGEs includes buffer components type and concentration, pH and takes into

account the request for chemical and temperature stability and biological activity of analyzed peptides [30]. Effective charges of peptides are strongly dependent on pH and pK_a of ionogenic groups of amino acid residues present in peptide chain. Analyzed peptides contain ionogenic groups—all except one α-NH_3^+ group of N-terminal of peptide chain (average pK_a 8.0), four of them guanidium of arginine (average pK_a 11.2) or hydroxy group of tyrosine (average pK_a 10.0) and form cyclic structures by disulfide bridges of cystine. The relative molecular mass of nonapeptides was around 1000. The pH dependence of effective charge was calculated with the earlier developed computer program Nabamfo [31] using the above given average values of pK_a of ionogenic groups. The program is based on mathematical model of acid–base equilibrium of general ampholyte. The effective charges of ionogenic peptides reached values +1 or +2 elementary charges in the whole acidic pH range. Some peptides behaved as weakly negatively charged in strongly alkaline BGE, which was not suitable for these peptides due to the lability of cystine bond at high pH. In conclusion, ionogenic peptides were analyzed by CZE as cations in acidic BGE. The pH dependence of the effective charges of analyzed nonapeptides is depicted in Fig. 1.

The solubility of peptides is given by their structure. The analyzed peptides were dissolved in deionized water or BGEs. Solubilization in deionized water is advantageous due to the possibility to apply the same sample solution for CE separations in different BGEs and in addition the concentrating effect is utilized. On the other hand using BGE as sample solvent ensures the constant separation conditions (BGE composition) in the whole CE experiment.

Ionogenic peptides were analyzed by CZE as cations in acidic BGEs. The best results were obtained in BGE composed of 100 mM phosphoric acid, 50 mM Tris, pH 2.25, and with the applied voltage 10 kV. The examples of peptide CZE analyses are shown in Fig. 2. The effective electrophoretic mobilities of analyzed peptides in the above tris-phosphate BGE are presented in Table 2. The average electroosmotic mobility of the tris-phosphate buffer was 3.46×10^{-9} m^2 V^{-1} s^{-1}. Peptides with two positive elementary charges migrated the fastest. Peptides containing tyrosine in the second position in peptide chain migrated slower than peptides with other amino acids in this position and the same total positive charge, obviously due to larger size of their hydrated molecules. On the other hand peptide containing arginine residue in position 8 instead of leucine migrated faster than peptides with free N-terminal group, the slowest migrating positively charged peptide had just free N-terminal group. The peptides with fluorescent label NBD were analyzed by CZE in 0.5 M acetic acid, pH 2.5, and with the applied voltage 15 kV. The examples of their electrophoregrams are shown in Fig. 3.

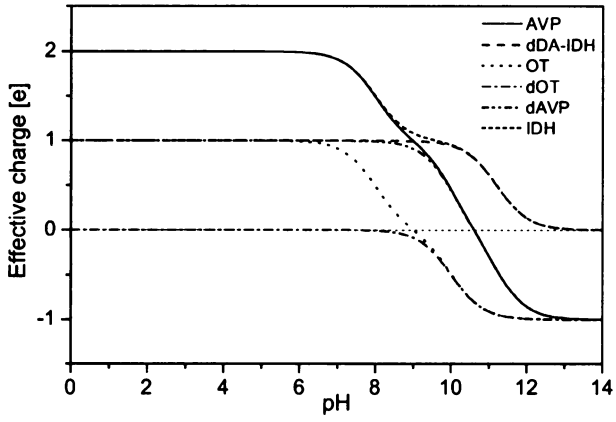

Fig. 1. The pH dependence of the effective charge of analyzed neurohypophyseal peptides. For peptide abbreviations see Table 1.

Table 2
Effective electrophoretic mobility and differently expressed purity degrees of peptides determined by CZE in home-made CE-IOCB device and in commercial CE-MDQ device with UV-absorption detection (206 nm) in BGE composed of 100 mM H_3PO_4, 50 mM Tris, pH 2.25

Peptide	m_{ef} (10^{-9} m^2 V^{-1} s^{-1})	P_h (%)	P_A (%)	P_{CA} (%)
Analyses in CE-IOCB device				
OT	11.6	95.6	95.0	94.5
dOT	0	93.3*	89.1*	89.3*
AVP	23.3	94.1	90.1	91.5
dDAVP	12.7	95.1	96.9	96.4
IDH	24.5	42.3	28.6	26.7
dDA-IDH	13.4	66.7	69.3	68.4
dAVP	12.6	92.0	89.9	89.3
DA-IDH	24.4	70.8	52.9	48.2
Analyses in CE-MDQ device				
OT	9.1	93.5	90.6	90.4
AVP	16.8	87.7	83.2	80.4

m_{ef}: Effective electrophoretic mobility; P_h, P_A, P_{CA}: purity degrees expressed on the basis of relative peak height, relative peak area and relative peak corrected area, respectively; (*): purity degrees of dOT obtained from MEKC analyses.

Non-ionogenic peptides with blocked or derivatized ionogenic groups were analyzed by MEKC in alkaline BGE—20 mM Tris, 5 mM H_3PO_4, pH 8.8, with micellar pseudophase formed by an anionic detergent sodium dodecylsulfate, see Fig. 4. The applied voltage was 20 kV. In all systems symmetrical peaks were obtained without any shoulders and with high separation efficiency in short times. All analyses did not take more than 7 min. The number of theoretical plates/meter was in the range 8×10^5 to 3×10^6.

3.2. Determination of purity degree

The purity degrees of the crude synthetic or semisynthetic peptide preparations after HPLC purification were determined. Standards of synthesized peptides were not available. Peptide purity and peptide content in the sample can be quantified by several ways: (i) relative peak height, $P_h(i)$ (1), (ii) relative peak area, $P_A(i)$ (2), and (iii) relative peak corrected area, P_{CA}(i) (3), of the UV-positive peaks

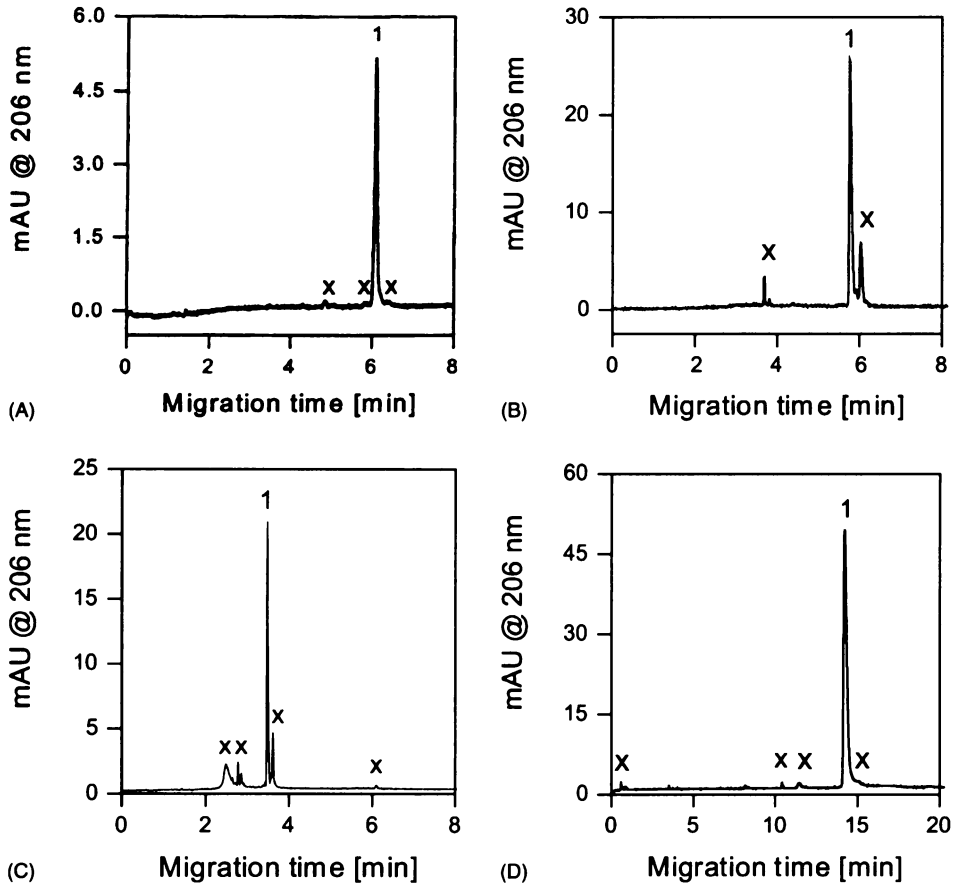

Fig. 2. CZE analyses of derivatives of hypophyseal neurohormones: (A) (deamino-Arg^8)-vasopressin, 0.40 mg ml^{-1}; (B) (deamino-D-Arg^8)-IDH, 1.15 mg ml^{-1}; (C) (D-Arg^8)-IDH, 1.0 mg ml^{-1}; all three analyses performed in CE-IOCB device, current 48–50 μA, injection 10 mBar × 5 s, (D) oxytocin, 0.95 mg ml^{-1}, in CE-MDQ device, 69–70 μA, injection 7 mBar × 5 s. All analyses performed in BGE composed of 100 mM H_3PO_4, 50 mM Tris, pH 2.25; applied voltage 10 kV; (1) main synthetic product; (×) non-identified admixtures.

for i-th component:

$$P_h(i) = \frac{h(i)}{\sum h(i)} \quad i = 1 \ldots n \tag{1}$$

$$P_A(i) = \frac{A(i)}{\sum A(i)} \quad i = 1 \ldots n \tag{2}$$

$$P_{CA}(i) = \frac{A_c(i)}{\sum A_c(i)} \quad i = 1 \ldots n \tag{3}$$

where $h(i)$ is height of the i-th peak, $A(i)$ is area of the i-th peak and $A_c(i)$ is corrected area of the i-th peak, corrected peak area is peak area corrected with respect to migration velocity of the given peak, i.e. it is equal to peak area divided by migration time of the given peak, n is the number of sample components.

The values of differently expressed purity degrees are presented in the Table 2. The values of purity degrees were determined as averages of two subsequent analyses, which differed less than 1%. Analyses of peptides with high purity degree are demonstrated by CZE of (deamino-Arg^8)-vasopressin in Fig. 2A and oxytocin in Fig. 2D. On the other hand analysis of peptide with low purity degree and with at least three major impurities is shown in electrophoregram of (deamino-D-Arg^8)-insect diuretic hormone in Fig. 2B. As follows from the above definitions, the most exact characteristic of peptide purity is the relative corrected peak area. Sometimes other, the simpler ways of purity evaluation, relative peak height or relative peak area, can be used, particularly in the cases when the peaks of sample components are uniformly dispersed and their migration velocities are not too different. The comparison of differently expressed purity degree is demonstrated on (D-Arg^8)-insect diuretic hormone in Fig. 2C. DA-IDH relative peak height differed in around 20% against relative peak area and relative peak corrected area. As follows from the presented data, the determination of purity degree depends on separation conditions and mostly also on the way of its determination.

3.3. Sensitivity of detection

3.3.1. UV-absorption detection

The most common detection of peptides in CE is UV-absorption detection in the range 200–220 nm, due to

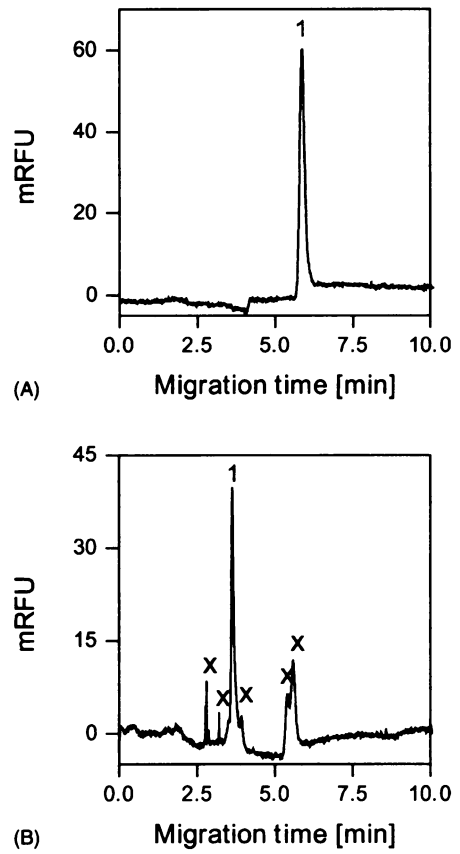

Fig. 3. CZE analyses of fluorescence labeled peptides in CE-MDQ device with LIF-detection: (A) NBD-B23-30-HI, 0.05 mg ml^{-1}; (B) NBD-HI, 0.5 μg ml^{-1}. Analyses performed in BGE composed of 0.5 M AcOH, pH 2.5; injection 10 mBar × 5 s; applied voltage 15 kV; current 20–21 μA; (1) main synthetic product; (×) non-identified admixtures.

the absorption of peptide bond CO–NH in this short wavelength UV region. The background electrolytes (BGEs) should not absorb light significantly in this range in order to prevent the decrease of the signal of analytes [7].

In this work two different UV-absorption detectors were tested. The comparison was performed from the analyses on new synthesized nonapeptides by CZE in acidic tris-phosphate buffer, pH 2.25. The first absorption detector used high-frequency excited iodine discharge lamp with emission at 206 nm and UV-sensitive silicon photodiode

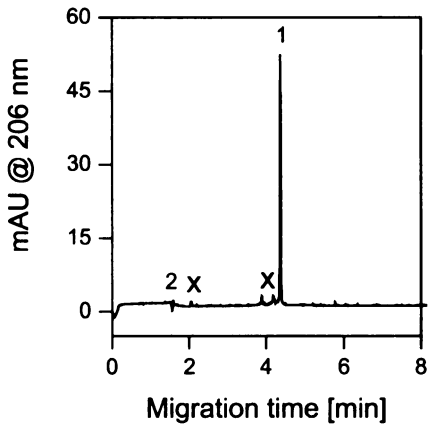

Fig. 4. MEKC analysis of non-ionogenic peptide, deamino-oxytocin, 1.15 mg ml^{-1}, in CE-MDQ device with PDA detector, BGE: 20 mM Tris, 5 mM H_3PO_4, 50 mM SDS, pH 8.8, injection 5 mBar × 10 s, applied voltage 20 kV, current 69–71 μA, (1) main synthetic product, (2) peak of electroosmotic flow marker, (×) non-identified admixtures.

as detector of radiation. The second one was based on multiple-wavelength detection realized by photodiode array and deuterium lamp. Both detectors operated at constant wavelength 206 nm. The characteristics of the detectors, noise, n, response of the detector, R, signal to noise ratio, R/n, detectability of substance, D, and sensitivity of detector, S, were compared. The sensitivity of detector was calculated as the ratio of response of detector and concentration of analyte, $S = R/c$. The detectability of substance was determined as treble of noise divided by sensitivity, $D = 3n/S$. The values of the above characteristics of single wavelength detector (CE-IOCB) measured with oxytocin and Arg^8-vasopressin are presented in Table 3 and for PDA detector in CE-MDQ device in Table 4. The values were determined as averages of two subsequent analyses with maximal difference 2% in response of the detector. The ratio R/n of the oxytocin and Arg^8-vasopressin was slightly higher in PDA detector. The detectability of substances copied with small deviations the increase of R/n in PDA detector.

The influence of BGEs absorption on detector sensitivity and detectability of substance was investigated by CZE of oxytocin and Arg^8-vasopressin, performed in tris-phosphate buffer and acetic acid-based BGEs, respectively.

Table 3
The characteristics of single wavelength (206 nm) UV-absorption detector of CE-IOCB device determined from CZE analyses of peptides in BGE composed of 100 mM H_3PO_4, 50 mM Tris, pH 2.25

Peptide	c (μmol dm^{-3})	R (mV)	R/n	S (V mol^{-1} dm^3)	D (μmol dm^{-3})
OT	89.1	64.0	89.0	717.7	3.00
AVP	84.4	141.8	197.3	1680.6	1.28
dDAVP	1036	658.5	916.4	635.4	3.39
IDH	329	181.8	253.0	553.5	3.89
dDA-IDH	818	300.9	418.7	367.7	5.86

c: Peptide concentration; R: detector response; n: noise, average value of noise was 0.72 mV; S: sensitivity of detector, $S = R/c$; D: detectability of substance, $D = 3n/S$.

Table 4
The characteristics of the UV-absorption PDA detector (operating at 206 nm) of CE-MDQ device determined from CZE analyses of peptides in different BGEs, BGE I: 100 mM H_3PO_4, 50 mM Tris, pH 2.25; BGE II: 0.5 M acetic acid, pH 2.5

Peptide	BGE	c (mmol dm^{-3})	R (mAU)	R/n	S (AU.mol^{-1} dm^3)	D (μmol dm^{-3})
OT	I	0.85	43.8	1093.2	51.4	2.34
	II	0.91	16.4	859.2	18.0	3.18
AVP	I	0.92	67.2	1675.6	72.9	1.65
	II	0.86	24.6	1285.8	28.4	2.02

c: Peptide concentration; R: detector response; n: noise, average value of noise was 0.04 mAU for BGE I and 0.02 mAU for BGE II; S: sensitivity of detector, $S = R/c$; D: detectability of substance, $D = 3n/S$.

Table 5
The characteristics of the UV-absorption PDA detector set to 206 nm and LIF detector (488 nm/520 nm) of CE-MDQ device determined from CZE analyses of peptides in BGE composed of 0.5 M acetic acid, pH 2.5

Peptide	c (mmol dm^{-3})	R (mAU)	R/n	S (AU.mol^{-1} dm^3)	D (μmol dm^{-3})
Analyses with UV detector					
NBD-HI	629	2.77	184.7	44.1	1.02
NBD-B23-30-HI	72.9	8.57	571.1	11.7	3.83
Peptide	c (μmol dm^{-3})	R (mRFU)	R/n	S (RFU.mol^{-1} dm^3)	D (μmol dm^{-3})
Analyses with LIF detector					
NBD-HI	5.09	505.7	136.6	99331	0.112
NBD-B23-30-HI	0.89	629.1	169.9	706590	0.016

c: Peptide concentration; R: detector response; n: noise, average value of noise was 3.70 mRFU for LIF detector and 0.02 mAU for PDA detector; S: sensitivity of detector, $S = R/c$; D: detectability of substance, $D = 3n/S$.

The acetic acid absorbs more light, the peaks were smaller and noise was also lower. The value of the noise in tris-phosphate buffer was 0.0401 mAU and in acetic acid reached 0.0191 mAU in Beckman CE-MDQ with PDA detector. The separation in acetic acid BGE was influenced by electromigration dispersion; the peaks were wide and non-symmetrical. The sensitivity of PDA detector decreased 2.5 times in acetic acid BGE; the detectability was lower in comparison with tris-phosphate buffer in both equipments. On the other hand, the differences were not dramatic (see Table 4) and acetic acid can be also used as BGE in CZE.

3.3.2. LIF detection

Laser-induced fluorescence detection is the most sensitive detection in CE, its sensitivity is two or three orders higher than UV-absorption detection. On the other hand it is necessary to derivatize peptides by fluorogenic labels. Only peptides with aromatic amino acid residues of tryptophane and tyrosine exhibit native fluorescence in the region 200–300 nm. The necessary condition for excitation is UV-laser systems or multiphoton excitation [7].

In this work, the sensitivity of PDA and LIF detectors of CE-MDQ device were compared. Firstly, the derivatives of human insulin and its B23-30 octapeptide fragment with NBD label, NBD-HI and NBD-B23-30-HI, respectively, were detected by PDA detector in CE-MDQ device in 0.5 M acetic acid, pH 2.5. Fluorescent probe NBD was bonded on ε-amino group of lysine B29, the excitation maximum was at 475–478 nm and the emission maximum at 530–534 nm in pH 3–8 [32]. Labeled human insulin is necessary for monitoring of interactions between insulin and insulin-receptor at low concentrations in in vivo conditions. Consequently, LIF detector with Ar-ion laser (excitation at 488 nm, emission at 520 nm) was used for analyses of NBD-derivatives of HI and its fragment. The electrophoregrams of peptide analyses in acetic acid, pH 2.5, with LIF detection are depicted in Fig. 3. Whereas single peak was obtained for NBD-derivative of B23-30 octapeptide fragment of human insulin (see Fig. 3A), several admixtures have been found by CZE analysis of NBD-labeled human insulin, as shown in Fig. 3B. This indicates that the rest of fluorescent probe was not completely removed from the octapeptide fragment and it reacted with non-protected groups of amino acid residues of desoctapeptide of HI. For LIF detection the concentration of human insulin was 10 times lower than for UV-absorption detection, for octapeptide the solution was diluted 1000 times due to too high signal in LIF detector. The main characteristics of detectors as well as the comparison of UV detectors are shown in Table 5. The detectability of substance is one or two orders better for fluorescence detection.

4. Conclusions

CZE and MEKC proved to be powerful and useful tools for fast and sensitive analyses of ionogenic or non-ionogenic derivatives of peptide hormones, oxytocin, vasopressin,

human insulin and its fragment. The purity degrees and effective mobilities of ionogenic peptides were determined by CZE in acidic BGEs. Purity degree of non-ionogenic peptides was evaluated by MEKC in alkaline BGE with SDS micellar pseudophase. Sensitivity of single wavelength UV-absorption detector in home-made CE device was found to be comparable with that of multiple-wavelength PDA detector in commercial Beckman CE-MDQ apparatus. LIF detector was able to detect NBD-labeled octapeptide fragment of human insulin with two orders lower detectability than UV-absorption detector.

Acknowledgements

We wish to acknowledge the financial support from the Grant Agency of the Czech Republic, grants no. 203/02/1467, 203/03/0716, and from the Czech Academy of Sciences, research project no. AVOZ4055 905. Mrs. V. Lišková is thanked for her skilful technical assistance and other collegues from our laboratory, Dr. P. Sázelová and Dr. Z. Prusík, for their help in preparation of this publication.

References

[1] P.G. Righetti, Biopharm. Drug Dispos. 22 (2001) 337.
[2] V. Kašička, Electrophoresis 22 (2001) 4139.
[3] H.J. Issaq, T.P. Conrads, G.M. Janini, T.D. Veenstra, Electrophoresis 23 (2002) 3048.
[4] M.T.W. Hearn, Biologicals 29 (2001) 159.
[5] S. Hu, N.J. Dovichi, Anal. Chem. 74 (2002) 2833.
[6] Z. Deyl, I. Mikšík, in: Z. Deyl (Ed.), Advanced Chromatographic and Electromigration Methods in BioSciences, Elsevier, Amsterdam, 1998, p. 465.
[7] V. Kašička, in: H.Y. Aboul-Enein (Ed.), Analytical and Preparative Separation Methods of Biomacromolecules, Marcel Dekker Inc., New York, 1999, p. 39.
[8] O. Hanč, Z. Pádr, Hormony, Academia, Praha, 1982, p. 274.
[9] N. Sewald, H.D. Jakubke, in: N. Sewald, H.D. Jakubke (Eds.), Peptides: Chemistry and Biology, Wiley-VCH Verlag, Weinheim, 2002, p. 61.
[10] J. Mařík, M. Buděšínský, J. Slaninová, J. Hlaváček, Collect. Czech. Chem. Commun. 67 (2002) 373.
[11] J. Jiskra, V. Pacáková, M. Tichá, K. Štulík, T. Barth, J. Chromatogr. A 761 (1997) 285.
[12] V. Pacáková, J. Suchánková, K. Štulík, J. Chromatogr. B. 681 (1996) 69.
[13] V. Kašička, Z. Prusík, J. Pospíšek, J. Chromatogr. 608 (1992) 13.
[14] N. Sutcliffe, P.H. Corran, J. Chromatogr. 636 (1993) 95.
[15] G. Mandrup, J. Chromatogr. 604 (1992) 267.
[16] J. Frenz, S.L. Wu, W.S. Hancock, J. Chromatogr. 480 (1989) 379.
[17] K. Huml, T. Barth, Chem. Listy 92 (1998) 294.
[18] K. Zaitsu, Y. Kimura, Y. Ohkura, Biol. Pharm. Bull. 17 (1994) 763.
[19] A. Kunkel, S. Günter, C. Dette, H. Wätzig, J. Chromatogr. A. 781 (1997) 445.
[20] A. Kunkel, S. Günter, H. Wätzig, Am. Lab. 30 (1998) C76.
[21] C. Arcelloni, L. Falqui, S. Martinenghi, A.E. Pontiroli, R. Paroni, Electrophoresis 19 (1998) 1475.
[22] W. Tong, E.S. Yeung, J. Chromatogr. B Bio. Med. Appl. 685 (1996) 35.
[23] J. Sowell, R. Parihar, G. Patonay, J. Chromatogr. B 752 (2001) 1.
[24] N. Sewald, H.D. Jakubke, in: N. Sewald, H.D. Jakubke (Eds.), Peptides: Chemistry and Biology, Wiley-VCH Verlag, Weinheim, 2002, p. 135.
[25] A. Ciencialová, L. Klasová, J. Jiráček, J. Barthová, T. Barth, in: J. Slaninová (Ed.), Biological Active Peptides, Collection Symposium Series, 4, Praha, 2001, p. 41.
[26] A. Ciencialová, L. Klasová, J. Barthová, T. Barth, Book of Abstracts "Biological Active Peptides", IOCB, Praha, 2003, p. 17.
[27] V. Kašička, Z. Prusík, P. Sázelová, E. Brynda, J. Stejskal, Electrophoresis 20 (1999) 2484.
[28] P.G. Righetti, Capillary Electrophoresis in Analytical Biotechnology, CRC Series in Analytical Biotechnology, CRC Press, Boca Raton, 1996, p. 39.
[29] H.J. Issaq, G.M. Janini, K.C. Chan, Z. El Rassi, in: P.R. Brown, E. Grushka (Eds.), Advances in Chromatography, vol. 35, Marcel Dekker Inc., New York, 1995, p. 101.
[30] G.M. Janini, H.J. Issaq, Chromatographia 53 (2001) S18.
[31] V. Kašička, Z. Prusík, J. Chromatogr. 470 (1989) 209.
[32] A. Ciencialová, Graduation Report, Faculty of Natural Sciences, Charles University, Praha, 2003.

Available online at www.sciencedirect.com
SCIENCE DIRECT
Journal of Chromatography A, 1081 (2005) 9–18
JOURNAL OF CHROMATOGRAPHY A
www.elsevier.com/locate/chroma

Analysis and separation of enkephalin and dalargin analogues and fragments by capillary zone electrophoresis

Veronika Šolínová[a], Václav Kašička[a,*], Tomislav Barth[a], Linda Hauzerová[a], Salvatore Fanali[b]

[a] *Institute of Organic Chemistry and Biochemistry, Academy of Sciences of the Czech Republic, Flemingovo 2, 16610 Prague 6, Czech Republic*
[b] *Institute of Chemical Methodologies, Consiglio Nazionale delle Ricerche, Area della Ricerca di Roma I, Via Salaria Km 29,300, 00016 Monterotondo Scalo, Rome, Italy*

Available online 30 January 2005

Abstract

Capillary zone electrophoresis (CZE) has been applied to qualitative and quantitative analysis and separation of synthetic analogues and fragments of enkephalins ([Leu^5]enkephalin, H-Tyr-Gly-Gly-Phe-Leu-OH, [Met^5]enkephalin, H-Tyr-Gly-Gly-Phe-Met-OH), and dalargin (H-Tyr-D-Ala-Gly-Phe-Leu-Arg-OH), biologically active peptides with morphin-like effects acting as ligands for the opiate receptors in the brain. These oligopeptides (dipeptides to hexapeptides) were analyzed as cations in two acidic background electrolytes (BGEs), BGE I (100 mM H_3PO_4, 50 mM Tris, pH 2.25), BGE II (100 mM iminodiacetic acid, pH 2.30), and both as cations and anions in alkaline BGE IV (40 mM Tris, 40 mM Tricine, pH 8.10). Purity degrees of peptides, expressed in three different ways (relative peak height, relative peak area and relative corrected peak area), were determined by their CZE analyses in the above BGEs, and their values were compared with respect to the peak shapes and migration times of the main synthetic products and their admixtures. Selected analogues and fragments of enkephalins and dalargin were successfully separated by CZE in acidic isoelectric buffers, 100 and 200 mM iminodiacetic acid, pH 2.30 and 2.32, respectively. The effective electrophoretic mobilities at standard temperature 25 °C, and effective and specific charges of all analyzed peptides in the above three BGEs were determined. Correlation between effective electrophoretic mobility of the analyzed peptides and their charge and size (relative molecular mass) was investigated, which revealed different molecular shape of analyzed peptides in acidic and alkaline BGEs. In addition, the selected characteristics of the UV-absorption detector (noise, signal to noise ratio, sensitivity, and limits of detection and quantification) were determined.

Keywords: Capillary zone electrophoresis; Peptides; Enkephalins; Dalargin

1. Introduction

Capillary zone electrophoresis (CZE), one of the high-performance capillary electromigration methods, providing fast (few minutes) and high-efficient separation (10^5–10^6 theoretical plates per meter) of picomole to attomole amounts of analytes in the nanolitre sample volume, possesses a high application potential in the field of separations of peptides: it is broadly utilized for analysis, preparation and physicochemical and biochemical characterization of peptides both in the research and in practical applications in chemistry, biochemistry, biomedicine, biotechnology, pharmaceutical industry, food and feed industry and fishing farming, as documented in several recent reviews [1–7].

Enkephalins (ENKs), ([Leu^5]enkephalin [Leu^5]ENK), pentapeptide H-Tyr-Gly-Gly-Phe-Leu-OH, and [Met^5]enkephalin ([Met^5]ENK), pentapeptide H-Tyr-Gly-Gly-Phe-Met-OH, and dalargin (DLR), hexapeptide H-Tyr-D-Ala-Gly-Phe-Leu-Arg-OH, are biologically active peptides with morphin-like effects acting as ligands for the opiate receptors in the brain [8]. Enkephalins are fragments of nature opioid hormones, dynorphin A (17 amino acid residues) and dynorphin B (13 amino acid residues).

* Corresponding author. Tel.: +420 220 183 239; fax: +420 220 183 592.
E-mail address: kasicka@uochb.cas.cz (V. Kašička).

0021-9673/$ – see front matter © 2005 Elsevier B.V. All rights reserved.
doi:10.1016/j.chroma.2005.01.046

Enkephalins and dynorphins originate from the two large precursor proteins, preproenkephalin and preprodynorphin [8]. They play significant roles in mediating stress and abatement of pain and are involved in temperature control, feeding behavior and respiration. These peptides and their analogues are used for the treatment of some mental illnesses (e.g. chronic schizophrenia, senile dementia of Alzheimer type).

CZE has been frequently used for analysis of enkephalins and dalargins, most often to check the purity of synthetic preparations of these peptides but also for their determination in biological fluids (serum, plasma, cerebrospinal fluids). Rational approach to selection and optimization of important experimental parameters (composition and pH of the background electrolyte (BGE), loading limit, capillary diameter and fraction collection) in analytical and preparative CZE of opioid peptides including enkephalin and dynorphin analogues with off-line mass spectrometric (MS) detection was reviewed by Lee and Desiderio [9]. [Leu^5]ENK, [Met^5]ENK and [desTyr^1-Leu^5]ENK were analyzed with high sensitivity (with limits of detection as low as 3–11 attomole) by CZE in citrate and phosphate BGEs using electrospray ionization time-of-flight mass spectrometry (ESI-TOF-MS) [10]. Analogues of enkephalins and dalargin and other biopeptides, such as e.g. vasopressin, desmopressin, insulin-like growth factors, have been separated by CZE in strongly acidic BGE, 150 mM phosphoric acid, pH 1.8 [11]. These analogues were also analyzed and separated by capillary micellar electrokinetic chromatography (CMEKC) with micellar pseudophase formed by anionic detergent sodium dodecylsulfate (SDS) in alkaline BGEs (20 mM tetraborate, pH 9.2, and 20 mM phosphate, pH 8.8) or by cationic detergent cetyltrimethylammonium bromide (CTAB) in acidic BGE (50 mM phosphate, pH 4.1) [11–13]. Analogue of dalargin, [D-Tle^{2,5}]dalargin, was analyzed by CZE in 0.5 M acetic acid, pH 2.5, and then purified in preparative scale by free-flow zone electrophoresis [14]. Six analogues and fragments of enkephalins were separated and determined in biological matrices by multidimensional separation system consisting of on-line coupling of size-exclusion chromatography (SEC), reverse-phase C18 trapping column and CZE [15,16] and by liquid secondary ion mass spectrometry and tandem mass spectrometry (LSI-MS–MS–MS) [17]. Dynorphin peptide analogues were separated by CMEKC employing anionic (SDS), cationic (CTAB) and zwitterionic (CHAPS) surfactants [18]. Enkephalin-related peptides were derivatized by fluorescein isothiocyanate and then separated by CMEKC in borate BGE with SDS micelles and detected with laser-induced fluorescence detector [19]. [D-Pen^{2,5}]ENK (D-Pen is D-penicillamine or D-3-mercaptovaline) and [D-Ser^2,Thr^6]DLR were analyzed in rat serum by CZE in phosphate (pH 2.4) and borate (pH 8.3) buffers [20,21]. ENKs and their fragments were electrochemically detected as in-capillary formed copper complexes after their CZE separation [22]. ENK analogues were separated in tris-phosphate and sodium phosphate BGEs, pH 2.5, in capillary noncovalently coated with two layers of oppositely charged polymers [23]. [Leu^5]ENK, [Met^5]ENK and other peptide hormones were separated in three BGEs, pH 2.61, 2.85 and 10.0, and their pK_a were determined from the pH dependence of their electrophoretic mobilities in the broad pH range, 2–12, [24], and subsequently analyzed with CE-ESI-MS in 50 mM acetic acid and 50 mM formic acid, pH 2.85 [25].

The aim of this work was to perform qualitative and quantitative analysis of synthetic preparations of opioid peptide hormones, enkephalins and dalargin, and their analogs and fragments, by CZE both in acidic and alkaline BGEs. Suitable experimental conditions should be found for CZE separation of the mixtures of these structurally related peptides. In addition to the purity degree also some physicochemical characteristics of the analyzed peptides, such as effective electrophoretic mobilities, effective and specific charges should be determined, and the correlation between effective electrophoretic mobility of analyzed peptides and their charge and size (relative molecular mass) should be investigated.

2. Experimental

2.1. Chemicals

All chemicals used were of analytical reagent grade. Iminodiacetic acid (IDAA) was obtained from Bachem (Bubendorf, Switzerland), Tris (tris(hydroxymethyl)aminomethane) was supplied by Serva (Heidelberg, Germany), phosphoric acid and dimethyl sulfoxide (DMSO) were obtained from Lachema (Brno, Czech Republic) and Tricine ([tris(hydroxymethyl)-methyl]-glycine) was from Merck (Darmstadt, Germany). Isophorone (3,5,5-trimethyl-2-cyclohexen-1-one) was supplied by Fluka (Buchs, Switzerland).

2.2. Peptides

The list of analyzed peptides and their abbreviations, sequences and relative molecular masses, M_r, are presented in Table 1. The oligopeptide fragments of ENKs, Tyr-Gly (YG) and Tyr-Gly-Gly (YGG), were obtained from Bachem (Bubendorf, Switzerland), the di- and tripeptide fragments of DLR, Tyr-Ala (YA) and Tyr-D-Ala-Gly (YaG), were purchased from Sigma (St. Louis, MO, USA). The analogs and derivatives of ENKs and DLR were prepared by solid phase synthesis [26]. The structure of DLR was altered by the substitution of leucine in position 5 by bulky amino acid such as D-tertiary leucine [27], by glycosylation [28] or iodination of tyrosine in position 1, by derivatization of the C-terminal arginine carboxyl group and by combination of these modifications.

2.3. Instrumentation

The capillary electrophoretic experiments were carried out in commercial P/ACE MDQ System (Beckman-Coulter,

Table 1
Sequences of analyzed peptides and their relative molecular masses (M_r)

Peptide	Abbreviation	Sequence in three-letters code	M_r
[Leu^5]enkephalin	[Leu^5]ENK	H-Tyr-Gly-Gly-Phe-Leu-OH	555.8
[Met^5]enkephalin	[Met^5]ENK	H-Tyr-Gly-Gly-Phe-Met-OH	573.8
ENK dipeptide fragment	YG	H-Tyr-Gly-OH	238.3
ENK tripeptide fragment	YGG	H-Tyr-Gly-Gly-OH	295.4
Dalargin	DLR	H-Tyr-D-Ala-Gly-Phe-Leu-Arg-OH	726.1
DLR dipeptide fragment	YA	H-Tyr-Ala-OH	252.3
DLR tripeptide fragment	YaG	H-Tyr-D-Ala-Gly-OH	309.4
[D-Tle^5]dalargin	[D-Tle^5]DLR	H-Tyr-D-Ala-Gly-Phe-D-Tle-Arg-OH	726.1
Dalargin ethylamid	DLR-NHEt	H-Tyr-D-Ala-Gly-Phe-Leu-Arg-NH-Et	749.0
[Tyr(I_2)]dalargin	I_2DLR	H-(3,5-di-I)-Tyr-D-Ala-Gly-Phe-Leu-Arg-OH	960.8
[D-Ser^2,Thr^6]dalargin	[D-Ser^{2}Thr^6]DLR	H-Tyr-D-Ser-Gly-Phe-Leu-Thr-OH	689.9
N-Phenylacetyl-dalargin	PacDLR	C_6H_5-Ac-Tyr-D-Ala-Gly-Phe-Leu-Arg-OH	859.1

Fullerton, CA, USA), data acquisition and evaluation were performed using the software P/ACE System MDQ, version 2.3 supplied by Beckman.

The apparatus was equipped with the internally non-coated fused silica capillary with outer polyimide coating, total/effective length 39.4/29.2 cm, I.D./O.D. 75/360 μm (Polymicro Technologies, Phoenix, AR, USA). The analytes were detected by UV–vis absorption spectrophotometric photodiode array detector (190–600 nm) set at constant wavelength 206 nm. The temperature was set at 25 °C with liquid coolant continuously circulating around the capillary.

The new capillary was gradually flushed with water, 0.1 M NaOH, water and BGE, each wash for 5 min. Finally, the capillary was conditioned by a 20 min application of the high voltage to equilibrate the inner surface and to stabilize electroosmotic flow. Between runs under the same conditions, the capillary was rinsed with the BGE for 2 min. Prior to any change of the BGE the capillary was rinsed with 0.1 M NaOH for 5 min and then repeatedly stabilized. The separation voltage was 10 kV. The samples were injected with pressure 5–10 mbar for 5–15 s. The samples were dissolved in deionized water or in BGE and their concentrations were in the range 0.1–1.5 mg/ml. The BGEs were filtered through a 0.45 μm syringe filter (Millipore, Bedford, MA, USA) before use.

3. Results and discussion

3.1. Selection of separation conditions

The strategy for the rational selection of experimental conditions for CZE analysis and separations of ENKs, DLR and their derivatives and fragments followed the general rules of selection of suitable CZE separation conditions [29] and took into account the specific properties of these peptides resulting from their structure—number and sequence of the linked amino acid residues, i.e. their amphoteric character and strong pH dependence of effective electrophoretic mobilities, which are governed by the effective electric charge, size (relative molecular mass) and shape (conformation) of these peptides.

The selection of the composition of the BGEs includes the type and concentration of buffer components and pH, and it also takes into account the requests for preserving chemical and temperature stability and biological activity of analyzed peptides [30,31]. Effective charges of peptides are strongly dependent on pH and pK_a of ionogenic groups of amino acid residues present in peptide chain. The analyzed peptides, see Table 1, contain several different types of ionogenic groups—all peptides, except Pac-DLR, possess α-amino group of the N-terminus of the peptide chain (average pK_a 8.0), and all peptides, except DLR-NHEt, contain α-carboxyl group of the C-terminus of the peptide chain (average pK_a 2.6), dalargin analogues (except [D-Ser^{2}Thr^6]DLR) possess guanidium group of arginine (average pK_a 11.3) and all of them hydroxy group of tyrosine (average pK_a 10.4). The relative molecular mass of analyzed peptides was in the range 238.3–1065, see Table 1.

One of the most important parameters for selection of suitable experimental conditions for CZE analysis and separation of peptides is the pH dependence of their effective and specific charges, since the electrophoretic mobility of peptides is directly proportional to their effective charge. For that reason the dependence of effective charge and specific charge (effective charges divided by relative molecular mass) of all peptides to be analyzed has been calculated by the earlier developed computer program Nabamfo [32] using the above given average values of pK_a of ionogenic groups. From the course of the pH dependence of the specific charge of peptides to be analyzed and separated (see Fig. 1) it follows, that these peptides can be analyzed both as cations (preferably in acid pH range) and as anions (preferably in alkaline pH range). Consequently, the two strongly acidic BGEs (pH 2.25–2.30) and one weakly alkaline BGE (pH 8.1) were selected for CZE analyses and separations of the above peptides. Full composition of the used BGEs together with the separation voltage and electric currents are presented in Table 2. Separation conditions are significantly influenced by solubility of peptides. With respect to the relatively hydrophilic character of the analyzed

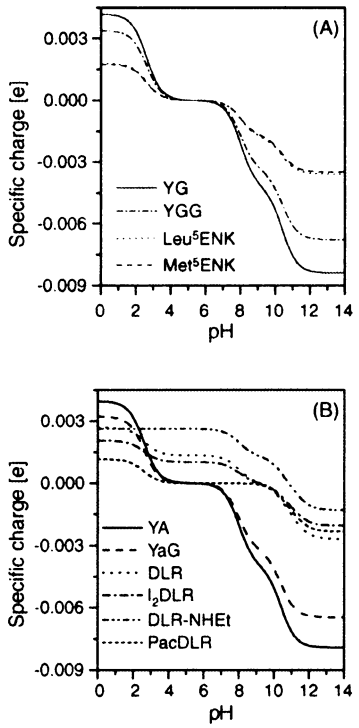

Fig. 1. The pH dependence of specific charge (effective charge divided by relative molecular mass) of selected peptides. (A) Enkephalin analogues and fragments and (B) dalargin analogues and fragments.

peptides most of them could be dissolved in deionized water, which brings an advantage that the same sample solution can be applied to CZE analyses in different BGEs, and in addition the electric-field-enhanced concentrating effect is utilized to concentrate the diluted peptide solutions. On the other hand using BGE as sample solvent ensures the constant separation conditions (movement in the BGE of the same composition) in the whole CZE experiment, which is important when CZE is applied for the physicochemical measurements.

3.2. Qualitative and quantitative analysis

The selected BGEs were used for qualitative and quantitative analysis of synthetic preparations of ENKs, DLR and their new analogues and fragments. For full characterization of these peptides before their application in the biological tests it is necessary to find out the content of their all admixtures, originating from the synthesis of peptides and/or from their subsequent purification procedures. Consequently, the purity degrees of these peptides, both crude synthetic products and peptides purified by chromatographic methods, size-exclusion chromatography and reverse phase high-performance liquid chromatography (RP-HPLC), were determined. Peptides were analyzed as cations in acidic BGEs and as anions or cations in weakly alkaline BGE. The examples of CZE analyses of some peptides are shown in Fig. 2. Standards of synthesized peptides were not available, therefore only relative degrees of purity could be determined. Peptide purity and peptide content in the sample was quantified by three ways: (i) relative peak height, $P_h(i)$ (1), (ii) relative peak area, $P_A(i)$ (2), and (iii) relative corrected peak area, $P_{CA}(i)$ (3), of the UV-positive peaks for the ith component of the peptide preparation:

$$P_h(i) = \frac{h(i)}{\sum h(i)}, \quad i = 1, \ldots, n \tag{1}$$

$$P_A(i) = \frac{A(i)}{\sum A(i)}, \quad i = 1, \ldots, n \tag{2}$$

$$P_{CA}(i) = \frac{A_c(i)}{\sum A_c(i)}, \quad i = 1, \ldots, n \tag{3}$$

where $h(i)$ is height of the ith peak, $A(i)$ is area of the ith peak and $A_c(i)$ is corrected area of the ith peak, corrected peak area is peak area corrected with respect to migration velocity of the given peak, which is obtained as peak area divided by the migration time of the given peak, n is the number of sample components.

The values of differently expressed purity degrees of analyzed peptides are presented in Table 3. The values of purity degrees were determined as averages of values obtained in two subsequent analyses, which differed less than 1%. The synthetic peptides exhibited rather different degree of purity. Analyses of peptides with high purity degree, [Leu^5]ENK and DLR-NHEt, are demonstrated in Fig. 2A and F, respectively. On the other hand analysis of peptide with low purity degree, with one major and several minor impurities, is shown in electrophoregram of [D-Tle^5]DLR in Fig. 2D. Analysis of peptide with some minor impurities is demonstrated in electrophoregram of I_2DLR in Fig. 2C. As follows from the above definitions, the most exact characteristic of peptide purity is the relative corrected peak area. Sometimes other, the simpler ways of purity evaluation, relative peak height or relative peak area, can be used, particularly in the cases when the peaks of sample components are uniformly dispersed and their migration times (velocities) are not too different. The great difference in differently expressed purity degree was found, e.g. in the CZE analysis of DLR presented in Fig. 2B. Relative peak height of DLR was about 10–15% lower than its relative peak area and relative peak corrected area in acidic BGEs I and II due to the relatively high height and small area of the sharp peak of the main admixture X. On the other hand relative peak height of tripeptide fragment of ENK, YGG, was about 6–7% higher than relative peak area

Table 2
Composition and pH of the BGEs applied for CZE analyses and separations of ENKs and DLR analogues and fragments, and electric current, I, in these BGEs at constant voltage 10 kV

BGE no.	BGE constituents	pH	I (μA)
I	50 mM Tris, 100 mM H_3PO_4	2.25	58–65
II	100 mM iminodiacetic acid	2.30	36.7–37
III	200 mM iminodiacetic acid	2.32	52.3–52.8
IV	40 mM Tris, 40 mM Tricine	8.10	13.2–14.2

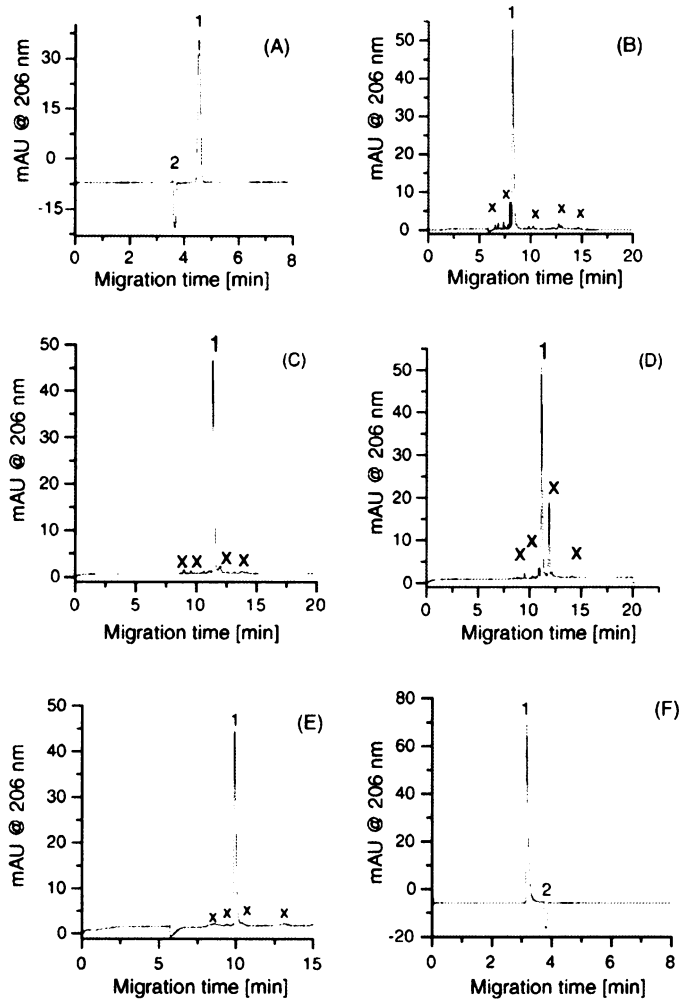

Fig. 2. CZE analyses of selected synthetic peptides. Experiments were carried out in uncoated fused-silica capillary: total/effective length 394/292 mm, I.D. 75 μm, O.D. 360 μm, constant voltage $U = 10$ kV, UV-absorption detection at 206 nm. (A) [Leu^5]ENK, 1.25 mg ml^{-1}, in BGE IV; (B) DLR, 1.25 mg ml^{-1}, in BGE II; (C) I_2DLR, 1.00 mg ml^{-1}, in BGE II; (D) [D-Tle^5]DLR, 1.00 mg ml^{-1}, in BGE I; (E) YGG, 1.10 mg ml^{-1}, in BGE II; (F) DLR-NHEt, 1.15 mg ml^{-1}, in BGE IV. (1) Main synthetic product; (2) neutral electroosmotic flow marker; and (X) non-identified impurities.

Table 3
Purity degrees of analyzed peptides, expressed alternatively as relative peak height, P_h, relative peak area, P_A, and relative peak corrected area, P_{CA}, determined by CZE in three BGEs

Peptide	BGE I, pH 2.25			BGE II, pH 2.3			BGE IV, pH 8.1		
	P_h (%)	P_A (%)	P_{CA} (%)	P_h (%)	P_A (%)	P_{CA} (%)	P_h (%)	P_A (%)	P_{CA} (%)
[Leu^5]ENK	94.5	92.7	92.7	93.3	89.4	89.4	95.8	93.1	93.0
[Met^5]ENK	94.0	92.6	92.6	91.3	95.7	95.6	97.5	97.8	97.8
YG	98.3	98.8	98.9	97.4	98.5	98.7	98.5	99.0	99.0
YGG	92.5	86.0	85.7	95.8	89.6	89.6	96.2	91.0	91.8
DLR	75.4	84.6	84.6	65.8	80.7	81.9	91.5	89.2	90.3
YA	99.2	99.2	99.3	99.7	99.8	99.9	99.3	99.4	98.2
YaG	92.7	93.1	93.4	96.3	96.3	94.4	98.5	98.7	98.7
[D-Tle^5]DLR	66.6	69.8	70.9	50.8	58.8	58.8	91.3	92.1	92.1
DLR-NHEt	94.5	96.8	96.9	95.0	94.2	94.2	94.7	94.3	94.2
I_2DLR	91.5	90.5	90.6	87.5	82.8	82.8	90.2	89.9	90.5
[D-Ser^{2}Thr^6]DLR	87.7	88.3	87.3	92.5	94.2	94.2	97.9	98.7	98.8
PacDLR	81.0	78.1	81.8	94.9	95.0	89.7	n.d.	n.d.	n.d.

n.d.: not determined.

or relative corrected peak area in acidic BGEs I and II due to the relatively small height and broad width of the peaks of its admixtures (see Fig. 2E). Similar values of purity degrees expressed by relative peak height, relative peak area and corrected peak area were obtained in analysis of highly purified peptides, as e.g. in analysis of DLR-NHEt both in acidic and alkaline BGEs, see Table 3 and Fig. 2F. As follows from the presented data, the purity degree of given peptide depends on BGE used and on the way of purity degree evaluation. Consequently, purity degree of peptides should be tested in more than one BGE and only the purity degrees obtained under the same conditions and evaluated in the same way can be compared.

As can be seen from the analyses presented in Fig. 1A–F, in all BGEs used symmetrical peaks were obtained with high separation efficiency in short times, with migration times of the main component between 3 and 12 min. The best results were obtained in BGE II (100 mM iminodiacetic acid, pH 2.30) using the separation voltage 10 kV. The separation efficiency in BGE II was in range $(0.5–1.0) \times 10^6$ theoretical plates per meter, concentration limit of detection (LOD = three times noise) was $(0.60–2.26) \times 10^{-6}$ mol dm^{-3}, concentration limit of quantification (LOQ = 10 times noise) was $(2.01–7.54) \times 10^{-6}$ mol dm^{-3}, sensitivity of the UV-absorption detector was 46.5–114.4 AU mol^{-1} dm^3 and the noise of UV-detector signal was 0.023 mAU. These parameters for BGE I were almost the same as for BGE II, however the time of analysis was longer because of the very low electroosmotic flow (EOF) in this BGE. BGE IV was found less suitable for analysis of these series of peptides due to the basic character of some of the analyzed peptides, DLR and its derivatives, which are positively charged even at pH 8.1 and due to the fast EOF at this pH, which means that the electrophoretically migrated trajectory of these peptides is relatively short and they could not be well separated from their admixtures and other structurally related peptides. The characteristics of the UV-absorption detector for all BGEs are presented in Table 4.

3.3. Separation of structurally related peptides

In addition to qualitative and quantitative analysis of individual synthetic peptide preparations, the separation of closely related structures of ENKs and their fragments, and DLR and its analogues and fragments was tested. These separations are important from the point of view of separations of the whole molecules of ENKs and DLR from their degradation products. The suitable conditions for the separations were derived from the course of the pH dependence of specific charge of these peptides (see Fig. 1), and from the experience obtained in the analysis of individual peptides by CZE in BGEs I, II, and IV. As it was already mentioned above from the BGEs tested the BGE II, composed of isoelectric buffer, 100 mM iminodiacetic acid (IDAA), provided the best results. To achieve the best

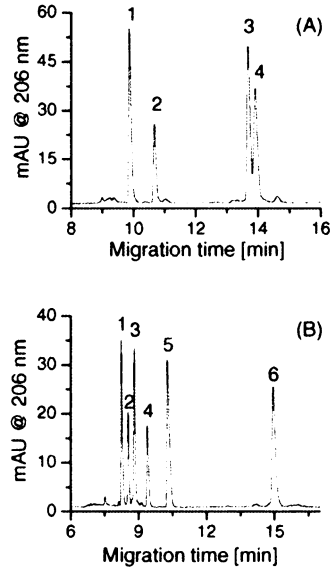

Fig. 3. CZE separations of structurally related peptides. Experiments were carried out in uncoated fused-silica capillary: total/effective length 394/292 mm, I.D. 75 μm, O.D. 360 μm, constant voltage $U = 10$ kV, UV-absorption detection at 206 nm. (A) Enkephalin analogues and fragments in BGE III: 1, YG; 2, YGG; 3, [Leu^5]ENK; 4, [Met^5]ENK. (B) Dalargin fragments and analogues in BGE II: 1, DLR-NHEt; 2, DLR; 3, I_2DLR; 4, YA; 5, YaG; and 6, PacDLR.

resolution different concentrations of IDAA and separation voltages were tested. Finally, 100 mM iminodiacetic acid, pH 2.30 and voltage 10 kV were selected as the best conditions for separation of DLR and its analogues and fragments. The doubled concentration of IDAA, i.e. 200 mM, pH 2.32, was found to be most suitable for separation of ENKs and their fragments, providing the best resolution at the same separation voltage, 10 kV. Separations of these two mixtures are shown in Fig. 3, mixture of [Leu^5]ENK, [Met^5]ENK and their fragments (YG, YGG) in Fig. 3A, and the mixture of DLR and its derivatives (DLR-NHEt, I_2DLR, PacDLR) and fragments (YA, YaG) in Fig. 3B. The resolution of any pair of peptides was higher than 2.1 with the exception of [Leu^5]ENK and [Met^5]ENK, which were separated with resolution 1.11. In the mixture of ENKs and their fragments the latter migrated faster, with migration times in the order YG < YGG < [Leu^5]ENK < [Met^5]ENK. In the mixture of DLR and their analogues and fragments the longer peptides with higher values of effective and specific charges migrated faster than the short fragments with lower specific charges.

3.4. Determination of effective mobility

From CZE analyses of ENKs, DLR and their analogues and fragments the effective electrophoretic mobilities of these peptides were determined. The effective electrophoretic mobility, m_{eff}, of peptide in the given BGE was calculated from the migration time of the peptide, t_{mig}, in this BGE, and from the migration time of the electroneutral marker of

Table 4
The characteristics of the UV-absorption photodiode array detector set at 206 nm

Peptide	BGE	c (mmol dm^{-3})	$R/n \times 10^{-3}$	S (AU mol^{-1} dm^3)	LOD (μmol dm^{-3})	LOQ (μmol dm^{-3})
[Leu^5]ENK	I	2.08	4.02	42.6	1.55	5.17
	II	2.01	4.06	46.5	1.48	4.95
	IV	2.16	1.04	32.9	6.20	20.7
[Met^5]ENK	I	1.61	5.46	74.7	0.88	2.95
	II	1.49	7.41	114.4	0.60	2.01
	IV	1.70	1.49	59.7	3.42	11.4
YG	I	4.56	4.75	22.9	2.88	9.60
	II	5.38	7.14	30.5	2.26	7.54
	IV	5.61	1.20	14.5	14.1	46.9
YGG	I	3.19	2.55	17.6	3.75	12.5
	II	3.34	1.85	12.8	5.41	18.0
	IV	3.58	0.44	8.35	24.4	81.4
DLR	I	1.46	4.50	67.8	0.97	3.24
	II	1.41	5.74	93.6	0.74	2.46
	IV	1.55	1.07	46.7	4.37	14.6
YA	I	4.32	2.63	13.4	4.93	14.4
	II	4.35	1.73	9.13	7.56	25.2
	IV	4.33	0.49	7.67	26.6	88.7
YaG	I	3.46	5.23	33.2	1.99	6.62
	II	3.58	4.02	25.8	2.70	8.90
	IV	3.66	1.54	28.7	7.12	23.7
[D-Tle^5]DLR	I	0.98	3.76	84.4	0.78	2.61
	II	0.81	3.00	85.3	0.81	2.70
	IV	1.11	0.83	50.9	4.01	13.4
DLR-NHEt	I	1.48	7.57	112.6	0.59	1.95
	II	1.45	5.21	82.7	0.83	2.78
	IV	1.45	2.25	105.3	1.94	6.46
I_2DLR	I	0.94	4.16	97.4	0.68	2.26
	II	1.16	4.52	89.6	0.77	2.57
	IV	0.94	1.16	83.6	2.44	8.14
[D-Ser^{2}Thr^6]DLR	I	1.33	2.74	45.4	1.45	4.85
	II	1.44	2.96	47.3	1.46	4.86
	IV	1.51	0.86	38.6	5.29	17.6
PacDLR	I	0.91	2.56	62.0	1.07	3.55
	II	1.38	4.02	67.0	1.03	3.43
	IV	n.d.	n.d.	n.d.	n.d.	n.d.

R: detector response, n: noise, c: concentration, S: sensitivity of detector $S = R/c$, LOD: limit of detection LOD = $3n/S$, LOQ: limit of quantification LOQ = $10n/S$, n.d.: not determined. BGE I: 100 mM H_3PO_4, 50 mM Tris, pH 2.25, $n = 0.022$ mAU; BGE II: 100 mM iminodiacetic acid, pH 2.30, $n = 0.023$ mAU; BGE IV: 40 mM Tris, 40 mM Tricine, pH 8.1, $n = 0.068$ mAU.

EOF (DMSO or isophorone), t_{eo}, according to the following relation:

$$m_{eff} = \frac{l_t l_{ef}}{U}\left(\frac{1}{t_{mig}} - \frac{1}{t_{eo}}\right) \quad (4)$$

where l_t is total capillary length, l_{ef} is effective capillary length, U is the separation voltage.

In CZE analyses in highly acidic BGEs with very low EOF due to the suppressed dissociation of silanol groups the effective electrophoretic mobility was determined using the pressure accelerated measurement of EOF as described in [33]. Briefly the sample was injected along with zone A of the neutral EOF marker into the capillary filled with BGE. Then the separation voltage was applied, the analytes were separated and the neutral marker zone A migrated with the velocity of EOF. Analysis was stopped (separation voltage switched-off) at a specific time, t_u, just after the peptide zone passed the detector. Then the second zone (B) of the (same or different) EOF marker was injected and the injection pressure (15 mbar) was applied onto the pure BGE vessel. Both zones of the EOF marker, A and B, reached the detector at times, t_A and t_B, respectively, which were recorded in the usual manner. Then the electrophoretic mobility can be calculated from the following relation:

$$m_{eff} = \frac{l_t l_{ef}}{U}\left(\frac{1}{t_{mig}} - \frac{1}{t_u} + \frac{t_A}{t_u t_B}\right) \quad (5)$$

where the symbols have the same meanings as in Eq. (4). The values of effective electrophoretic mobility were determined as averages of two subsequent measurements, which differed less than 1%.

The real temperature inside the capillary was higher than the temperature of the coolant due to Joule heating. The real temperature in the capillary for each BGE was obtained from the dependence of temperature increase in fused silica capillary on the input power per unit length of the capillary, which was determined from the measurement of specific electric conductivity of standard solution of 0.01 mol dm^{-3} KCl in the capillary at different values of input power as described in [34]. The temperature increase in fused silica capillary was 4.5 °C for BGE I, 2.0 °C for BGE II, 3.2 °C for BGE III and 0.7 °C for BGE IV. The effective electrophoretic mobility corrected to standard temperature (25 °C), $m_{eff,25}$, was calculated according to the equation:

$$m_{eff,25} = m_{eff,t}[1 - 0.022(t - 25)] \quad (6)$$

where $m_{eff,25}$ is effective electrophoretic mobility at 25 °C, $m_{eff,t}$, is effective electrophoretic mobility measured at real temperature, t, inside the capillary.

The values of effective electrophoretic mobilities of peptides in different BGEs corrected to standard temperature, 25 °C, are presented in Table 5. The effective electrophoretic mobilities measured at real temperature inside the capillary differed up to 10% in the most conductive BGE I in comparison with standard effective electrophoretic mobilities at 25 °C.

Generally the effective mobilities of analyzed peptides were in agreement with the values predicted from the course of the dependence of the specific charge on pH, i.e. peptides with higher specific charge exhibited higher effective mobilities than those with lower specific charge. Peptides containing guanidium group of arginine, particularly DLR and its analogues with the exception of [D-Ser^2Thr^6]DLR and PacDLR, migrated faster than the enkephalins, and due to their strongly basic character they migrated as cations even in the weak alkaline BGE IV, pH 8.10. Enkephalin dipeptide and tripeptide fragments (YG, YGG) migrated faster than enkephalins, all these peptides had almost the same charge (see Table 5). DLR analogs, [D-Ser^2Thr^6]DLR and PacDLR, lacking positive charged group of arginine behaved similarly as ENKs, however their mobilities were lower than those of ENKs due to their larger molecules.

3.5. Relationship between mobility of peptides and their charge and size

Several models correlating effective electrophoretic mobilities of peptides, m_{eff}, with their effective charge, q, and molecular size expressed as relative molecular mass, M_r, or number of amino acids in polypeptide chain, n, respectively, have been developed [35–39]. The models are based on Stoke's law, describing the motion of a particle in liquid medium, and on the action of electric field force on charged molecule. The semiempirical models describe the electrophoretic behavior of various conformations of molecules, which can be utilized to predict secondary or tertiary structure of peptides and proteins in solution [40].

In the current work we have used Cross's model [41], due to its suitability for prediction of the most probable secondary structure of peptides:

$$\log\left(\frac{m_{eff}}{q}\right) = k \log M_r \quad (7)$$

where the constant of proportionality, k, is the exponent of M_r in the non-logarithmic expression of this relation, which can be determined as a slope of this dependence and which is related to the shape of the charged molecule. The graph of these dependences in three BGEs is shown in Fig. 4. Because not all of the analyzed peptides formed a homologous series, some points did not fit well in the linear part of this dependence. This concerns especially DLR, and its analogs [D-$Tle^{2,5}$]DLR and DLR-NHEt, analyzed at alkaline pH in BGE IV, where their effective mobilities were rather low with respect to their estimated effective charges (see Table 5). The best coefficient of the correlation of the dependence expressed by Eq. (7)

Table 5
Calculated effective charges, q, and CZE determined effective electrophoretic mobilities, m_{eff}, corrected to standard temperature, 25 °C, of analyzed peptides in three different BGEs

Peptide	q (e)			m_{eff} ($\times 10^{-9}$ m^2 $V^{-1}s^{-1}$)		
	BGE I, pH 2.25	BGE II, pH 2.30	BGE IV, pH 8.1	BGE I, pH 2.25	BGE II, pH 2.30	BGE IV, pH 8.1
[Leu^5]ENK	0.72	0.62	−0.57	9.44	11.4	−9.99
[Met^5]ENK	0.71	0.61	−0.56	9.12	11.3	−10.0
YG	0.69	0.69	−0.57	14.3	17.6	−13.9
YGG	0.69	0.69	−0.56	12.8	15.3	−12.8
DLR	1.71	1.63	0.42	15.7	19.0	1.91
YA	0.69	0.69	−0.57	14.5	16.7	−13.3
YaG	0.69	0.69	−0.55	12.3	15.2	−12.7
[D-Tle^5]DLR	1.63	1.55	0.42	15.7	18.7	2.13
DLR-NHEt	2.00	2.00	1.42	15.9	20.0	10.3
I_2DLR	1.75	1.59	0.45	15.4	18.1	7.58
[D-Ser^2Thr^6]DLR	0.68	0.64	−0.56	7.83	9.78	−8.91
PacDLR	0.71	0.68	0.00	7.49	9.32	0.00

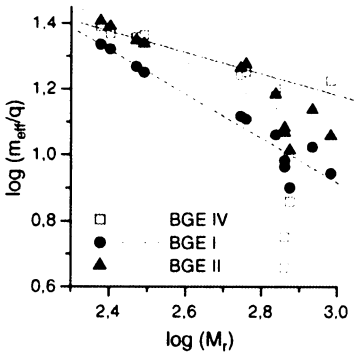

Fig. 4. Dependence of the decadic logarithm of the ratio of the effective electrophoretic mobility and effective charge on the decadic logarithm of relative molecular mass of analyzed enkephalin and dalargin analogues and fragments.

was obtained in BGE I, pH 2.25, $R = 0.9602$. When "outlier" points of DLR and its derivatives in BGE IV were omitted, the high coefficient of correlation was obtained also for BGE IV, reaching the value 0.9566. From the graph in Fig. 4 it is obvious, that the slopes of these dependences, k, are similar for two acidic BGEs, $k = -0.67386$ for BGE I, and $k = -0.5958$ for BGE II, whereas the slope of this dependence in alkaline BGE IV, is significantly different, $k = -0.3233$. The values of k in acidic BGEs are close to the value 2/3, which indicates that at this pH the peptides molecules have the shape of a wide thin disk, whereas the value of k in alkaline BGE is close to 1/3, which corresponds to the spherical shape of the molecule [40].

4. Conclusions

CZE proved to be powerful and useful tool for the fast and sensitive analyses and highly efficient separations of opioid peptide hormones, enkephalins, dalargins, and their analogues and fragments, in picomole to femtomole level in the nanolitre applied sample volume. The purity degree of analyzed peptides was best evaluated by relative corrected peak area. From the CZE analyses of peptides also their important physicochemical characteristics, particularly effective electrophoretic mobilities at both acidic and alkaline pH, could be determined. From the investigated correlation between effective electrophoretic mobility of analyzed peptides and their charge and size (relative molecular mass) the probable secondary structure of peptides could be predicted.

Acknowledgements

This work was supported by the Grant Agency of the Czech Republic, grants no. 203/02/1467, 203/03/0716, 203/04/0098, from the Grant Agency of the Academy of Sciences of the Czech Republic (ASCR), grant no. S4055006 and research project AV0Z 4055905, and by the CNR-ASCR cooperation project for the years 2004–2006. We thank Mrs. V. Lišková for her skilful technical assistance and other colleagues from our laboratory, Dr. P. Sázelová, Mgr. D. Koval and Dr. Z. Prusík, for their cooperation and assistance.

References

[1] W.W.C. Quigley, N.J. Dovichi, Anal. Chem. 76 (2004) 4645.
[2] V. Kašička, Electrophoresis 24 (2003) 4013.
[3] H.J. Issaq, T.P. Conrads, G.M. Janini, T.D. Veenstra, Electrophoresis 23 (2002) 3048.
[4] P.G. Righetti, Biopharm. Drug Dispos. 22 (2001) 337.
[5] M.T.W. Hearn, Biologicals 29 (2001) 159.
[6] Z. Deyl, I. Mikšík, in: Z. Deyl (Ed.), Advanced Chromatographic and Electromigration Methods in BioSciences, Amsterdam, Elsevier, 1998, p. 465.
[7] V. Kašička, in: H.Y. Aboul-Enein (Ed.), Analytical and Preparative Separation Methods of Biomacromolecules, Marcel Dekker Inc., New York, 1999, p. 39.
[8] N. Sewald, H.D. Jakubke, Peptides: Chemistry and Biology, Wiley-VCH Verlag, Weinheim, 2002, p. 61.
[9] H.G. Lee, D.M. Desiderio, Anal. Chim. Acta 383 (1999) 79.
[10] I.M. Lazar, E.D. Lee, A.L. Rockwood, M.L. Lee, J. Chromatogr. A 829 (1998) 279.
[11] V. Pacáková, J. Suchánková, K. Štulík, J. Chromatogr. B 681 (1996) 69.
[12] J. Jiskra, V. Pacáková, M. Tichá, K. Štulík, T. Barth, J. Chromatogr. A 761 (1997) 285.
[13] A. Furtosmatei, J.J. Li, K.C. Waldron, J. Chromatogr. B 695 (1997) 39.
[14] V. Kašička, Z. Prusík, J. Pospíšek, J. Chromatogr. 608 (1992) 13.
[15] T. Stroink, G. Wiese, J. Teeuwsen, H. Lingeman, J.C.M. Waterval, A. Bult, G.J. de Jong, W.J.M. Underberg, Electrophoresis 24 (2003) 897.
[16] T. Stroink, P. Schravendijk, G. Wiese, J. Teeuwsen, H. Lingeman, J.C.M. Waterval, A. Bult, G.J. de Jong, W.J.M. Underberg, Electrophoresis 24 (2003) 1126.
[17] D.M. Desiderio, J. Chromatogr. B 731 (1999) 3.
[18] A. Furtosmatei, R. Day, S.A. Stpierre, L.G. Stpierre, K.C. Waldron, Electrophoresis 21 (2000) 715.
[19] Y. Huang, J.P. Duan, Q.R. Chen, G.N. Chen, Electrophoresis 25 (2004) 1051.
[20] C.P. Chen, G.M. Pollack, J. Chromatogr. B 681 (1996) 363.
[21] C.P. Chen, D. Jeffery, J.W. Jorgenson, M.A. Moseley, G.M. Pollack, J. Chromatogr. B 697 (1997) 149.
[22] A.J. Gawron, S.M. Lunte, Electrophoresis 21 (2000) 3205.
[23] J.R. Catai, G.W. Somsen, G.J. de Jong, Electrophoresis 25 (2004) 817.
[24] V. Sanz-Nebot, F. Benavente, I. Toro, J. Barbosa, Electrophoresis 22 (2001) 4333.
[25] V. Sanz-Nebot, F. Benavente, E. Balaguer, J. Barbosa, Electrophoresis 24 (2003) 883.
[26] N. Sewald, H.D. Jakubke, Peptides: Chemistry and Biology, Wiley-VCH Verlag, Weinheim, 2002, p. 135.
[27] J. Pospíšek, Z.D. Bespalova, E. Kovaříková, M.I. Titov, T. Barth, K. Medzihradszky, Collect. Czech. Chem. Commun. 52 (1987) 1867.
[28] M. Tichá, T. Trnka, T. Barth, J. Pospíšek, V. Pacáková, V. Kašička, L. Hauzerová, K. Ubik, Book of Abstracts "Biological Active Peptides", IOCB, Praha, 1997, p. 52.
[29] H.J. Issaq, G.M. Janini, K.C. Chan, Z. El Rassi, in: P.R. Brown, E. Grushka (Eds.), Advances in Chromatography, vol. 35, Marcel Dekker Inc., New York, 1995, p. 101.
[30] G.M. Janini, H.J. Issaq, Chromatographia 53 (2001) S18.

[31] B.H. Hu, L.M. Martin, in: P.A. Millner (Ed.), High Resolution Chromatography A Practical Approach, Oxford University Press, Oxford, 1999, p. 77.
[32] V. Kašička, Z. Prusík, J. Chromatogr. 470 (1989) 209.
[33] D. Koval, V. Kašička, J. Jiráček, M. Collinsová, Electrophoresis 24 (2003) 774.
[34] D. Koval, V. Kašička, J. Jiráček, M. Collinsová, T.A. Garrow, J. Chromatogr. B 770 (2002) 145.
[35] N.J. Adamson, E.C. Reynolds, J. Chromatogr. B 699 (1997) 133.
[36] A. Cifuentes, H. Poppe, Electrophoresis 18 (1997) 2362.
[37] J. Kim, R. Zand, D.M. Lubman, Electrophoresis 24 (2003) 782.
[38] S.K. Basak, M.R. Ladisch, Anal. Biochem. 226 (1995) 51.
[39] J.M. Miller, A.C. Blackburn, Y. Shi, A.J. Melzak, O.Y. Ando, Electrophoresis 23 (2002) 2833.
[40] J.C. Colburn, in: P.D. Grossman, J.C. Colburn (Eds.), Capillary Electrophoresis: Theory and Practice, Academic Press, San Diego, 1992, p. 111.
[41] R.F. Cross, N.F. Garnham, Chromatographia 54 (2001) 639.

Veronika Šolínová
Václav Kašička
Dušan Koval
Jan Hlaváček

Institute of Organic Chemistry and Biochemistry, Academy of Sciences of the Czech Republic, Prague, Czech Republic

Separation and investigation of structure-mobility relationships of insect oostatic peptides by capillary zone electrophoresis

Capillary zone electrophoresis (CZE) has been applied to qualitative analysis, separation, and physicochemical characterization of synthetic insect oostatic peptides (IOPs) and their derivatives and fragments. Series of homologous IOPs were separated in three acidic background electrolytes (BGEs; pH 2.25, 2.30, 2.40) and an alkaline BGE (pH 8.1). Best separation was achieved in acid BGE composed of 100 mM H_3PO_4, 50 mM Tris, pH 2.25. The effective electrophoretic mobilities, μ_{ep}, of all IOPs in four BGEs were determined and several semiempirical models correlating effective mobility with charge-to-size ratio (μ_{ep} *versus* q/M_r^k) were tested to describe the migration behavior of IOP in CZE. None of models was found to be unambiguously applicable for the whole set of 20 IOPs differing in size (dipeptide – decapeptide) and charge (−2 to +0.77 elementary charges). However, a high coefficient of correlation, 0.9993, was found for the subset of homologous series of IOPs with decreasing number of proline residues at *C*-terminus, H-Tyr-Asp-Pro-Ala-Pro_x-OH, x = 6 – 0, for the dependence of μ_{ep} on q/M_r^k with k = 0.5 for IOPs as anions in alkaline BGE and with k = 2/3 for IOPs as cations in optimized acidic Tris-phosphate BGE. From these dependences the probable structure of IOPs in solution could be predicted.

Keywords: Capillary zone electrophoresis / Insect oostatic peptides / Structure-mobility relationships
DOI 10.1002/elps.200405924

1 Introduction

1.1 General aspects

Capillary zone electrophoresis (CZE) has developed into a fast, high-efficient, and high-sensitive separation technique which is now frequently used for analysis, micropreparation, and physicochemical characterization of peptides [1–7]. CZE can provide not only the information on qualitative and quantitative composition of peptide samples but also important physicochemical characteristics of separated peptides such as effective and absolute mobilities, charges, and parameters of molecular size and conformation. Using capillary electrophoresis (CE) methods for physicochemical characterization is advantageous, since only small amounts of analyzed compounds are sufficient, and, in addition, the admixtures separable by CZE need not to be removed in advance from the sample. Several models of the correlation between electrophoretic mobility, and the effective charge and size of polypeptide molecules, expressed as relative molecular mass or number of amino acid residues, respectively, have been developed [8–21]. The models are based on Stoke's law, describing the motion of a particle in liquid medium, and on the action of electric field force on the charged molecule. The semiempirical models describe the electrophoretic behavior of various conformation of molecules, which can be utilized to predict the secondary or tertiary structure of peptides and proteins in solution [8, 22–25].

Insect oostatic peptides (IOPs) are antigonadotropic insect hormones. Borovsky *et al.* [26] have firstly described the oostatic factor *Aed*-TMOF (trypsin modulating oostatic factor) as native decapeptide H-Tyr-Asp-Pro-Ala-Pro-Pro-Pro-Pro-Pro-Pro-OH, which was isolated from the mosquito *Aedes aegypti*. IOPs have specific effects on the reproduction of the flies, they cause the changes in the follicular epithelium, proliferation of nuclei, and cell division toward the inner part of the egg chamber. Consequently, IOPs are considered as a potential new type of biologically degradable insecticides. Borovsky *et al.* [27] also suggested the probable structure of the decapeptide as left-handed helix. Later, analogs with shortened *C*-terminal sequences, cyclic structure, and analogs with proline-substituted dehydroproline were synthesized

Correspondence: Dr. Václav Kašička, Institute of Organic Chemistry and Biochemistry, Academy of Sciences of the Czech Republic, Flemingovo 2, CZ-166 10 Prague 6, Czech Republic
E-mail: kasicka@uochb.cas.cz
Fax: +420-220-183-592

Abbreviations: IDAA, iminodiacetic acid; **IOP**, insect oostatic peptide

[28, 29], and characterized by NMR and circular dichroism spectra [29, 30]. Their biological activities were tested in the fly *Neobellieria bullata* (Diptera). The peptides with the *C*-terminus shortened linear chain-affected processes of egg development in 20–80% of ovarioles [28]. Weak oostatic activity was observed with the cyclic analogs due to their changed conformation in comparison with linear peptides possessing the ability in receptor binding [29]. Determination of secondary structure of IOPs is of great importance for estimation of their interactions with receptors.

In the current work, the first aim was to analyze qualitatively the synthetic IOPs, to determine their purity degree before they are used for biological tests, and to develop a BGE suitable for separation of closely related IOPs. The second aim was to determine effective electrophoretic mobilities of IOP at standard temperature (25°C), to test different models of the dependence of mobility of IOPs on their charge and size, and, consequently, to predict the structure of IOPs in solution.

1.2 Theory

1.2.1 Electrophoretic mobility

Electrophoretic mobility of a peptide is a complex function of the properties of the peptide itself (charge, size, and shape), properties of a medium in which the peptide is moving (composition, pH, ionic strength, viscosity, permittivity, and temperature) and interactions of the peptide with medium components (solvatation, dissociation, complex formation). Consequently, the experimental conditions must be strictly defined for determination of peptide's effective electrophoretic mobility, which has to be related to given composition, pH, and temperature of the BGE. The effective electrophoretic mobility, μ_{ep}, of a charged particle moving in liquid medium in an electric field, can be described [8] by the following equation:

$$\mu_{ep} = \frac{q}{6\pi\eta r} \tag{1}$$

where q is the effective charge of the ion, η is the viscosity of the solution, and r is the hydrodynamic radius of the ion.

1.2.2 Calculation of effective charge

Peptides are amphoteric electrolytes containing different types of ionogenic groups. The effective charge of peptides is given by the sum of charges (including their sign) of all ionogenic groups present in the polypeptide chain. The relationships usually used for the calculation of the effective charge are based on the Henderson-Hasselbalch equation [31]. The effective charge of peptide is a function of pH of liquid medium and pK_a values of the ionogenic groups of amino acid residues in the peptide [31]:

$$q = \sum_{i=1}^{m} \frac{1}{1 + 10^{pH - pK_a(i)}} - \sum_{j=1}^{p} \frac{1}{1 + 10^{-pK_a(j) - pH}} \tag{2}$$

where m and p are the integral number of cationic and anionic groups, and pK_a (i) and pK_a (j) are negative decadic logarithms of acid dissociation constants of the i-th and j-th ionogenic group of the analyte, respectively.

1.2.3 Models of correlations between mobility of peptides and their charge and size

Several models correlating effective electrophoretic mobilities of peptides, μ_{ep}, with their effective charge, q, and molecular size expressed as relative molecular mass, M_r, or number of amino acids in polypeptide chain, n, respectively, have been developed [8–21, 32].

Offord [12] has firstly quantitatively described this relationship for the series of oligo- and polypeptides separated by paper electrophoresis:

$$\mu_{ep} = \frac{k\,q}{M_r^{2/3}} \tag{3}$$

where k is a constant of proportionality. This relationship was found also by some other authors, Issaq *et al.* [13], Rickard *et al.* [14], and Basak and Ladisch [15] for peptides separated in free solution by CZE.

For rigid spherically shaped molecules in low-ionic-strength buffers the following relationship was derived [8] from Eq. (1):

$$\mu_{ep} = \frac{k\,q}{M_r^{1/3}} \tag{4}$$

Another semiempirical model has been proposed from the study of the synthetic polymers with cylindrical or rod-shaped molecules [33]:

$$\mu_{ep} = \frac{k\,q}{M_r^{1/2}} \tag{5}$$

Cross and Garnham [16] modified Offord's relation by expressing it in logarithmic form:

$$\log\left(\frac{\mu_{ep}}{q}\right) = k \log M_r \tag{6}$$

where k is the exponent of M_r in nonlogarithmic relation, which can be determined as a slope of this dependence.

Kim *et al.* [20] suggested another formula, which fitted well to his set of peptides originating from enzyme digests of proteins. It is similar to the semiempirical model for polymers:

$$\mu_{ep} = \frac{k\ q}{M_r^{0.56}} \quad (7)$$

Compton [21] combined two relationships for small (Eq. 4) and large (Eq. 3) molecules and obtained the relation:

$$\mu_{ep} = \frac{k\ q}{k_1\ M_r^{1/3} + k_2\ M_r^{2/3}} \quad (8)$$

where the first term in the denominator, $M_r^{1/3}$, represents smaller molecules, and the second term, $M_r^{2/3}$, larger molecules, both in low-ionic-strength buffers.

In all these cases the relative molecular mass was used as size parameter. Another possibility is to express the molecular size by the number of amino acid residues in the peptide chain, *n*. This approach was used by Grossman *et al.* [17], who derived the following relation for dependence of effective mobility on charge and size:

$$\mu_{ep} = \frac{k\ \ln(q+1)}{n^{0.43}} \quad (9)$$

Cifuentes and Poppe [18] reported the modification of Grossman's classical linear model, where the logarithmic dependence of mobility on the charge expressed electrostatic charge suppression in highly charged peptides:

$$\mu_{ep} = \frac{k_1\ \log(1 + k_2 q)}{M_r^{0.411}} \quad (10)$$

The same equation, only with different exponent of M_r, 0.435 instead of 0.411, was derived by Adamson and Reynolds [9].

Sanz-Nebot *et al.* [19] tested relationships (Eq. 10) with *q* compensated for electrostatic charge suppression in highly charged peptides and the relationships of classical semiempirical models (Eqs. 3–5), compared their results, and found a better correlation for the formula:

$$\mu_{ep} = \frac{k_1\ \ln(k_2 q + 1)}{M_r^k} \quad (11)$$

where k = 1/3 for small molecules, k = 1/2 for medium-sized polymers, k = 2/3 for large molecules, respectively.

These models can be used for prediction of the possible structure of the peptides and proteins in free solution. The structure of the molecule is derived from the relationship between frictional coefficient or electrophoretic mobility, respectively, and the exponent of the relative molecular mass or alternatively exponent of the number of amino acid residues in the peptide [8]. Each type of correlation corresponds to the specific shape of a molecule in free solution. For determination of molecular conformations it is important to find the best way in which electrophoretic mobility in free solution is related to molecular size. Usually at the low-molecular-mass range the short oligopeptides, such as di- and tripeptide fragments of IOPs studied in this paper, have no secondary structure and behave as simple organic ions. Peptides with more amino acids in their molecules form more organized secondary structures, which are strongly dependent on the medium [34]. α-Helical or β-sheet conformation features are preferable to random coil structures under CZE experimental conditions. At the high-molecular-mass range as long-chain polymers, polypeptides may form different types of ordered structures [11]. The structure is dependent on solvent, ionic strength, and pH of the BGE [22, 25]. The structure of synthetic peptides has been studied by CZE with MS detection [23]. The peptide structures help to predict shapes of proteins in free solution [24] and also in peptide mapping of proteins [10]. The data on secondary peptide structures derived from the relation between electrophoretic mobility and charge-to-size ratio are advantageously utilized in the structure-activity studies of biologically active peptides.

2 Materials and methods

2.1 Chemicals

All chemicals used were of analytical reagent grade. Iminodiacetic acid (IDAA) was obtained from Sigma (St. Louis, MO, USA), Tris was purchased from Serva (Heidelberg, Germany), phosphoric acid and dimethyl sulfoxide (DMSO) were supplied by Lachema (Brno, Czech Republic), and Tricine was from Merck (Darmstadt, Germany).

2.2 Peptide synthesis

All samples were synthesized in the group of Dr. Hlaváček in our institute by a procedure described in [28, 29]. Linear di-, tri-, and tetrapeptides were prepared by stepwise synthesis in solution [35]. Larger peptides were prepared by solid-phase approach using a polymer with a 2-chlorotritylchloride linker [28]. 9-Fluorenylmethoxycarbonyl/tertiary-butyl (Fmoc/*t*Bu) protection of amino acids was utilized. The synthesized peptides were purified by preparative HPLC and characterized by amino acid analysis, mass spectrophotometry, and analytical HPLC. The synthesis of cyclic peptides was carried out by a cyclization of their linear, *t*Bu side-chain protected, tetra- and pentapeptide precursors followed by side-chain deprotection [29].

2.3 Instrumentation

All experiments were carried out on a capillary electrophoretic analyzer P/ACE MDQ System (Beckman-Coulter, Fullerton, CA, USA). Data were recorded on a personal computer with software supplied by Beckman. The analyses were performed in an uncoated fused-silica capillary 402 mm long with 75 μm ID, 360 μm OD, with outer polyimide coating (Polymicro Technologies, Phoenix, AZ, USA), the detection window was located 300 mm from the injection end. The new capillary was flushed with water, 0.1 M NaOH, again water followed by the BGE, each for 5 min, and then the capillary was conditioned by a 20 min application of high voltage to equilibrate the inner surface and to stabilize the electroosmotic flow. Between runs at the same pH, the capillary was rinsed with BGE for 2 min. Prior to any change of the BGE, the capillary was rinsed with 0.1 M NaOH for 5 min and then repeatedly stabilized by the above-described procedure. The samples were injected with pressure (5–10 mbar for 5–15 s). The samples were dissolved in deionized water, their concentrations ranging from 0.05–0.5 mg·mL^{-1}. The BGEs were filtered through a 0.45 μm syringe filter (Millipore, Bedford, MA, USA) before use. The analytes were detected by a spectrophotometric photodiode array detector (190–600 nm) at constant wavelength (206 nm). The separation voltage was 10 kV, with the anode at the inlet side of the capillary. The temperature of the coolant continuously circulating around the capillary was set to 25°C.

3 Results and discussion

3.1 Determination of peptide charge

Effective charges of IOPs were calculated in all BGEs on the basis of Eq. (2) and utilizing the computer program Nabamfo [36] earlier developed to calculate the pH dependence of the effective and specific charges of peptides. The analyzed IOPs contain the following ionogenic groups – all of them, except of cyclic ones, possess an α-NH_3^+ group of the *N*-terminal of the peptide chain and an α-COOH group of the *C*-terminal of the peptide chain, most of the peptides contain the hydroxy group of tyrosine and the β-COOH group of aspartic acid. The average values of pK_a of amino acid residues in peptides [2] were used: *C*-terminal of peptide chain 2.6, hydroxy group of tyrosine 10.0, *N*-terminal of peptide chain 8.0, β-carboxy group of aspartic acid 4.0. The pH dependence of the specific charge (effective charge divided by relative molecular mass) of seven linear IOPs with decreasing number of proline residues at the *C*-terminus, $YDPAP_x$, where $x = 6 - 0$, is depicted in Fig. 1. The calculated pH dependence of the effective or specific charge is important for finding a pH region of BGE suitable for the separation of the given analytes. The experimental conditions, particularly composition and pH of BGE, used for IOPs separation were selected on the basis of this dependence. They are presented together with other parameters, voltage, currents, and electroosmotic mobilities, in Table 1.

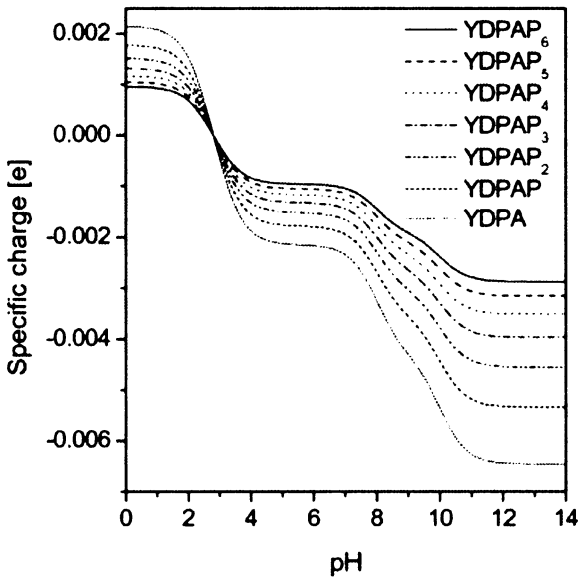

Figure 1. pH dependence of the specific charge (effective charge divided by relative molecular mass) of seven selected IOPs with decreasing number of proline residues at the *C*-terminus of the peptide chain.

The calculated values of effective charge at four different pH of the BGEs used and relative molecular mass of the whole set of 20 analyzed IOPs are given in Table 2. In acidic BGEs the linear IOPs had positive charges in the

Table 1. CZE conditions

BGE No.	BGE constituents	pH	$I^{a)}$ (μA)	$\mu_{eo}{}^{b)}$ ($10^{-9}m^2V^{-1}s^{-1}$)
I	50 mM Tris, 100 mM H_3PO_4	2.25	69–70	4.98 (0.13)[c]
II	100 mM iminodiacetic acid	2.30	38.5	7.90 (0.09)[c]
III	50 mM iminodiacetic acid	2.40	28.5	11.92 (0.08)[c]
IV	40 mM Tris, 40 mM Tricine	8.1	13–14	57.91 (0.81)[c]

a) Constant voltage, 10 kV
b) Average value from 20 experiments
c) Value in parentheses is the standard deviation.

Table 2. Relative molecular mass and calculated effective charge of 20 IOPs in four different BGEs

Peptide sequence[a]	M_r	Effective charge (e)			
		BGE I	BGE II	BGE III	BGE IV
$YDPAP_6$	1044.1	0.778	0.737	0.686	−1.594
$YDPAP_5$	950.0	0.778	0.737	0.686	−1.594
$YDPAP_4$	852.9	0.778	0.737	0.686	−1.594
$YDPAP_3$	755.8	0.778	0.737	0.686	−1.594
$YDPAP_2$	658.7	0.778	0.737	0.686	−1.594
YDPAP	561.6	0.778	0.737	0.686	−1.594
YDPA	464.47	0.778	0.737	0.686	−1.594
YDP	393.4	0.778	0.737	0.686	−1.594
YD	296.3	0.778	0.737	0.686	−1.594
$c(YDPAP)_2$	1087.2	−0.019	−0.023	−0.029	−2.000
c(YDPAP)	543.6	−0.014	−0.019	−0.029	−1.000
c(YDPA)	446.5	−0.014	−0.019	−0.029	−1.000
$YDPAP_5\Delta P$	1044.5	0.778	0.737	0.686	−1.594
YDPAΔP	559.6	0.778	0.737	0.686	−1.594
YDΔPA	462.5	0.778	0.737	0.686	−1.594
YDΔP	391.4	0.778	0.737	0.686	−1.594
DPAP	399.0	0.778	0.737	0.686	−1.594
DPA	301.3	0.778	0.737	0.686	−1.594
DΔPA	299.3	0.778	0.737	0.686	−1.594
HtyDPA	476.6	0.778	0.737	0.686	−1.594

a) Peptide sequences are given in single letter code: Y, tyrosine; D, aspartic acid; P, proline; A, alanine; c, with peptide sequence in parentheses indicates cyclic peptide, ΔP, dehydroproline; Hty, homotyrosine

range of 0.686 to 0.778 of elementary charge and in alkaline BGE they had a negative charge (−1.594 e). The pK_a values of ionogenic groups presented in all linear IOPs were considered to be identical, consequently, the effective charges of all linear IOPs were also identical at given pH of the appropriate BGE. The cyclic derivatives behaved differently in comparison with linear IOPs, in acid BGEs their charge was close to zero, in alkaline BGE their charge was −2.000 or −1.000 e.

3.2 Qualitative analysis of IOPs and determination of purity degree

As follows from the course of pH dependence of specific charge (see Fig. 1), either a strong acid region, pH < 2.5, or alkaline pH region, pH > 8, are suitable for separation of the set of linear IOPs. Consequently, three acidic BGEs (pH 2.25, 2.30, 2.40) and an alkaline BGE (pH 8.1) were tested for peptide analysis. The cyclic analogs were analyzed only in alkaline BGE, in acidic BGE they migrated with an electroosmotic marker as neutral components. The best separation of linear IOPs was achieved in BGE I, composed of 100 mM H_3PO_4, 50 mM Tris, pH 2.25.

Other BGEs were also applicable for analyses, the obtained peaks of analytes were symmetrical but the resolution was lower.

For full characterization of peptide preparations, especially pharmaceuticals and peptides used in biological tests, it is important to know the content of admixtures, originating from peptide synthesis and purification procedures. The purity degrees of IOPs were determined as the ratio of the corrected peak area of the peptide itself to the sum of corrected areas of all peaks presented in electropherograms; the correction is done with respect to migration velocity of the given peak. The analyzed peptides were mostly well purified by HPLC, the values of purity degrees reached 95–99%. The minor impurities of longer IOPs were sometimes identified as their shorter fragments. The CZE analysis of a highly pure tripeptide, DPA, with a purity degree 98.7% is depicted in Fig. 2A. CZE analysis of a decapeptide, $YDPAP_6$, (see Fig. 2B) demonstrates an example of a peptide with four admixtures, which were identified as shorter fragments of this decapeptide by their effective mobilities and by addition of the standards of these shorter peptides to the decapeptide sample. The purity degree in this case was only 86.7%.

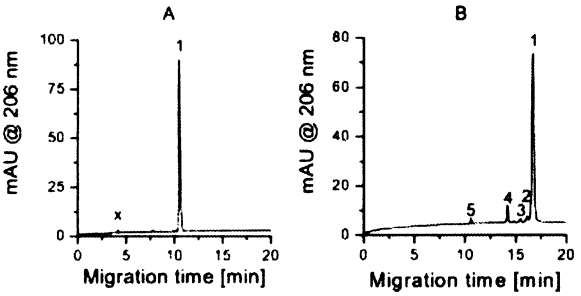

Figure 2. CZE analyses of IOPs. (A) Tripeptide DPA, (B) Decapeptide $YDPAP_6$. Experiments were carried out in BGE I, 100 mM H_3PO_4, 50 mM Tris, pH 2.25, at constant voltage U = 10 kV; fused-silica capillary, total/effective length 402/300 mm, ID 75 μm, OD 360 μm; UV-absorption detection at 206 nm. Peak 1, main synthetic product DPA (A) and $YDPAP_6$ (B); x, nonidentified admixture; 2–5, identified admixtures (2 = $YDPAP_5$, 3 = $YDPAP_4$, 4 = $YDPAP_2$, 5 = YD).

3.3 Separation of peptide mixtures and determination of peptide mobilities

In addition to qualitative analysis of individual synthetic peptide preparations, the separation of closely related structures of several IOPs was tested. CZE separations of mixtures of IOPs differing in the number of amino acid residues in linear or cyclic chain or in small changes of amino acid composition, *e.g.*, peptides with dehydropro-

line instead of proline, or peptides with homotyrosine instead of tyrosine, were performed in the same four BGEs, as those used for CZE analysis of individual IOPs. The electropherograms of the separation of peptides with decreasing number of proline residues at the *C*-terminus sequences $YDPAP_x$, $x = 6 - 0$, and di- and tripeptide, YD, YDP, in four different BGEs are depicted in Fig. 3. The best resolution was obtained in BGE I (pH 2.25, 100 mM H_3PO_4, 50 mM Tris; Fig. 3A). In isoelectric buffer, BGE II (100 mM IDAA, pH 2.30), the electroosmotic flow was faster and the peaks were closer to each other and have not been baseline-separated (Fig. 3B). In BGE III (50 mM IDAA, pH 2.40) peptides YD (1) and YDP (2) comigrated (Fig. 3C). And finally, in alkaline BGE IV (see Fig. 3D) the slower IOP were not baseline-separated and faster IOPs had a triangular peak shape because of electromigration dispersion.

Separation of some other closely related peptides from the set of 20 IOPs was achieved at least in some of the above BGEs. The tetrapeptide, YDPA, and its analog with homotyrosine at the *N*-terminus, HtyDPA, were well separated in alkaline BGEs, the resolution was 1.92. Furthermore, the resolution was in the range of 1.01–1.51 in acid BGEs and the samples were not baseline-separated in BGE II and BGE III. The analogs with a longer peptide chain, decapeptides, $YDPAP_6$ and $YDPAP_5\Delta P$, and pentapeptides, YDPAP and YDPAΔP, were completely baseline-separated in all acid BGEs. On the other hand, shorter analogs, tetrapeptides, YDPA and YDΔPA, and tripeptides, YDP and YDΔP, were separated only partly or comigrated. No derivatives with dehydroproline were separated from their analogs with proline in alkaline BGE. The cyclic IOPs were separated in alkaline BGE.

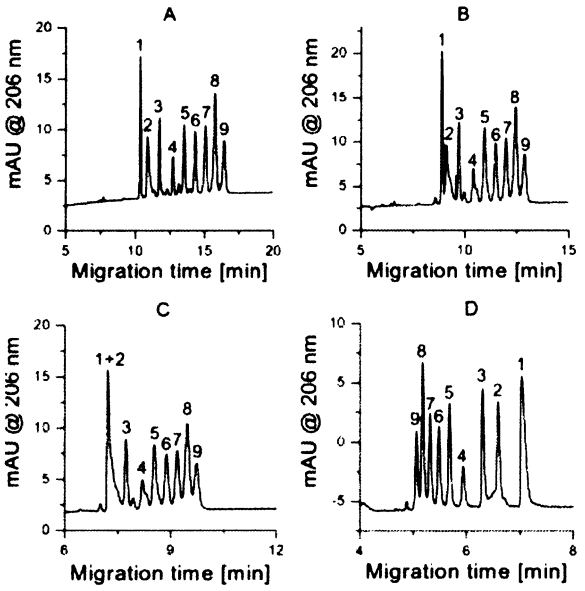

Figure 3. Electropherograms of nine IOPs in (A) BGE I, pH 2.25, (B) BGE II, pH 2.30, (C) BGE III, pH 2.40, and (D) BGE IV, pH 8.1. Other conditions as in Fig. 2. Peak 1, YD; 2, YDP; 3, YDPA; 4, YDPAP; 5, $YDPAP_2$; 6, $YDPAP_3$; 7, $YDPAP_4$; 8, $YDPAP_5$; 9, $YDPAP_6$.

From CZE analyses of IOPs their effective electrophoretic mobilities were determined. The effective electrophoretic mobility, μ_{ep}, of peptides in BGE was calculated from the migration time of the peptide, t_{mig}, and the migration time of the neutral electroosmotic marker, t_{eo}, according to Eq. (12) with upper signs of the terms in parenthesis for cations and with lower signs of these terms for anions (due to logarithmic plots of mobility, the mobilities of both cations and anions were considered as positive values):

$$\mu_{ep} = \frac{l_c l_d}{U}\left(\pm\frac{1}{t_{mig}} \mp \frac{1}{t_{eo}}\right) \quad (12)$$

where l_c is total capillary length, l_d is the effective capillary length, and U is the applied voltage. The values of effective electrophoretic mobility were determined as averages of two subsequent measurements, which differed by less than 1%. DMSO was used as electroosmotic flow marker.

The real temperature inside the capillary was higher than the temperature of the coolant due to Joule heating. The real temperature in the capillary for each BGE was obtained from the dependence of temperature increase in fused-silica capillary on the input power per unit length of the capillary (see Fig. 4), which was determined by the measurement of the specific electric conductivity of the standard solution of 0.01 mol·dm^{-3} KCl in the capillary at different values of input power as described in [37]. The temperature increase in the fused-silica capillary was 4.5°C for BGE I, 2.1°C for BGE II, 1.5°C for BGE III,

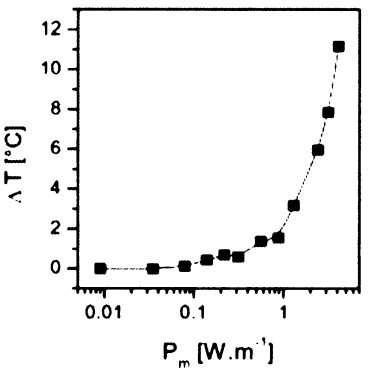

Figure 4. Dependence of temperature increase, ΔT, inside the fused-silica capillary (ID/OD 75/360 µm, effective/total length 30/40.2 cm, thermostated at outer surface to 25°C) on the input power, per unit length of the capillary, P_m.

and 0.7°C for BGE IV. The effective electrophoretic mobility corrected to standard temperature (25°C), μ_{ep25}, was calculated according to the equation:

$$\mu_{ep,25} = \mu_t [1 - 0.022 (t - 25)] \quad (13)$$

where $\mu_{ep,25}$ is the effective electrophoretic mobility at 25°C and μ_t is the effective electrophoretic mobility measured at real temperature t inside the capillary.

The values of effective electrophoretic mobilities of IOPs in different BGEs corrected to standard temperature, 25°C, are presented in Table 3. The effective electrophoretic mobilities measured at real temperature inside the capillary differed by up to 10% in the most conductive BGE (BGE I) in comparison with standard effective electrophoretic mobilities, at 25°C. The increasing values of effective mobilities of IOPs from BGE I (pH 2.25) to BGE III (pH 2.40) in spite of increasing pH of these BGEs in the same order can be explained by the fact that the increase of pH is rather small (0.05 – 0.15 pH unit) and the mobilities are not corrected to the same ionic strength. A significantly higher ionic strength of the BGE I than that of BGEs II and III is the cause of the lower effective mobilities in BGE I than in BGEs II and III, respectively. In addition, the different capabilities of the BGE counterions, phosphate in BGE I and iminodiacetate in BGEs II and III, to form ionic pairs with cationic peptides may also contribute to the different effective mobilities of peptides. The difference of effective mobilities of IOPs in BGE II and III is smaller than that in BGE I and II and it can be explained by the lower ionic strength of BGE III than BGE II.

Table 3. Effective electrophoretic mobilities, μ_{ep}, corrected to standard temperature, 25°C, of 20 analyzed IOPs in four BGEs

Peptide sequence[a)]	μ_{ep} (10^{-9} $m^2V^{-1}s^{-1}$)			
	BGE I	BGE II	BGE III	BGE IV
$YDPAP_6$	6.66	7.83	8.44	14.19
$YDPAP_5$	7.16	8.34	9.00	15.07
$YDPAP_4$	7.73	8.94	9.63	16.07
$YDPAP_3$	8.31	9.64	10.37	17.19
$YDPAP_2$	9.13	10.46	11.24	18.45
YDPAP	9.95	11.36	12.17	19.97
YDPA	11.26	12.70	13.62	21.88
YDP	12.33	14.01	15.10	23.28
YD	13.38	14.52	15.40	25.18
$c(YDPAP)_2$	0	0	0	18.50
c(YDPAP)	0	0	0	14.01
c(YDPA)	0	0	0	15.21
$YDPAP_5\Delta P$	6.18	7.40	7.80	14.43
YDPAΔP	9.34	10.55	11.05	20.17
YDΔPA	11.38	13.00	13.83	22.18
YDΔP	11.79	13.89	14.84	23.82
DPAP	10.95	12.19	12.70	20.76
DPA	12.98	14.17	14.82	23.83
DΔPA	12.86	14.17	14.82	25.71
HtyDPA	10.89	12.38	13.11	20.15

a) See comment in Table 2.

3.4 Testing semiempirical models

Several various models of the correlations between the effective electrophoretic mobility of peptides and their effective charge and size parameters were suggested (see Section 1.2.3) but none of them was found to be generally applicable to the unambiguous description of migration behavior of different peptide sets and for prediction of peptide structure. In the current work, we have tested and compared seven semiempirical models of the correlation between effective electrophoretic mobility of IOPs and their charge/size ratio: the rigid spherical model, Eq. (4) [8], the classical linear polymer model, Eq. (5) [33], Offord's model, Eq. (3) [12], Grossman's model, Eq. (9) [17], Cifuentes's and Poppe's model, Eq. (10) [18], Kim's model, Eq. (7) [20], and Cross's model, Eq. (6) [16]. The set of 20 IOPs was tested in the range of relative molecular masses from 299.3 to 1087.2 and sizes from 2 to 10 amino acid residues. The graphs of the correlations of the above semiempirical models applied to all 20 IOPs are depicted in Fig. 5. As expected, none of the models gave the full agreement between theory and experimental data for the whole set of IOPs. The values of the slope and correlation coefficient of the linear plot log (μ_{ep}/q) *versus* log M_r (Fig. 5A) suggested us the most suitable semiempirical model for each electrolyte; parameters of this linear regression are given in Table 4. The rigid spherical model (Fig. 5B) fitted best in acidic BGE II (curve 2) with R = 0.972 and BGE III (curve 3) with R = 0.958. However, the classical linear polymer model (R = 0.972) was found best in alkaline BGE IV (Fig. 5C, curve 4), alternatively the Offord's model (Fig. 5D, curve 1), where R = 0.963, the classical polymer model with R = 0.981 (Fig. 5C, curve 1) suited to acidic BGE I. On the other hand, Grossman's model (Fig. 5E) with R = 0.888 – 0.936, Cifuentes's and Poppe's model (Fig. 5F) with R = 0.911 – 0.965 as well as Kim's model (Fig. 5G) with R = 0.933 – 0.965 were found less suitable for our set of IOPs. As follows from the data presented in Fig. 5, none of the models was able to describe the correlation between mobility and charge-to-size ratio with high precision for the whole set of IOPs. Therefore, the peptides were divided in smaller groups with more related structures.

The number of peptides in the set was reduced and just nine analogs with decreasing number of proline residues at *C*-terminal sequences, from decapeptide, $YDPAP_6$, to

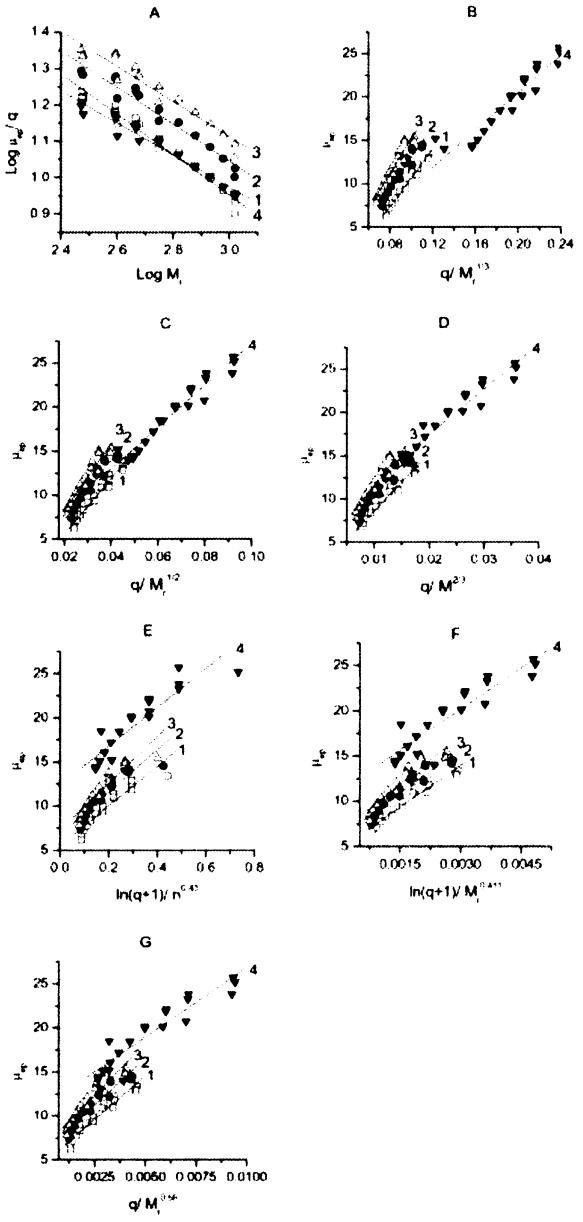

Figure 5. Semiempirical models of the correlation between effective mobility, μ_{ep}, and peptide charge, q, and size (expressed by relative molecular mass, M_r, or by number of amino acid residues in peptide chain, n) applied to all IOPs and their fragments in four different BGEs (1, BGE I 50 mM Tris, 100 mM H_3PO_4, pH 2.25; 2, BGE II, 100 mM iminodiacetic acid, pH 2.30; 3, BGE III, 50 mM iminodiacetic acid, pH 2.40; 4, BGE IV, 40 mM Tris, 40 mM Tricine, pH 8.1). (A) Cross's model, Eq. (6), (B) rigid spherical model, Eq. (4), (C) classical linear polymer model, Eq. (5), (D) Offord's model, Eq. (3), (E) Grossman's model, Eq. (9), (F) Cifuentes's and Poppe's model, Eq. (10), (G) Kim's model, Eq. (7). The mobilities were taken from Table 3, effective charges and relative molecular masses from Table 2. Other conditions as in Fig. 2.

Table 4. Parameters of linear regression log μ_{ep}/q *versus* log M_r for the whole set of twenty analyzed IOPs and for the subset of seven linear IOPs with decreasing number of proline residues at the *C*-terminus, $YDPAP_x$ (x = 6 – 0), in four different BGEs

BGE No.	Set of 20 IOPs			Subset of linear IOPs, $YDPAP_x$ (x = 6 – 0)		
	k	*b*	*R*	*k*	*b*	*R*
I	−0.5567	2.6217	0.9821	−0.6376	2.8626	0.9992
II	−0.5062	2.5641	0.9738	−0.5935	2.8213	0.9993
III	−0.4813	2.5568	0.9546	−0.5831	2.8547	0.9993
IV	−0.4410	2.2970	0.9792	−0.5309	2.5573	0.9988

k, slope of curve; b, intercept; *R*, coefficient of correlation

dipeptide, YD, were selected. Better values of correlation coefficients were obtained but from the regression analysis it was evident, that di- and tripeptide did not fit well in this linear part of the graphs. Due to nonlinearity of the correlations between effective mobility and charge-to-size ratio of these two short peptides and with respect to their low potential to form more organized secondary structures, the set of IOPs was further reduced to the series of seven peptides with linearly decreasing number of proline residues at the *C*-terminal of the peptide chain, from decapeptide, $YDPAP_6$, to tetrapeptide, YDPA, with constant decrement of the relative molecular mass, 97.1. The graphs of semiempirical models of correlations of electrophoretic mobility and effective charge and size parameters applied to this series of seven linear IOPs are depicted in Fig. 6. As evident from the plots, the correlation has improved significantly – the experimental data fitted well in the linear parts of the graphs, indicating similar migration behavior and structure of this homologous series of IOP.

3.5 Predicted probable structure of peptides

Fitting the experimental data into the graphs of different semiempirical models helped us to solve the question with the secondary structure of IOPs. As expected, the group of peptides in the whole range of relative molecular mass and with different number of amino acid residues tested, *i.e.*, from dipeptides to decapeptides, did not exhibit the same structure. From the series of the homologous nine IOPs with decreasing number of proline residues at the *C*-terminus, $YDPAP_6$ – YD, the smallest two peptides, YD and YDP, behaved differently, and did not fit to the linear part of regression plot of any model.

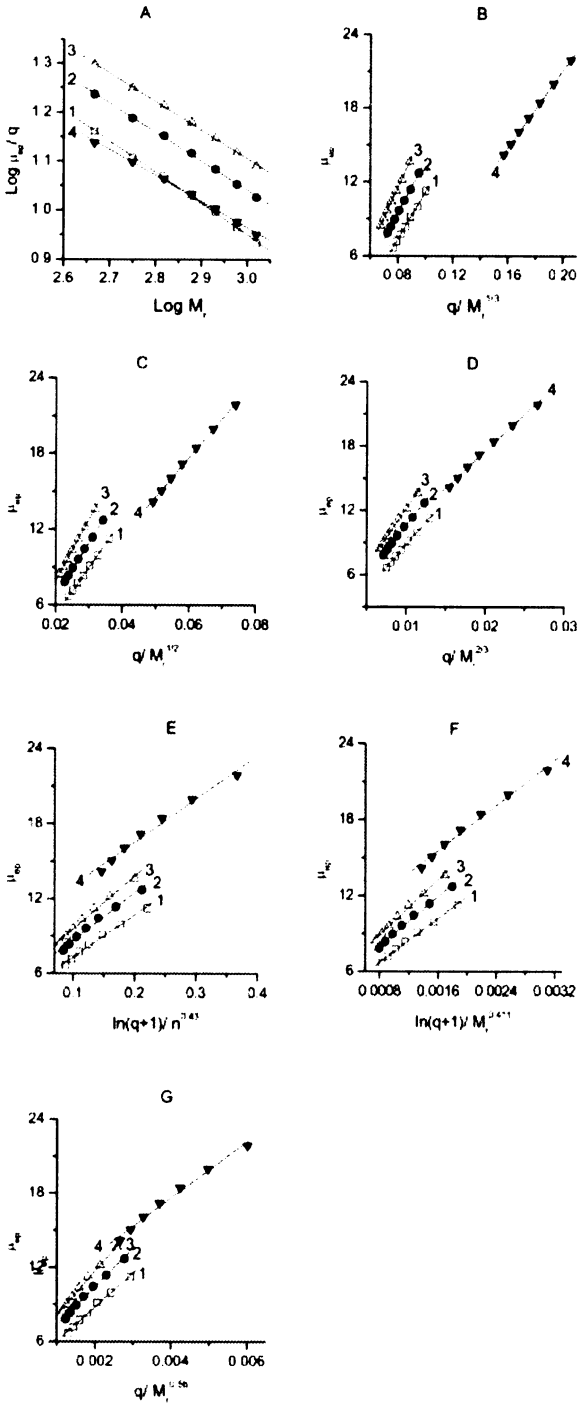

Figure 6. Semiempirical models of the correlation between effective mobility, μ_{ep}, and peptide charge, q, and size (expressed by relative molecular mass, M_r, or by number of amino acid residues in peptide chain, n) applied to seven IOPs with decreasing number of proline residues at the C-terminus, $YDPAP_6$–YDPA, in four different BGEs. BGEs, models, and other conditions as in Fig. 5.

Cross's plot seems to be the most suitable for predicting the peptide structure, because it directly provides the value of exponent k in the μ_{ep} *versus* q/M_r^k plot as the slope of the line expressed by Eq. (6). Parameters of linear regression (slope of curve, intercept, coefficient of correlation) of the Cross's plot, log (μ_{ep}/q) *versus* log M_r, for the whole set of 20 IOP and for the subset of seven linear IOPs are presented in Table 4. As follows from the data presented in this table for the subset of seven linear IOPs, where also high values of correlation coefficients were obtained, the exponent k of the above dependence in alkaline BGE was close to 1/2, *i.e.*, migration of this set of peptides can be best described by the classical linear polymer model. Consequently, the most probable structure of these peptides in alkaline solution is random coil. In acid BGE I the exponent k was close to 2/3, which means that the migration of these peptides fits best to Offord's model and their molecules have the shape of wide thin discs [8]. In the two isoelectric buffers, BGE II and BGE III, differing only in ionic strength, the exponents k were almost identical, with the values ranging from 0.5–0.6, which indicate the shape of random coils. The difference of exponent k for BGE I (k = 0.64) and for BGE II (k = 0.58) may reflect some differences in the peptide structure caused rather by the change of the ionic strength and quality of the peptide counterions (iminodiacetates instead of phosphates) than by the relatively very small change of pH. However, with respect to small differences in correlation coefficients of different models of correlation between electrophoretic mobility and charge and size presented in Fig. 6, the predicted structures should be considered as the most probable but not determined quite unambiguously.

4 Concluding remarks

CZE proved to be a suitable technique for analysis and physicochemical characterization of IOPs. From the CZE analyses not only the purity degree of synthetic IOPs could be obtained but also their effective electrophoretic mobilities. The probable secondary structure of IOPs in solutions of different composition could be predicted as the result of testing various models of the correlations between electrophoretic mobility of peptides and their effective charge and size.

This work was supported by the Grant Agency of the Czech Republic, grants No. 203/02/1467, 203/03/0716, and by the Czech Academy of Sciences, research project AV0Z 4055905. We thank to Mrs. V. Lišková for her skilful technical assistance and Dr. P. Sázelová and Dr. Z. Prusík for their cooperation and assistance in the presented results.

Received January 5, 2004

5 References

[1] Deyl, Z., Mikšík, I., in: Deyl, Z. (Ed.), *Advanced Chromatographic and Electromigration Methods in BioSciences*, Elsevier, Amsterdam 1998, pp. 465–523.

[2] Kašička, V., in: Aboul-Enein, H. Y. (Ed.), *Analytical and Preparative Separation Methods of Biomacromolecules*, Marcel Dekker, New York 1999, pp. 39–97.

[3] Kašička, V., *Electrophoresis* 2001, *22*, 4139–4162.

[4] Righetti, P. G., *Biopharm. Drug Dispos.* 2001, *22*, 337–351.

[5] Issaq, H. J., Conrads, T. P., Janini, G. M., Veenstra, T. D., *Electrophoresis* 2002, *23*, 3048–3061.

[6] Hearn, M. T. W., *Biologicals* 2001, *29*, 159–178.

[7] Issaq, H. J., *J. Liq. Chromatogr. Relat. Technol.* 2002, *25*, 1153–1170.

[8] Grossman, P. D., in: Grossman, P. D., Colburn, J. C. (Eds.), *Capillary Electrophoresis: Theory and Practice*, Academic Press, San Diego, CA 1992, pp. 111–132.

[9] Adamson, N. J., Reynolds, E. C., *J. Chromatogr. B* 1997, *699*, 133–147.

[10] Janini, G. M., Metral, C. J., Issaq, H. J., Muschik, G. M., *J. Chromatogr. A* 1999, *848*, 417–433.

[11] Cifuentes, A., Poppe, H., *Electrophoresis* 1997, *18*, 2362–2376.

[12] Offord, R. E., *Nature* 1966, *211*, 591–593.

[13] Issaq, H. J., Janini, G. M., Atamna, I. Z., Muschik, G. M., Lukszo, J., *J. Liq. Chromatogr.* 1992, *15*, 1129–1142.

[14] Rickard, E. C., Strohl, M. M., Nielsen, R. G., *Anal. Biochem.* 1991, *197*, 197–207.

[15] Basak, S. K., Ladisch, M. R., *Anal. Biochem.* 1995, *226*, 51–58.

[16] Cross, R. F., Garnham, N. F., *Chromatographia* 2001, *54*, 639–646.

[17] Grossman, P. D., Colburn, J. C., Lauer, H. H., *Anal. Biochem.* 1989, *179*, 28–33.

[18] Cifuentes, A., Poppe, H., *J. Chromatogr. A* 1994, *680*, 321–340.

[19] Sanz-Nebot, V., Benavente, F., Barbosa, J., *J. Chromatogr. A* 2002, *950*, 99–111.

[20] Kim, J., Zand, R., Lubman, D. M., *Electrophoresis* 2003, *24*, 782–793.

[21] Compton, B. J., *J. Chromatogr.* 1991, *559*, 357–366.

[22] Hearn, M. T. W., Keah, H. H., Boysen, R. I., Messana, I., Misiti, F., Rossetti, D. V., Giardina, B., Castagnola, M., *Anal. Chem.* 2000, *72*, 1964–1972.

[23] Sitaram, B. R., Keah, H. H., Hearn, M. T. W., *J. Chromatogr. A* 1999, *857*, 263–273.

[24] Micinski, S., Gronvald, M., Compton, B. J., in: Karger, B. L., Hancock, W. S. (Eds.), *High Resolution Separation and Analysis of Biological Macromolecules,*, Academic Press, San Diego, CA 1996, pp. 342–358.

[25] Verzola, B., Perduca, M., Mezo, G., Hudecz, F., Righetti, P. G., *Electrophoresis* 2003, *24*, 794–800.

[26] Borovsky, D., Mahmoot, T., Carlson, D. A., *J. Fla. Anti-Mosqv. Assoc.* 1989, *60*, 66–70.

[27] Borovsky, D., Carlson, D. A., Griffin, P. R., Shabanowitz, J., Hunt, D. F., *Insect Biochem. Mol. Biol.* 1993, *23*, 703–712.

[28] Hlaváček, J., Tykva, R., Bennettová, B., Barth, T., *Bioorg. Chem.* 1998, *26*, 131–140.

[29] Hlaváček, J., Buděšínský, M., Bennettová, B., Mařík, J., Tykva, R., *Bioorg. Chem.* 2001, *29*, 282–292.

[30] Maloň, P., Dlouhá, H., Bennettová, B., Tykva, R., Hlaváček, J., *Collect. Czech. Chem. Commun.* 2003, *68*, 1309–1318.

[31] Sillero, A., Ribeiro, J. M., *Anal. Biochem.* 1989, *179*, 319–325.

[32] Hilser, V. J., Worosila, G. D., Rudnick, S. E., *J. Chromatogr.* 1993, *630*, 329–336.

[33] Tanford, C., *Physical Chemistry of Macromolecules*, Wiley, New York 1961, pp. 390–392.

[34] Gaus, H. J., Becksickinger, A. G., Bayer, E., *Anal. Chem.* 1993, *65*, 1399–1405.

[35] Hlaváček, J., Bennettová, B., Barth, T., Tykva, R., *J. Pept. Res.* 1997, *50*, 153–158.

[36] Kašička, V., Prusík, Z., *J. Chromatogr.* 1989, *470*, 209–221.

[37] Koval, D., Kaššička, V., Jiráček, J., Collinsová, M., Garrow, T. A., *J. Chromatogr. B* 2002, *770*, 145–154.

IV

Separation and investigation of structure-mobility relationship of gonadotropin-releasing hormones by capillary zone electrophoresis in conventional and isoelectric acidic background electrolytes

Veronika Šolínová [a], Václav Kašička [a,*], Petra Sázelová [a], Tomislav Barth [a], Ivan Mikšík [b]

[a] Institute of Organic Chemistry and Biochemistry, Academy of Sciences of the Czech Republic, Flemingovo 2, 166 10 Prague 6, Czech Republic

[b] Institute of Physiology, Academy of Sciences of the Czech Republic, Vídeňská 1083, 142 20 Prague 4, Czech Republic

*Corresponding author

Dr. Václav Kašička

Institute of Organic Chemistry and Biochemistry

Academy of Sciences of the Czech Republic

Flemingovo 2

166 10 Prague 6

Czech Republic

Phone: +420-220-183-239

Fax: +420-220-183-592

e-mail: kasicka@uochb.cas.cz

Abstract

Capillary zone electrophoresis (CZE) has been applied to qualitative and quantitative analysis, separation and physicochemical characterization of synthetic gonadotropin-releasing hormones (GnRHs) and their analogs and fragments. Structurally related peptides were separated in conventional and isoelectric acidic background electrolytes (BGEs), pH 2.18-2.50. Best separation was achieved in isoelectric BGE composed of 200 mM iminodiacetic acid, pH 2.32. The effective electrophoretic mobilities, m_{ep}, of GnRHs in five BGEs were determined and several semiempirical models correlating effective mobility with charge, q, and relative molecular mass, M_r, (m_{ep} versus q/M_r^k) were tested to describe the migration behavior of GnRHs in CZE. None of the models was found to be definitively applicable for the set of ten GnRHs differing in size (tetrapeptide – decapeptide) and positive charge (0.91 – 3.00 elementary charges). However, high coefficient of correlation, 0.995-0.999, was found for the GnRHs, for the dependence of m_{ep} on q/M_r^k with k (related to molecular shape) close to 0.5 in all five acidic BGEs. From these dependences the probable structure of GnRHs in solution was predicted as random coil.

Keywords:

Capillary electrophoresis; GnRH; LHRH; Peptides; Effective electrophoretic mobility; Structure-mobility relationship

1. Introduction

Gonadotropin-releasing hormone (GnRH) is present in different biological species such as human, pig, lamb, chicken, sea bream and salmon with small modifications in its peptide sequence. Human GnRH, hGnRH, alternatively termed luteinizing hormone-releasing hormone (LHRH), is physiologically important decapeptide (pGlu-His-Trp-Ser-Tyr-Gly-Leu-Arg-Pro-Gly-NH_2), which is synthesized in neurosecretory cells within the hypothalamus and regulates reproductive functions and maintenance of secondary sex characteristics in males and females. LHRH agonists are used for the treatment of hormone-dependent breast and prostate cancers [1]. In reproductive medicine, they serve to prevent a premature LH surge prior to stimulation of ovulation. Synthetic hGnRH is produced under the name gonadorelin. Several commercially available analogs are used as drugs. Buserelin, [Des-Gly^{10},D-Ser(tBu)^6,Pro-NHEt^9]hGnRH, and triptorelin, [D-Trp^6]hGnRH, are used in treatment of prostate cancer, deslorelin, [Des-Gly^{10},D-Trp^6,Pro-NHEt^9]hGnRH, for treatment of true precocious puberty, goserelin, [D-Ser(tBu)^6,Azagly^{10}]hGnRH for treatment of advanced breast cancer and nafarelin, [D-2-Nal^6]hGnRH, in treatment of endometriosis.

Synthetic GnRHs and their analogs and fragments are frequently used as model analytes, usually in mixtures with other peptides, to demonstrate new methodology and/or instrumentation developments and optimization of separation conditions for analysis and separation of peptides by capillary electromigration methods [2]. Successful combination of capillary electrophoresis (CE) with mass spectrometry (MS) detection without make-up flow or nebulizing gas was demonstrated by analysis of gonadorelin with sensitivity on the level of immunoassay [3]. Home-made on-line preconcentration CE was optimized for the purity control of synthetic biologically active peptides including GnRH in BGE composed of 25 mM K_2HPO_4, pH 3.5 [4]. Membrane preconcentration CE-MS/MS was appropriately constructed for sequencing biologically active peptides at the sub-100 femtomole level [5]. The analysis of nine model peptides was performed in 2 mM ammonium acetate and 1 % v/v acetic acid. Successful application of fused silica (FS) capillary modified by positively charged alkylaminosilyl monomer to capillary zone electrophoresis (CZE) and capillary electrochromatographic (CEC) separations of the mixture of peptides and proteins was demonstrated using UV-absorption and MS detection [6]. Rapid separation of five peptides including GnRH was achieved in 5 mM acetic acid in 50% v/v MeCN. A new CE-nanoflow electrospray ionization (ESI) interface, where separation column, an electrical porous junction and spray tip were integrated on single FS capillary, was found as a suitable device for analysis and separation of nine peptides including GnRH and proteins in 1 M acetic acid, pH 2.4 [7]. Human GnRH and its four analogs, [D-Ala^6]GnRH, [D-Lys^6]GnRH, [D-Phe^2,D-Ala^6]GnRH and [Gly-OH^{10}]GnRH were analyzed in

capillary derivatized with 3-(aminopropyl)trimethoxysilane in 0.01 M acetic acid, pH 3.5, to demonstrate suitability of CE-ESI-MS using high performance magnetic sector MS for identification of toxins in snake venom [8]. For determination of side products of buserelin synthesis, CE with field-amplified sample injection was used [9]. Optimal separation conditions were found in acidic BGEs with pH less than 3.5. An off-line coupling of CE and MALDI-MS was successfully applied for the analysis of four standard peptides, proteins and real tear fluid in 50 mM ammonium acetate buffer, pH 7.4 [10]. According to the known or established characteristics, such as dissociation constants of ionogenic groups of therapeutic peptides optimal separation conditions were determined for set of seven peptides including buserelin and triptorelin for CE [11]. The conditions were tested in a wide pH range 2-12; the best separation was achieved at pH 2.85, in BGE composed of 50 mM acetic acid and 50 mM formic acid, pH adjusted by NH_4OH. The same set of peptides was successfully applied for separation and characterization in hydroorganic mixture of formic acid, acetic acid and 2-propanol by CE-ESI-MS with commercial [12] and home-made graphite coated sheath-flow interface [13] and as well for comparison of predicted and experimentally obtained resolution, electrophoretic mobility and retention factor in CE and HPLC [14]. Complete separation of gonadorelin and its five analogs was provided by RP-HPLC in mobile phase consisting of MeCN and phosphate buffer, pH 2.5, by CE in phosphate or borate buffer and as well by micellar electrokinetic chromatography (MEKC) with the same BGE with addition of CTAB (cetyltrimethylammonium bromide), CHAPS (3-[(3-choloamidopropyl)dimethylammonio]-1-propanesulfonate) and Triton X-100 as micellar constituents [15]. Alternative detection technique to UV-absorption, contactless conductivity detection was employed for the analysis of mixture of nine peptides including GnRH in phosphate buffer, pH 2.5 [16]. Detection limits at the μM level in combination with good resolution were shown. Native GnRHs are generally used to study biological regulatory processes such as kinetics and mechanism of their action. A rapid CE assay for measuring the stability of human and salmon GnRH in the presence of intestinal enzymes was developed and validated [17]. The analysis was performed in acetic acid-based BGE, pH 4.0, and applied to the stability of GnRH analogs in salmon intestinal digest. Determination of gonadorelin in plasma by on-capillary preconcentration CE system was demonstrated [18]. For suppressing adsorption on the wall, the capillary had cationic coating and for increasing sensitivity and selectivity MS detection was used. CE was also applied for determination of proteins during the investigation of influence of GnRH in human ovarian fluid and sera in pre-treatment for in vitro fertilization [19]. The aim of this work was to perform qualitative and quantitative analysis of synthetic preparations of human, salmon and chicken GnRH, and their analogs and fragments, by CZE in acidic conventional and isoelectric BGEs. Suitable experimental conditions should be developed

for CZE separation of the mixtures of these structurally related peptides. In addition to the purity degree also some physicochemical characteristics of the analyzed peptides, such as effective electrophoretic mobilities of GnRHs at standard temperature, 25°C, should be determined, and different models of the dependence of mobility of GnRHs on their charge and size should be tested in order to predict the probable structure of GnRHs in solution.

2. Theory

Models of correlations between peptide mobility and their charge and size

Several semiempirical models correlating effective electrophoretic mobilities of peptides, m_{ep}, with their effective charge, q, and molecular size expressed as relative molecular mass, M_r, or number of amino acids in polypeptide chain, n, respectively, have been developed. The models are based on Stokes law, describing the motion of a particle in liquid medium, and on the action of electric field force on charged molecule.

Offord [20] has firstly quantitatively described this relationship for the series of oligo- and polypeptides separated by paper electrophoresis:

$$m_{ep} = \frac{k_1.q}{M_r^{2/3}} \tag{1}$$

where k_1 is a constant of proportionality. This relationship was applied by some other authors, Issaq et al. [21], Rickard et al. [22], Basak and Ladisch [23], Tessier et al. [24] and Jalali-Heravi et al. [25] for peptides separated in free solution by CZE.

For rigid spherically shaped molecules in low ionic strength buffers the following relationship was gained by Grossman [26]:

$$m_{ep} = \frac{k_1.q}{M_r^{1/3}} \tag{2}$$

Another semiempirical model was suggested for the synthetic polymers with cylindrical or rod-shaped molecules [27]:

$$m_{ep} = \frac{k_1.q}{M_r^{1/2}} \tag{3}$$

Cross [28] adapted Offord's relation to logarithmic form:

$$\log(\frac{m_{ep}}{q}) = k.\log M_r \tag{4}$$

where k is the exponent of M_r in non-logarithmic relation, which can be determined as a slope of this dependence.

Another formula has been proposed by Kim [29] in which set of peptides originating from enzyme digests of proteins fitted well. The value of exponent was close to that used in semiempirical model for polymers:

$$m_{ep} = \frac{k_1.q}{M_r^{0.56}} \tag{5}$$

Compton [30] combined two relationships for small (2) and large (1) molecules and obtained the relation:

$$m_{ep} = \frac{k_1.q}{k_2.M_r^{1/3} + k_3.M_r^{2/3}} \tag{6}$$

where the first term in the denominator, $M_r^{1/3}$, represents smaller molecules, and the second term, $M_r^{2/3}$, larger molecules, both in low ionic strength buffers.

In all these cases relative molecular mass was used as size parameter. Other possibility is to express the molecular size by the number of amino acid residues in peptide chain, n. This approach was used by Grossman et al. [31], who derived the following relation for dependence of effective mobility on charge and size:

$$m_{ep} = \frac{k_2.\ln(q+1)}{n^{0.43}} \tag{7}$$

Cifuentes and Poppe [32] firstly published the modification of the Grossman's classical linear model, where logarithmic dependence of mobility on charge expressed electrostatic charge suppression in highly charged peptides:

$$m_{ep} = \frac{k_2.\log(1+k_1q)}{M_r^{0.411}} \tag{8}$$

The same equation, only with different exponent of M_r, 0.435 instead of 0.411, was derived by Adamson [33].

Sanz-Nebot [34] tested relationships (9) with q compensated for electrostatic charge suppression with highly charged peptides and the relationships of classical semiempirical models (1), (2) and (3), compared their results, and found better correlation for the formula:

$$m_{ep} = \frac{k_2.\ln(k_1q+1)}{M_r^k} \tag{9}$$

where k = 1/3 for small molecules, k = 1/2 for medium size polymers, k = 2/3 for large molecules, respectively.

These semiempirical models can be used for prediction of possible structure of the peptides and proteins in a free solution. The structure of the molecule is derived from the relationship between frictional coefficient or electrophoretic mobility, respectively, and the exponent of the relative molecular mass or alternatively exponent of the number of amino acid residues in peptide [26].

Each type of correlation corresponds to the specific shape of molecule in a free solution. For determination of molecular conformations it is very important to find the best way in which electrophoretic mobility in a free solution is related to molecular size. Peptides form more organized secondary structures, which are strongly dependent on the medium [35]. The structure is dependent on solvent, ionic strength and pH of BGE [36, 37]. At the high molecular mass range as long-chain polymers, polypeptides may form different types of ordered structures such as α-helical or β-sheet conformation [32, 38]. The peptide structures help to predict shapes of proteins in free solution [39] and also in peptide mapping of proteins [26]. The data on secondary peptide structures derived from relation between electrophoretic mobility and charge to size ratio, are advantageously utilized in the structure-activity studies of peptide hormones.

3. Experimental

3.1 Chemicals

All chemicals used were of analytical reagent grade. Iminodiacetic acid (IDAA) was obtained from Bachem (Bubendorf, Switzerland), phosphoric and acetic acids were obtained from Lachema (Brno, Czech Republic) and Tris (tris(hydroxymethyl)aminomethane) was supplied by Serva (Heidelberg, Germany). Isophorone (3,5,5-trimethyl-2-cyclohexen-1-one) was supplied by Fluka (Buchs, Switzerland).

3.2 Peptides

The list of analyzed peptides and their abbreviations, sequences and relative molecular masses, M_r, are presented in Table 1. The oligopeptide fragments of human GnRH, YGLRPG-NH_2, LRPG-NH_2, (pGlu)HWSTGLRPG-NH_2 and (pGlu)HWS, were purchased from Sigma (St. Louis, MO, USA). The other analogs and fragments of GnRHs were prepared by solid phase synthesis in the Institute of Organic Chemistry and Biochemistry.

3.3 Instrumentation

The capillary electrophoretic experiments were carried out in commercial P/ACE MDQ System (Beckman-Coulter, Fullerton, CA, USA), data acquisition and evaluation were performed using the software P/ACE System MDQ, version Karat supplied by Beckman.
The apparatus was equipped with the internally non-coated FS capillary with outer polyimide coating, total/effective length 39.0/28.8 cm, I.D./O.D. 50/375 μm (Polymicro Technologies, Phoenix, AR, USA). The analytes were detected by UV-Vis absorption spectrophotometric

photodiode array detector (190-600 nm) set at constant wavelength 206 nm. The temperature of capillary liquid coolant was set at 25°C.

The new capillary was gradually flushed with water, 1 M NaOH, water and BGE, each wash for 10 min. Finally, the capillary was conditioned by a 20 min application of the high voltage to equilibrate the inner surface with BGE and to stabilize electroosmotic flow. Between runs under the same conditions, the capillary was rinsed with the BGE for 2 minutes. Before a change of the BGE the capillary was rinsed with 0.1 M NaOH for 5 min and then repeatedly stabilized. The samples were injected with pressure 6.9-13.8 mbar for 5-15 s. The samples were dissolved in deionized water and their concentrations were in the range 0.6-1.3 mg/ml. The BGEs were filtered through a 0.45-μm syringe filter (Millipore, Bedford, MA, USA) before use. The list of composition and pH of BGEs, separation voltage and electric current are presented in Table 2.

4. Results and discussion

4.1 Selection of separation conditions and determination of peptide charge

The strategy for the rational selection of experimental conditions for CZE analysis and separations of GnRHs and their analogs and fragments followed the general rules of selection of suitable CZE separation conditions [40] and took into account the specific properties of these peptides resulting from their structure. The selection of the composition of the BGEs includes the type and concentration of buffer components and pH, and it also takes into account the requests for solubility and chemical stability of analyzed peptides [41, 42]. Effective charges of peptides are strongly dependent on pH and pK_a of ionogenic groups of amino acid residues present in peptide chain. The analyzed peptides, see Table 1, contain several types of ionogenic groups; all peptides, except fragments of hGnRH 4-10 and 7-10, possess imidazolyl group of the histidine (average pK_a 6.3), and all peptides, except fragments of hGnRH 1-4 and 7-10, contain phenol group of tyrosine (average pK_a 10.4), all hGnRHs except [Des-Arg-Pro-Gly-NH_2]hGnRH and fragment of hGnRH 1-4, possess guanidinyl group of arginine (average pK_a 11.3), three peptides (fragments of hGnRH 4-10 and 7-10 and [Des-pGlu^1-D-Orn^6]sGnRH) possess α–amino group of the N-terminus of the peptide chain (average pK_a 8.1), five peptides ([Des-Arg-Pro-Gly-NH_2]hGnRH, [Des-Pro-Gly-NH_2] hGnRH, fragment of hGnRH 1-4, [Des-Gly-NH_2]sGnRH and [Des-Gly-NH_2]cGnRH II) contain α–carboxyl group of the C-terminus of the peptide chain (average pK_a 3.5) and salmon fragment of its analog [Des-pGlu^1-D-Orn^6]sGnRH contains amino group of ornithine (average pK_a 9.9). The relative molecular mass of analyzed peptides was in the range 440.6 – 1262.5, see Table 1.

One of the most important parameters for selection of suitable experimental conditions for CZE analysis and separation of peptides is the pH dependence of their effective and specific charges, since the electrophoretic mobility of peptides is directly proportional to their effective charge. For that reason the dependence of effective charge and specific charge (effective charges divided by relative molecular mass) of all peptides to be analyzed has been calculated by the earlier developed computer program Nabamfo [43] using the above given average values of pK_a of ionogenic groups. From the course of the pH dependence of the specific charge of peptides to be analyzed and separated (see Fig. 1) it follows, that these peptides can be analyzed as cations at pH < 7 and as anions mostly at pH > 10. Consequently, the strongly acidic conventional and isoelectric BGEs (pH 2.18-2.50) were selected for CZE analyses and separations of the above peptides. Full composition and pH of the used BGEs together with the separation voltage and electric currents are presented in Table 2. In all used BGEs, the GnRHs had positive charges in the range from 0.91 to 3.00 of elementary charge. The calculated values of effective charge at five selected pHs of the BGEs used are given in Table 3. With respect to their relatively hydrophilic character all analyzed peptides were dissolved in deionized water, which brought an advantage that the same sample solution could be applied to CZE analyses in different BGEs, and in addition the electric-field-enhanced concentrating effect was utilized to concentrate the diluted peptide solutions.

4.2 Qualitative analysis of GnRHs and determination of purity degree

For full characterization of peptide preparations, especially pharmaceuticals and peptides used in biological tests it is important to know the content of admixtures, originating from peptide synthesis and purification procedures. The purity degrees of GnRHs were determined as the ratio of the corrected peak area of peptide itself to the sum of corrected areas of all peaks presented on electrophoregrams, corrected peak area is peak area corrected with respect to migration velocity of the given peak. The qualitative analyses of GnRHs were carried out in BGE II, 100 mM H_3PO_4 and 50 mM Tris, pH 2.25, peptides with purity degree lower than 75 % were not used for further experiments. The analyzed peptides were mostly well purified by HPLC, the values of purity degrees reached 88-99 %. The CZE analysis of highly pure tetrapeptide, fragment of hGnRH 7-10, with purity degree 96.2 % is depicted in Fig. 2A. CZE analysis of nonapeptide, [Des-Gly-NH_2]cGnRH II, (see Fig. 2B) demonstrates example of impure peptide with four major and a lot of minor admixtures, which could not be used for further experiments. The purity degree in this case was only 55.1 %.

4.3 Separation of structurally related peptides and determination of peptide mobilities

In addition to qualitative analysis of individual synthetic peptide preparations, the separation of closely related GnRHs and their analogs and fragments was tested. These separations are important from the point of view of simultaneous analysis of the whole molecules of GnRHs and their degradation products. The suitable separation conditions for the separations were derived from the course of the pH dependence of specific charge of these peptides (see Fig. 1), and from the experience obtained in the analysis of individual peptides by CZE in different BGEs. Three mixtures of four GnRHs were separated in five BGEs in pH range 2.18-2.50. The mixture I contained hGnRH and its fragments, mixture II contained GnRH decapeptides of three species and in mixture III sGnRH, its two fragments and hGnRH fragment were present. The efficiency and resolution of separation in conventional and isoelectric BGEs as well as composition of mixtures are given in Table 4. 0.5 M acetic acid, pH 2.5, was the best BGE for fast separation, but the efficiency and the resolution were the worst in comparison with other BGEs. The shortest time of analyses in range 3.4-4.5 minutes were achieved in 500 mM acetic acid, pH 2.5, the electrophoregrams are depicted in Fig. 3C for mixture I and Fig. 3F for mixture III. The best efficiency of separation was achieved in isoelectric BGE, BGE IV, 200 mM IDAA, pH 2.32, with theoretical plates number in range $0.5\text{-}1.6\cdot10^6$/m, CZE separations of mixture I are shown in Fig. 3B and separations of mixture III in Fig. 3E. The resolution of separations in BGE IV and BGE II (100 mM H_3PO_4, 50 mM Tris, pH 2.25) was comparable as can be seen from CZE separations of mixture I in Figs. 3B and 3A. [Des-Gly-NH_2]sGnRH and sGnRH in mixture III comigrated in a single peak in BGE II (see Fig. 3D), but in BGE IV and BGE V the partial resolution of these two peptides was achieved, as shown in Fig. 3E and 3F. As follows from the above results it is clear that in some cases better separation can be achieved with isoelectric buffer iminodiacetic acid than with classical phosphate buffer or acetic acid-based BGEs.

From CZE separations of GnRHs their effective electrophoretic mobilities were determined. The effective electrophoretic mobility, m_{ep}, of peptide in BGE was calculated from migration time of the peptide, t_{mig}, and migration time of neutral electroosmotic marker, t_{eo}, according to equation:

$$m_{ep} = \frac{l_t l_{ef}}{U}\left(\frac{1}{t_{mig}} - \frac{1}{t_{eo}}\right) \tag{11}$$

where l_t is total capillary length, l_{ef} is effective capillary length, U is the applied separation voltage. In CZE analyses in highly acidic BGEs with very low electroosmotic flow (EOF) due to the suppressed dissociation of silanol groups of FS capillary the effective electrophoretic mobility was determined using the pressure accelerated measurement of EOF according to [44]. The effective electrophoretic mobilities were determined as averages of two subsequent measurements, the values of which differed less than 1%.

The real average temperature inside the capillary was higher than the temperature of the capillary coolant due to Joule heating. The real temperature in the capillary for each BGE was obtained from the experimentally determined dependence of temperature increase inside the FS capillary capillary on the input power per unit length of the capillary as described in [45]. The average temperature increase inside the capillary was 3.6°C for BGEs I and V, 4.8°C for BGE II, 4.5°C for BGE III and 3.9°C for BGE IV. The values of effective electrophoretic mobilities of GnRHs in different BGEs corrected to standard temperature, 25°C, are presented in Table 3. The effective electrophoretic mobilities determined at real temperature inside the capillary differed about 8-11 % in all BGEs in comparison with standard effective electrophoretic mobilities, at 25°C. Relatively large differences of effective mobilities of GnRHs in different BGEs in spite narrow pH range (0.07 – 0.32 pH unit) are caused by different ionic strength of individual BGEs. For that reason the effective mobilities of GnRHs are minimal in BGE II, the ionic strength of which is maximal, and the mobilities are maximal in BGE V, the ionic strength of which is minimal. In addition, the different capabilities of the BGE counterions, acetate in BGE I and V, phosphate in BGE II and iminodiacetate in BGEs III and IV, to form even very weak ionic pairs with cationic peptides may also contribute to the different effective mobilities of peptides.

4.4 Semiempirical models

In the current work we have tested and compared six semiempirical models of the correlation between effective electrophoretic mobility of GnRHs and their charge/size ratio – rigid spherical model, Eq. (2) [26], classical linear polymer model, Eq. (3) [27], Offord's model, Eq. (1) [20], Grossman's model, Eq. (7) [31], Cifuentes's and Poppe's model, Eq. (8) [32] and Cross's model, Eq. (4) [28], which were utilized for prediction of secondary or tertiary structure of peptides and proteins in solution [26]. The graphs of the correlations of the above semiempirical models applied to ten GnRHs are depicted in Fig. 4. According to the figures it is evident that the best model was classical linear polymer model, Eq. (3), the correlation coefficients, R, reached values 0.995-0.999 in all five BGEs. Offord's model was also suitable for description of peptides in solution for four BGE, BGE I-IV (R = 0.994-0.998), and rigid spherical model could be alternative model for BGE V. Grossman's model and Cifuentes's and Poppe's model did not fit for acetic acid as BGE (R = 0.990 and 0.984). The most suitable model, classical linear polymer model, is in agreement with model predicted for set of similar peptides containing triptorelin and buserelin in pH 2.85 [46] and our former work concerning on insect oostatic peptides in pH 2.30 and 2.40 [47].

4.5 Estimation of probable structure of peptide

Fitting the experimental data into the graphs of different semiempirical models helped us to predict the secondary structure of GnRHs. Cross's plot seems to be the most suitable for predicting the peptide structure, because it directly provides the value of exponent k in the m_{ep} versus q/M_r^k plot as the slope of the line expressed by equation (4). Parameters of linear regression (slope of curve, intercept, and coefficient of correlation) of the Cross's plot, log (m_{ep}/q) versus log M_r, and coefficients of correlation of other five models for the GnRHs are presented in Table 5.

As follows from the data of Cross's model the exponent k in all five BGEs was close to 0.5, i.e. migration of this set of GnRHs can be best described by classical linear polymer model (C). Behavior of peptides in BGE II and BGE III can be also described by Cifuentes's and Poppe's (F) or Offord's (D) model. Consequently, the most probable structure of these peptides is random coil. In BGE V the exponent k was between 1/3 and 1/2, which means that the migration of these peptides fits also to rigid spherical model (B) and their molecules could possibly have the shape of solid sphere. The selection of the most probable model was supported by the high value of correlation coefficient R = 0.995-0.999. The predicted structures should be considered as the most probable, but not determined definitely.

Acknowledgements

This work was supported by the Grant Agency of the Czech Republic, grants no. 203/04/0098, 203/05/2539, 203/06/1044, and by the Czech Academy of Sciences, research project Z40550506. We thank to Mrs. V. Lišková for her skilful technical assistance and Dr. D. Koval for his help in preparation of this manuscript.

References

[1] M. M. Marelli, R. M. Moretti, J. Januszkiewicz-Caulier, M. Motta, P. Limonta, Current Cancer Drug Targets, 6 (2006) 257.

[2] V. Kašička, Electrophoresis 27 (2006) 142.

[3] J. C. M. Waterval, P. Bestebreurtje, H. Lingeman, C. Versluis, A. J. R. Heck, A. Bult, W. J. M. Underberg, Electrophoresis 22 (2001) 2701.

[4] N. M. Vizioli, M. L. Rusell, C. N. Carducci, Anal. Chim. Acta 514 (2004) 167.

[5] S. Naylor, A. J. Tomlinson, Talanta 45 (1998) 603.

[6] N. Johannesson, M. Wetterhall, K. E. Markides, J. Bergquist, Electrophoresis 25 (2004) 809.

[7] G. M. Janini, T. P. Conrads, K. L. Wilkens, H. J. Issaq, T. D. Veenstra, Anal. Chem. 75 (2003) 1615.

[8] J. R. Perkins, K. B. Tomer, Anal. Chem. 66 (1994) 2835.

[9] H. Watzig, M. Degenhardt, J. Chromatogr. A. 817 (1998) 239.

[10] A. Zuberovic, S. Ullsten, U. Hellman, K. E. Markides, J. Bergquist, Rapid Commun. Mass Spectrom. 18 (2004) 2946.

[11] V. Sanz-Nebot, F. Benavente, I. Toro, J. Barbosa, Electrophoresis 22 (2001) 4333.

[12] V. Sanz-Nebot, F. Benavente, E. Balaguer, J. Barbosa, Electrophoresis 24 (2003) 883.

[13] V. Sanz-Nebot, E. Balaguer, F. Benavente, J. Barbosa, Electrophoresis 26 (2005) 1457.

[14] V. Sanz-Nebot, F. Benavente, I. Toro, J. Barbosa, J. Chromatogr. A 985 (2003) 411.

[15] P. H. Corran, N. Sutcliffe, J. Chromatogr. 636 (1993) 87.

[16] E. Baltussen, R. M. Guijt, G. van der Steen, F. Laugere, S. Baltussen, G. W. K. van Dedem, Electrophoresis 23 (2002) 2888.

[17] R. Ledger, I. G. Tucker, G. F. Walker, J. Chromatogr. B 769 (2002) 235.

[18] J. C. M. Waterval, G. Hommels, P. Bestebreurtje, C. Versluis, A. J. R. Heck, A. Bult, H. Lingeman, W. J. M. Underberg, Electrophoresis 22 (2001) 2709.

[19] M. Rezeli, B. Vilaghy, F. Kilar, K. Kanyo, B. Torok, A. Torok, J. Biochem. Biophys. Methods 53 (2002) 151.

[20] R. E. Offord, Nature 211 (1966) 591.

[21] H. J. Issaq, G. M. Janini, I. Z. Atamna, G. M. Muschik, J. Lukszo, J. Liq. Chromatogr. 15 (1992) 1129.

[22] E. C. Rickard, M. M. Strohl, R. G. Nielsen, Anal. Biochem. 197 (1991) 197.

[23] S. K. Basak, M. R. Ladisch, Anal. Biochem. 226 (1995) 51.

[24] B. Tessier, F. Blanchard, R. Vanderesse, C. Harscoat, I. Marc, J. Chromatogr. A 1024 (2004) 255.

[25] M. Jalali-Heravi, Y. Shen, M. Hassanisadi, M. G. Khaledi, Electrophoresis 26 (2005) 1874.

[26] P. D. Grossman, J. C. Colburn, in P. D. Grossman, J. C. Colburn (Editors) Capillary Electrophoresis: Theory and Practice, Academic Press, Inc., San Diego, 1992, p. 352.
[27] C. Tanford, Physical Chemistry of Macromolecules, Wiley, New York 1961, p. 392.
[28] A. R. F. Cross, N. F. Garnham, Chromatographia 54 (2001) 639.
[29] J. Kim, R. Zand, D. M. Lubman, Electrophoresis 24 (2003) 782.
[30] B. J. Compton, J. Chromatogr. 559 (1991) 357.
[31] P. D. Grossman, J. C. Colburn, H. H. Lauer, Anal. Biochem. 179 (1989) 28.
[32] A. Cifuentes, H. Poppe, Electrophoresis 18 (1997) 2362.
[33] N. J. Adamson, E. C. Reynolds, J. Chromatogr. B 699 (1997) 133.
[34] V. Sanz-Nebot, F. Benavente, J. Barbosa, J. Chromatogr. A 950 (2002) 99.
[35] H. J. Gaus, A. G. Becksickinger, E. Bayer, Anal. Chem. 65 (1993) 1399.
[36] M. T. W. Hearn, H. H. Keah, R. I. Boysen, I. Messana, F. Misiti, D. V. Rossetti, B. Giardina, M. Castagnola, Anal. Chem. 72 (2000) 1964.
[37] B. Verzola, M. Perduca, G. Mezo, F. Hudecz, P. G. Righetti, Electrophoresis 24 (2003) 794.
[38] B. R. Sitaram, H. H. Keah, M. T. W. Hearn, J. Chromatogr. A. 857 (1999) 263.
[39] S. Micinski, M. Gronvald, B. J. Compton, in B. L. Karger, W. S. Hancock (Eds.), High Resolution Separation and Analysis of Biological Macromolecules, Pt A, Academic Press Inc, San Diego, 1996, p. 342.
[40] H. J. Issaq, G. M. Janini, K. C. Chan, Z. Elrassi, in P. R. Brown, E. Grushka (Editors), Advances in Chromatography, Vol.35., Marcel Dekker, Inc., New York, 1995, p. 101.
[41] G. M. Janini, H. J. Issaq, Chromatographia 53 (2001) S18-S26.
[42] V. Kašička, in H.Y. Aboul-Enein (Editor), Analytical and Preparative Separation Methods of Macromolecules, Marcel Dekker Inc., New York, 1999, p. 39.
[43] V. Kašička, Z. Prusík, J. Chromatogr. 470 (1989) 209.
[44] D. Koval, V. Kašička, J. Jiráček, M. Collinsová, Electrophoresis 24 (2003) 774.
[45] D. Koval, V. Kašička, J. Jiráček, M. Collinsová, T. A. Garrow, J. Chromatogr. B 770 (2002) 145.
[46] F. Benavente, E. Balaguer, J. Barbosa, V. Sanz-Nebot, J. Chromatogr. A 1117 (2006) 94.
[47] V. Šolínová, V. Kašička, D. Koval, J. Hlaváček, Electrophoresis 25 (2004) 2299.

Legends to Figures

Figure 1

The pH dependence of specific charge (effective charge divided by relative molecular mass) of analyzed peptides, 1 – fragment of hGnRH 7-10, 2 – fragment of hGnRH 4-10, 3 – [Des-pGlu^1-D-Orn^6]sGnRH, 4 – hGnRH, 5 – sGnRH, 6 – cGnRH, 7 – [βAla^6-ProNHEt^{10}]hGnRH, 8 – [Des-Gly-NH_2]sGnRH, 9 – [Des-Gly-NH_2]cGnRH, 10 – [Des-Pro-Gly-NH_2]hGnRH, 11 – [Des-Arg-Pro-Gly-NH_2]hGnRH, 12 – fragment of hGnRH 1-4.

Figure 2

CZE analyses of (A) HPLC purified fragment of hGnRH 7-10, 1.40 mg.ml^{-1}, and (B) crude synthetic product of [Des-Gly-NH_2]cGnRH II, 1.10 mg.ml^{-1}, 1 – main synthetic product, x – non-identified impurities. Analyses were performed in BGE II (see Table 2). Other experimental conditions are given in the text (see section 3.3).

Figure 3

CZE separations of structurally related GnRHs and their analogs and fragments. Mixture I in (A) BGE II, (B) BGE IV, (C) BGE V, and mixture III in (D) BGE II, (E) BGE IV, (F) BGE V. For composition of BGEs see Table 2. Mixture I, 1 – fragment of hGnRH 4-10, 2 – hGnRH, 3 – fragment of hGnRH 1-4, 4 – [Des-Arg-Pro-Gly-NH_2]hGnRH; mixture III, 1 – [Des-pGlu^1-D-Orn^6]sGnRH, 2 – [Des-Pro-Gly-NH_2]hGnRH, 3 – sGnRH, 4 – [Des-Gly-NH_2]sGnRH.

Figure 4

Semiempirical models of the correlation between effective mobility, m_{ep}, and peptide charge, q, and size (expressed by relative molecular mass, M_r, or by number of amino acid residues in peptide chain, n) applied to ten peptides in five BGEs, 1 – BGE I, 2 – BGE II, 3 – BGE III, 4 – BGE IV, 5 – BGE V, for BGEs composition see Table 2. (A) Cross's model, Eq. (4), (B) rigid spherical model, Eq. (2), (C) classical linear polymer model, Eq. (3), (D) Offord's model, Eq. (1), (E) Grossman's model, Eq. (7), (F) Cifuentes's and Poppe's model, Eq. (8).

Table 1

Sequences of analyzed peptides and their relative molecular masses (M_r)

Peptide	Sequence in three-letter code	M_r
Human GnRH (hGnRH)	pGlu-His-Trp-Ser-Tyr-Gly-Leu-Arg-Pro-Gly-NH_2	1181.5
[βAla^6-ProNHEt^{10}]hGnRH	pGlu-His-Trp-Ser-Tyr-β-Ala-Leu-Arg-Pro-Pro-NHEt	1262.5
[Des-Pro-Gly-NH_2]hGnRH	pGlu-His-Trp-Ser-Tyr-Gly-Leu-Arg-OH	1028.3
[Des-Arg-Pro-Gly-NH_2]hGnRH	pGlu-His-Trp-Ser-Tyr-Gly-Leu-OH	872.1
Fragment of hGnRH 1-4	pGlu-His-Trp-Ser-OH	538.6
Fragment of hGnRH 4-10	H-Ser-Tyr-Gly-Leu-Arg-Pro-Gly-NH_2	766.0
Fragment of hGnRH 7-10	H-Leu-Arg-Pro-Gly-NH_2	440.6
Salmon GnRH (sGnRH)	pGlu-His-Trp-Ser-Tyr-Gly-Trp-Leu-Pro-Gly-NH_2	1211.5
[Des-Gly-NH_2]sGnRH	pGlu-His-Trp-Ser-Tyr-Gly-Trp-Leu-Pro-OH	1155.4
[Des-pGlu^1-D-Orn^6]sGnRH	H-His-Trp-Ser-Tyr-D-Orn-Trp-Leu-Pro-Gly-NH_2	1058.3
Chicken GnRH I (cGnRH)	pGlu-His-Trp-Ser-Tyr-Gly-Leu-Gln-Pro-Gly-NH_2	1180.4
[Des-Gly-NH_2]cGnRH II	pGlu-His-Trp-Ser-His-Gly-Trp-Tyr-Pro-OH	1179.4

Table 2

Composition and pH of the BGEs applied for CZE analyses and separations of GnRHs and their analogs and fragments, separation voltage, *U*, and electric current, *I*.

BGE no.	BGE constituents	pH	U (kV)	I (μA)
I	2 M acetic acid	2.18	20	19.9
II	100 mM H_3PO_4, 50 mM Tris	2.25	15	43.2
III	100 mM iminodiacetic acid	2.30	20	33.0
IV	200 mM iminodiacetic acid	2.32	15	35.0
V	500 mM acetic acid	2.50	25	15.6

Table 3

Calculated effective charges, q, and CZE determined effective electrophoretic mobilities, m_{ep}, corrected to standard temperature, 25°C, of analyzed peptides in five different BGEs. Full composition of BGEs is given in Table 2.

Peptide	q [e]					m_{ep} (10^{-9} $m^2V^{-1}s^{-1}$)				
	BGE I	BGE II	BGE III	BGE IV	BGE V	BGE I	BGE II	BGE III	BGE IV	BGE V
Human GnRH (hGnRH)	2.00	2.00	2.00	2.00	2.00	14.26	11.69	14.60	12.87	16.85
[βAla^6-ProNHEt^{10}]hGnRH	2.00	2.00	2.00	2.00	2.00	14.68	12.05	15.22	13.47	17.90
[Des-Pro-Gly-NH_2]hGnRH	2.00	2.00	2.00	2.00	2.00	14.97	12.27	15.37	13.52	17.29
[Des-Arg-Pro-Gly-NH_2]hGnRH	0.95	0.94	0.93	0.92	0.91	8.33	7.15	8.54	7.66	9.55
Fragment of hGnRH 1-4	0.95	0.94	0.93	0.92	0.91	10.81	9.44	11.18	10.13	11.94
Fragment of hGnRH 4-10	2.00	2.00	2.00	2.00	2.00	18.21	15.22	18.96	16.86	21.99
Salmon GnRH (sGnRH)	1.00	1.00	1.00	1.00	1.00	7.63	6.38	7.98	7.01	9.42
[Des-Gly-NH_2]sGnRH	0.95	0.94	0.93	0.92	0.91	7.43	6.37	7.68	6.85	8.78
[Des-pGlu^1-D-Orn^6]sGnRH	3.00	3.00	3.00	3.00	3.00	22.16	17.24	22.47	20.95	27.20
Chicken GnRH I (cGnRH)	1.00	1.00	1.00	1.00	1.00	7.63	6.38	7.98	7.01	9.42

Table 4

Separation efficiency (number of theoretical plates) and resolution of CZE separation of three mixtures of GnRHs and their fragments and analogs in five BGEs. Composition of BGEs is given in Table 2.

Mixture no.	Peptide	Efficiency (number of theoretical plates)					Resolution				
		BGE I	BGE II	BGE III	BGE IV	BGE V	BGE I	BGE II	BGE III	BGE IV	BGE V
I	Fragment of hGnRH 4-10	21709	125188	60959	164189	14299	-	-	-	-	-
	hGnRH	18605	67104	43677	112854	12955	6.3	16.8	11.2	15.7	4.8
	Fragment of hGnRH 1-4	21967	56571	40334	106615	13811	6.7	10.9	9.6	11.5	5.4
	[Des-Arg-Pro-Gly-NH_2]hGnRH	17631	75473	47091	123868	12119	5.6	14.6	9.2	12.2	3.0
II	[βAla^6-ProNHEt^{10}]hGnRH	28602	104971	67695	152187	17714	-	-	-	-	-
	hGnRH	16941	58881	42961	100696	11929	0.8	2.1	1.8	2.5	1.2
	sGnRH	12807	36244	26417	55750	8739	6.9	24.9	17.9	23.6	8.0
	cGnRH I	12807	36244	26417	55750	8739	0	0	0	0	0
III	[Des-pGlu^1-D-Orn^6]sGnRH	27892	211526	74027	148832	14898	-	-	-	-	-
	[Des-Pro-Gly-NH_2]hGnRH	17129	106062	54877	120507	13414	10.7	25.8	18.3	24.7	9.2
	sGnRH	12985	36711	18131	59590	6529	13.4	29.3	18.2	29.6	10.6
	[Des-Gly-NH_2]sGnRH	12985	36711	13857	48050	4681	0	0	0.7	1.1	0.2

Table 5

Parameters of linear regression of Cross's (k_A, b_A, R_A), rigid spherical (R_B), classical linear polymer (R_C), Offord's (R_D), Grossman's (R_E), Cifuentes's and Poppe's (R_F) model for analyzed GnRHs, in five BGEs. For BGEs composition see Table 2.

BGE no.	k_A	b_A	R_A	R_B	R_C	R_D	R_E	R_F
I	-0.519	2.468	0.9827	0.9926	0.9989	0.9943	0.9895	0.9897
II	-0.589	2.604	0.9520	0.9826	0.9952	0.9977	0.9948	0.9965
III	-0.534	2.531	0.9725	0.9902	0.9981	0.9956	0.9911	0.9921
IV	-0.557	2.552	0.9723	0.9893	0.9967	0.9940	0.9898	0.9863
V	-0.457	2.468	0.9654	0.9945	0.9975	0.9901	0.9836	0.9839

k - slope of curve, b - intercept, R - coefficient of correlation

Figure 1

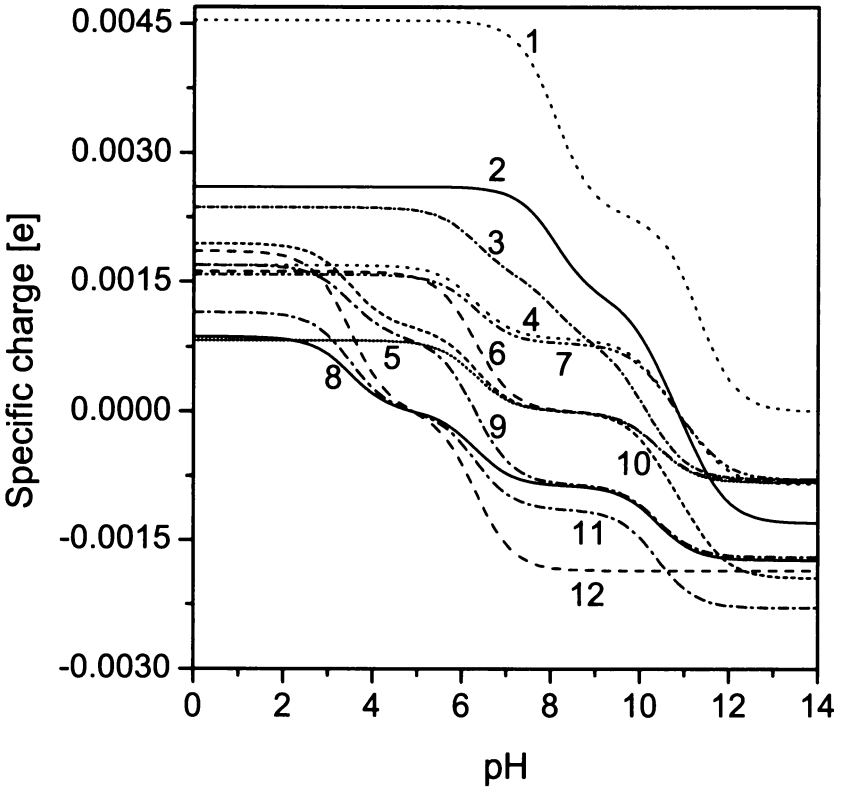
0.0045
0.0030
0.0015
0.0000
-0.0015
-0.0030
Specific charge [e]
0
2
4
6
8
10
12
14
pH
1
2
3
4
5
6
7
8
9
10
11
12

Figure 2

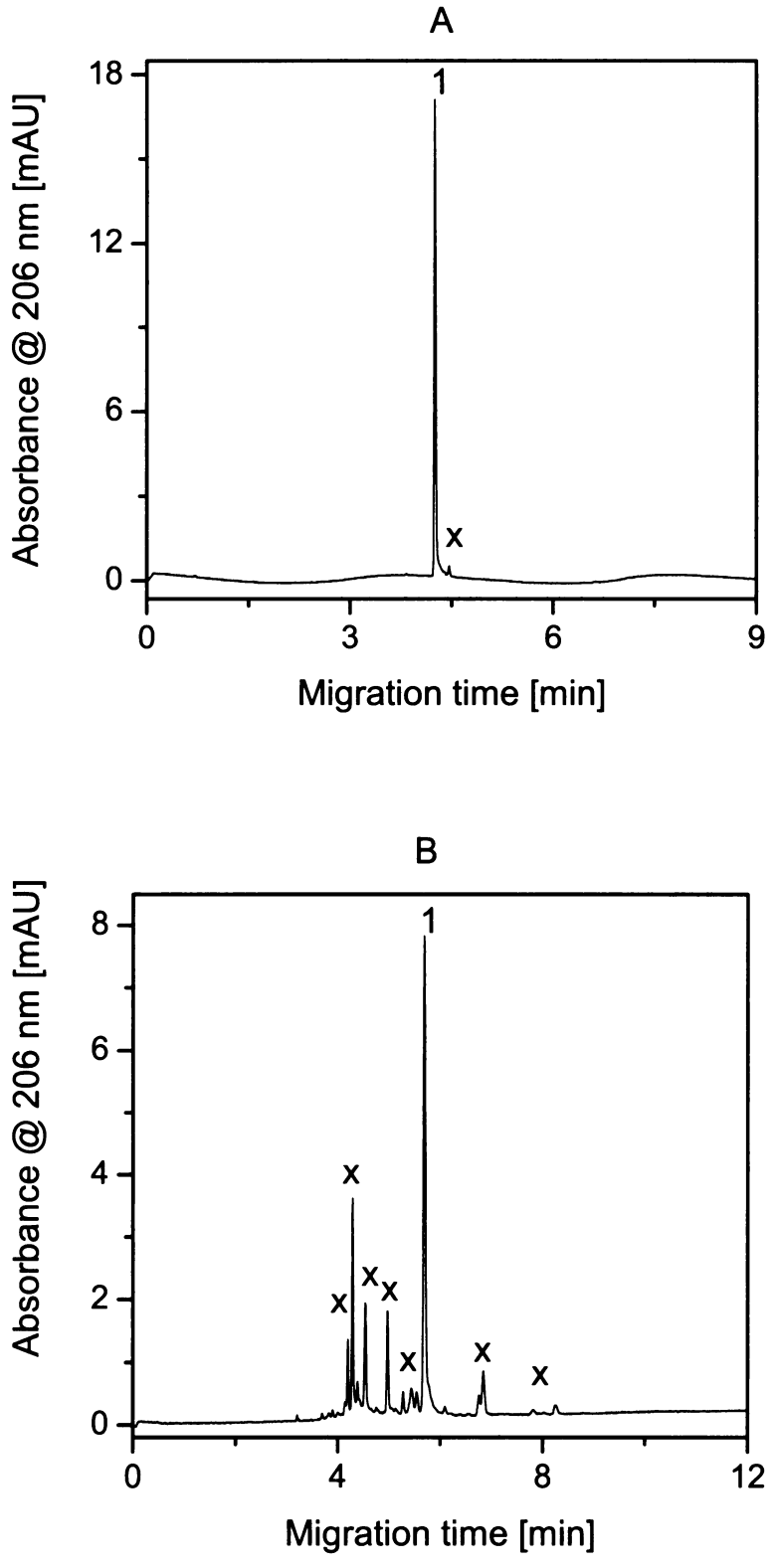
A
Absorbance @ 206 nm [mAU]
18
12
6
0
1
x
0
3
6
9
Migration time [min]
B
Absorbance @ 206 nm [mAU]
8
6
4
2
0
1
x
x
x
x
x
x
0
4
8
12
Migration time [min]

Figure 3

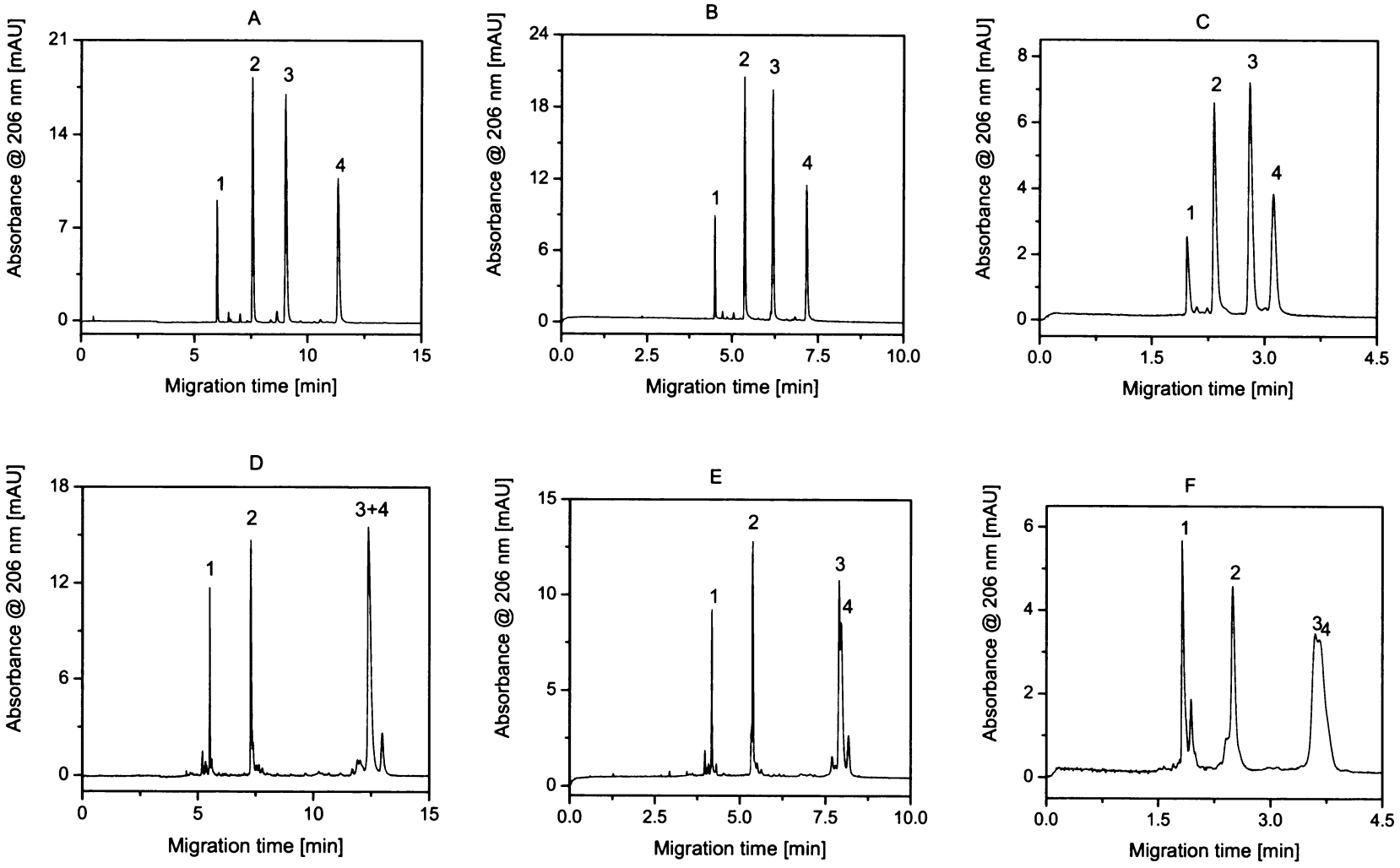
A
Absorbance @ 206 nm [mAU]
21
14
7
0
1
2
3
4
0
5
10
15
Migration time [min]
B
Absorbance @ 206 nm [mAU]
24
18
12
6
0
1
2
3
4
0.0
2.5
5.0
7.5
10.0
Migration time [min]
C
Absorbance @ 206 nm [mAU]
8
6
4
2
0
1
2
3
4
0.0
1.5
3.0
4.5
Migration time [min]
D
Absorbance @ 206 nm [mAU]
18
12
6
0
1
2
3+4
0
5
10
15
Migration time [min]
E
Absorbance @ 206 nm [mAU]
15
10
5
0
1
2
3
4
0.0
2.5
5.0
7.5
10.0
Migration time [min]
F
Absorbance @ 206 nm [mAU]
6
4
2
0
1
2
3
4
0.0
1.5
3.0
4.5
Migration time [min]

Figure 4

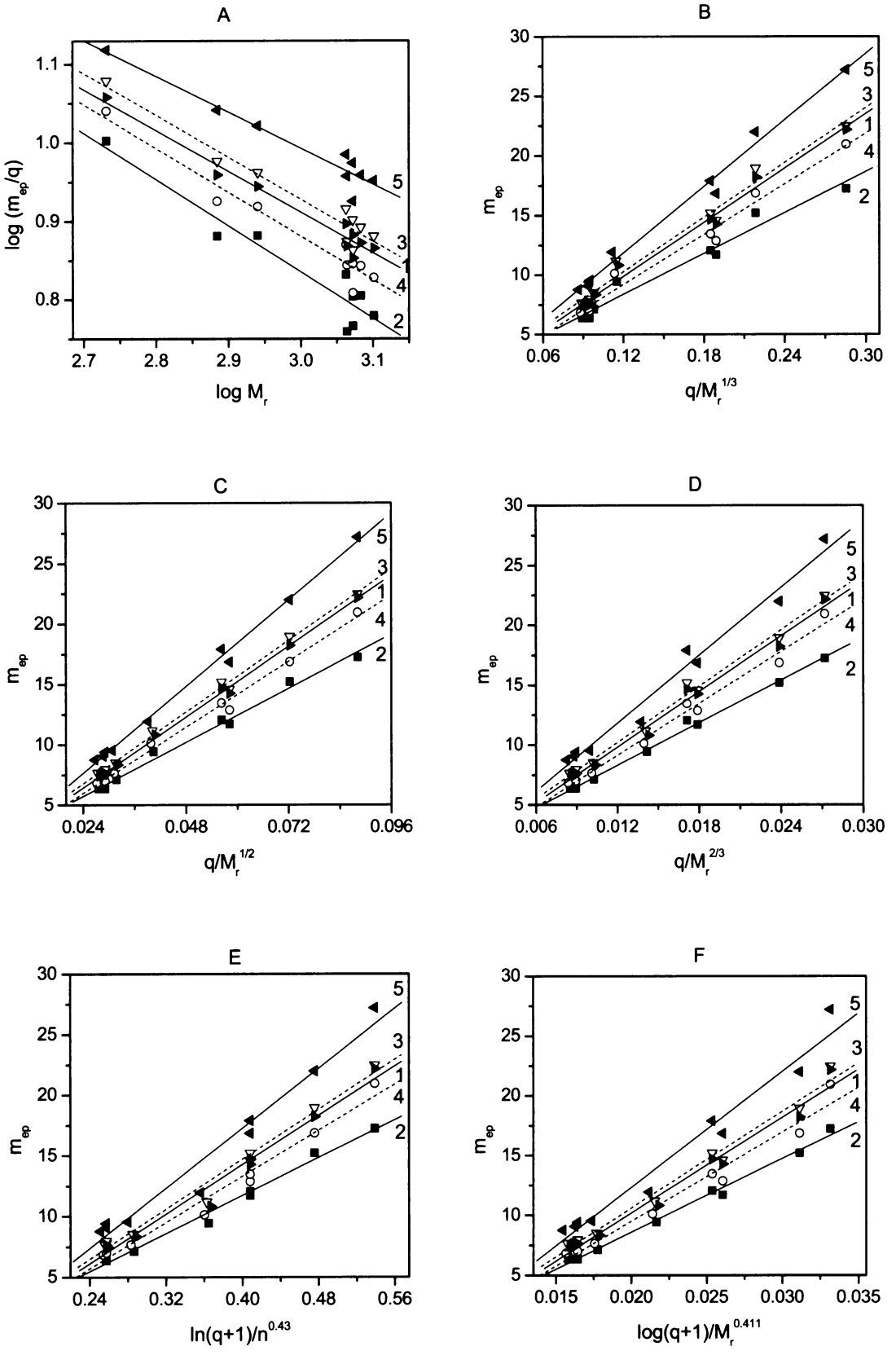
A
log (m_{ep}/q)
log M_r
B
m_{ep}
$q/M_r^{1/3}$
C
m_{ep}
$q/M_r^{1/2}$
D
m_{ep}
$q/M_r^{2/3}$
E
m_{ep}
$\ln(q+1)/n^{0.43}$
F
m_{ep}
$\log(q+1)/M_r^{0.411}$

Electrophoresis 2006, *27*, 1006–1019

Veronika Šolínová
Václav Kašička
Dušan Koval
Michal Česnek
Antonín Holý

Institute of Organic Chemistry and Biochemistry, Academy of Sciences of the Czech Republic, Prague, Czech Republic

Received November 1, 2005
Accepted November 8, 2005

Research Article

Determination of acid–base dissociation constants of amino- and guanidinopurine nucleotide analogs and related compounds by capillary zone electrophoresis

CZE has been applied for determination of acid–base dissociation constants (pK_a) of ionogenic groups of newly synthesized amino- and (amino)guanidinopurine nucleotide analogs, such as acyclic nucleoside phosphonate, acyclic nucleoside phosphonate diesters and other related compounds. These compounds bear characteristic pharmacophores contained in various important biologically active substances, such as cytostatics and antivirals. The pK_a values of ionogenic groups of the above compounds were determined by nonlinear regression analysis of the experimentally measured pH dependence of their effective electrophoretic mobilities. The effective mobilities were measured by CZE performed in series of BGEs in a broad pH range (3.50–11.25), at constant ionic strength (25 mM) and temperature (25°C). pK_a values were determined for the protonated guanidinyl group in (amino)guanidino 9-alkylpurines and in (amino)guanidinopurine nucleotide analogs, such as acyclic nucleoside phosphonates and acyclic nucleoside phosphonate diesters, for phosphonic acid to the second dissociation degree (−2) in acyclic nucleoside phosphonates of amino and (amino)guanidino 9-alkylpurines, and for protonated nitrogen in position 1 (N1) of purine moiety in acyclic nucleoside phosphonates of amino 9-alkylpurines. Thermodynamic pK_a of protonated guanidinyl group was estimated to be in the range of 7.75–10.32, pK_a of phosphonic acid to the second dissociation degree achieved values of 6.64–7.46, and pK_a of protonated nitrogen in position 1 of purine was in the range of 4.13–4.89, depending on the structure of the analyzed compounds.

Keywords: Acyclic nucleoside phosphonates / Aminopurine nucleosides / Capillary electrophoresis / Dissociation constant (pK_a) / Guanidinopurine nucleosides
DOI 10.1002/elps.200500815

1 Introduction

The knowledge of physicochemical characteristics of new synthetic compounds, such as water solubility, lipophilicity, and acid–base properties, is necessary when these compounds start to be tested as potential new drug candidates. The determination of these characteristics plays an important role in the optimization stage of a new drug development project. Particularly, the acid–base dissociation constant (pK_a) is a key parameter for compounds containing at least one ionogenic (acidic or basic) functional group for understanding the passage of drugs into and across cell membranes, for estimation of the concentration of the individual ionic forms of the drug in blood, for assessment of reaction rate and for investigation of the biological uptake, and metabolism mechanism. Moreover, the knowledge of pK_a values is important for prediction of the effective charge, effective electrophoretic mobility, and migration order of the analytes in CZE, which has become a method of choice for determination of pK_a values [1]. In comparison with the traditional potentiometric and spectrophotometric titration methods, the particular advantage of CZE is that it allows

Correspondence: Dr. Václav Kašička, Institute of Organic Chemistry and Biochemistry, Academy of Sciences of the Czech Republic, Flemingovo 2, CZ-166 10 Prague 6, Czech Republic
E-mail: kasicka@uochb.cas.cz
Fax: +420-220-183-592

Abbreviations: **PMEDAP**, 2,6-diamino-9-(2-(phosphonomethoxy) ethyl)-9*H*-purine; **PMEG**, 9-(2-(phosphono-methoxy)ethyl)guanine; **PMEMAP**, 2-amino-9-(2-(phosphonomethoxy)ethyl)-9*H*-purine

working with a very small amount of sample (nanolitre applied sample volume *per* analysis) and knowledge of the analyte precise concentration is not necessary. In addition, the analyte need not to be perfectly pure, since its potential admixtures are separated during the analysis.

Newly synthesized amino and (amino)guanidino 9-alkylpurines [2, 3], *e.g.*, 2-amino-6-guanidino-9-isopropylpurine, 6-amino-2-guanidino-9-isopropylpurine, 2- or 6-guanidino-9-isopropylpurine, 2-amino-9-alkylpurine, their acyclic nucleoside phosphonates and alkyl (isopropyl) esters of these acyclic nucleoside phosphonates, bear characteristic pharmacophores contained in various important biologically active substances, such as cytostatics and antivirals. The derivatives of 9-alkylpurines also show a broad spectrum of biological activity; they influence the metabolic pathway of cytokinins and cyclin-dependent kinases. The 6-amino group not only plays an important role in purine derivatives by its Watson–Crick basepairing capacity, but is also essential for substrate/inhibitor binding to diverse enzymes of purine metabolism as well as in important regulatory pathways. The guanidinyl group is closely related to the amino function but it is more basic than amino group. Among others, the inhibitors of the influenza virus neuramidinase, inhibitors of polyamine synthesis and the minor groove binding agent netropsin belong to the biologically active compounds bearing this functional group.

CZE has proved to be a convenient and precise method for determination of dissociation constants of ionogenic groups of various types of compounds, such as different types of drugs [4–9], alkaloids [10], flavonoids [11], amino acids [12], peptides [13–15], morpholinyl group of Mannich ketones [16], cytokinins [17], imidazole derivatives [18], guanosine monophosphate and adenosine monophosphate [19], xanthones [20], enolizable compounds [21], 2-amino-2-oxazolines [22], saccharides [23], heterocyclic aromatic amines [24], and secondary and tertiary amines [25].

The pK_a values of the above types of compounds were mostly determined in aqueous media, but several papers deal with pK_a estimation in nonaqueous [15, 26] or aqueous–organic solvents [27–29]. The most frequently applied detection for CZE estimation of pK_a is the direct UV-absorption detection [6, 7, 9, 10, 13, 30–32]; however, conductometric [12], amperometric [23], and indirect UV-absorption [33] detection schemes have been also used. The pK_a values of the ionogenic groups in both aqueous and nonaqueous media were determined using the different linear or nonlinear regression analysis of the pH dependence of effective electrophoretic mobility of analyzed compounds [1].

The aim of this work was to employ CZE for determination of the thermodynamic dissociation constants (pK_a) of ionogenic groups of amino- and guanidinopurines and their analogs, particularly pK_a of the protonated guanidinyl group in (amino)guanidino 9-alkylpurines, their acyclic nucleoside phosphonates and acyclic nucleoside phosphonate diisopropyl esters, pK_a of phosphonic acid to the second dissociation degree in acyclic nucleoside phosphonates of (amino)guanidino 9-alkylpurines, and pK_a of protonated nitrogen in position 1 (N1) of purine moiety in acyclic nucleoside phosphonates of amino 9-alkylpurines. To achieve this goal, it was necessary to measure the pH dependence of the effective electrophoretic mobilities of the above compounds by CZE performed in the BGEs within a broad pH range, 3.50–11.25, at constant ionic strength and constant temperature.

2 Materials and methods

2.1 Chemicals

All chemicals used were of analytical reagent grade. MES (2-morpholinoethanesulfonic acid), CHES (2-(cyclohexylamino)ethanesulfonic acid), CAPS, and Tris were obtained from Serva (Heidelberg, Germany); phosphoric acid, acetic acid, formic acid, sodium hydroxide, and DMSO were supplied by Lachema (Brno, Czech Republic); SDS and isophorone (3,5,5-trimethyl-2-cyclohexen-1-one) were from Fluka (Buchs, Switzerland); MOPS (4-morpholinopropanesulfonic acid) was obtained from Calbiochem (San Diego, CA, USA); and Tricine ((tris(hydroxymethyl)-methyl)-glycine) was from Merck (Darmstadt, Germany).

2.2 Analyzed compounds

The list of analyzed compounds (analytes), amino- and (amino)guanidinopurine nucleotide analogs, such as acyclic nucleoside phosphonates and acyclic nucleoside phosphonate diesters, their identification numbers and M_r are presented in Table 1. 6-Guanidinopurines and 2-amino-6-guanidinopurine derivatives were synthesized by reaction of the 6-chloropurine derivatives with guanidine solution in DMF (dimethylformamide) in the presence of 1,4-diazo-bicyclo(2,2,2,)octane (DABCO) [2]. Acyclic guanidinopurine nucleosides and acyclic guanidinopurine nucleoside phosphonates were obtained by alkylation of the 6-guanidinopurine bases [2]. 9-Alkyl and 9-heteroalkyl substituted derivatives of the 2-amino-6-guanidinopurine were synthesized by alkylation of 2-amino-6-chloropurine and subsequent guanidinolysis [3].

Table 1. List of analyzed compounds, their identification numbers and M_r

Compound	Identification number	M_r
6-Guanidino-9-methyl-9*H*-purine	**1**	191.2
2-Amino-6-guanidino-9-isopropyl-9*H*-purine	**2**	234.3
2-Guanidino-9-isopropyl-9*H*-purine	**3**	219.2
6-Amino-2-guanidino-9-isopropyl-9*H*-purine	**4**	234.3
9-{2-((Diisopropyloxy)phosphorylmethoxy)ethyl)-2-guanidino-9*H*-purine	**5**	399.4
6-Amino-9-(2-((diisopropyloxy)phosphorylmethoxy)ethyl)-2-guanidino-9*H*-purine	**6**	414.4
2-Amino-9-(2-(phosphonomethoxy)ethyl)-9*H*-purine	**7** (PMEMAP)	273.2
2,6-Diamino-9-(2-(phosphonomethoxy)ethyl)-9*H*-purine	**8** (PMEDAP)	288.2
9-(2-(Phosphonomethoxy)ethyl)guanine	**9** (PMEG)	289.2
6-Guanidino-9-(2-(phosphonomethoxy)ethyl)-9*H*-purine	**10**	315.3
2-Amino-6-guanidino-9-(2-(phosphonomethoxy)ethyl)-9*H*-purine	**11**	330.2
2-Guanidino-9-(2-(phosphonomethoxy)ethyl)-9*H*-purine	**12**	315.2
6-Amino-2-guanidino-9-(2-(phosphonomethoxy)ethyl)-9*H*-purine	**13**	330.2

2.3 Instrumentation

CZE analyses were carried out in the capillary electrophoretic analyzer P/ACE MDQ (Beckman Coulter, Fullerton, CA, USA) using the software 32 Karat System, version 7.0 (Beckman) for data acquisition and evaluation. Origin 6.1 (OriginLab Corp., Northampton, MA, USA) was used for data plotting and regression analysis. The analyzer was equipped with the internally uncoated fused-silica capillary with outer polyimide coating, total/effective length 394/292 mm, ID/OD 75/360 μm (Polymicro Technologies, Phoenix, AR, USA). The analytes were detected by UV-Vis spectrophotometric photodiode array detector (190–600 nm) set to operate in the range 190–300 nm. Absorbance of analyzed compounds and of EOF markers (DMSO or isophorone) was monitored at 225 and 250 nm, respectively. The analyses were performed at constant temperature of the BGE inside the capillary, 25°C.

The new capillary was gradually flushed with water, 0.1 M NaOH, water, and BGE, each wash for 5 min. Finally, the capillary was conditioned by a 20 min application of the high voltage to equilibrate the inner surface and to stabilize EOF. Between runs under the same conditions, the capillary was rinsed with the BGE for 1 min. Prior to any change of the BGE the capillary was rinsed with 0.1 M NaOH for 5 min and then repeatedly stabilized. The samples were injected hydrodynamically, with pneumatically induced pressure 6.9–13.8 mbar for 5–10 s. The samples were dissolved in concentrations of 0.1 mmol/L in deionized water or in deionized water slightly alkalized by a small addition of NaOH to ensure solubility of some compounds.

BGE solutions with pH values covering a broad pH range (3.50–11.25) with 0.25 pH unit increment were prepared by mixing the appropriate amounts of stock solutions listed in Table 2 and then diluted to the constant ionic strength 25 mmol/L. The pH was measured at 25°C by pH meter CyberScan pH 2100 (Oakton Instruments, Vernon Hills, IL, USA). The BGEs were filtered through a 0.45 μm pore NC syringe filter (Millipore, Bedford, MA, USA) before use.

Table 2. Composition of the stock solutions and pH range of the BGEs, applied separation voltage, *U*, and electric current, *I*, of the CZE analyses

BGE number	Composition of stock solutions	pH range	*U* range, kV	*I* range, μA
BGE I–IV	0.95 M HCOOH, 0.7 M Tris	3.50– 4.25	9.8–10.7	26.4–24.1
BGE V–X	1 M CH_3COOH, 1 M NaOH	4.25– 5.50	8.6–10.6	30.0–24.4
BGE XI–XV	0.4 M MES, 1 M NaOH	5.50– 6.50	11.0–11.5	24.8–23.4
BGE XVI–XX	0.4 M MOPS, 1 M NaOH	6.50– 7.50	11.3–11.5	23.4–21.7
BGE XXI–XXVI	0.4 M Tricine, 1 M NaOH	7.50– 8.75	11.1–12.3	23.1–19.7
BGE XXVII–XXXI	0.5 M CHES, 1 M NaOH	8.75– 9.75	11.0–11.5	23.5–22.5
BGE XXXII–XXXVIII	0.4 M CAPS, 1 M NaOH	9.75–11.25	10.0–13.0	27.1–19.8

2.4 Determination of the effective electrophoretic mobility

The effective electrophoretic mobility, m_{eff}, of the analyte at pH of the given BGE was calculated from the experimental data of its CZE analysis, using the following equation:

$$m_{eff} = \frac{l_t l_{eff}}{U}\left(\frac{1}{t_m} - \frac{1}{t_{eo}}\right) \quad (1)$$

where l_t is the total capillary length, l_{eff} is the effective capillary length, U is the applied separation voltage, t_m is the migration time of the analyte, and t_{eo} is the migration time of the electroneutral EOF marker.

Electrophoretic mobility is relatively strongly dependent on the temperature: it varies by about 2% *per* °C in the aqueous solutions. Therefore, it was necessary to ensure that all mobilities were measured at the same temperature, best at the standard temperature of 25°C. It was achieved by thermostating the outer polyimide capillary surface to constant temperature of 24°C and by setting the input power to the value of 0.66 W *per* meter of capillary length, which causes 1°C temperature increase inside the capillary, resulting in the constant temperature 25°C of the BGE inside the capillary. The value of 0.66 W/m for 1°C temperature increase was determined from the electric conductivity measurements of an aqueous standard solution of potassium chloride in the same capillary and from the known temperature dependence of its conductivity, as described in our previous paper [32].

3 Theory of the acid–base equilibria of the analyzed compounds

From the standpoint of the acid–base behavior in the applied pH range (3.50–11.25) of BGEs four different types of the analyzed compounds can be distinguished.

(i) (Amino)guanidino 9-alkylpurines (compounds **1–4**, see Table 1 and Fig. 1A) and their acyclic nucleoside phosphonate diisopropyl esters (compounds **5** and **6**, see Table 1 and Fig. 1B) behave as monovalent bases due to the presence of a single strongly basic (cationogenic) guanidinyl group. (ii) Acyclic nucleoside phosphonates of amino 9-alkylpurines (compounds **7** and **8**, see Table 1 and Fig. 1C) behave as zwitterions with single weakly basic (cationogenic) nitrogen group in position 1 (N1) of purine moiety and two acidic (anionogenic) phosphonic acid groups. (iii) Acyclic nucleoside phosphonates of (amino)guanidino 9-alkylpurines (compounds **10–13**, see Table 1 and Fig. 1D) behave as zwitterions due to the presence of single strongly basic (cationogenic) guanidinyl group and two acidic (anionogenic) phosphonic acid groups. (iv) 9-(2-(Phosphonomethoxy)ethyl)guanine (PMEG, **9**) behaves as trivalent acid due to the presence of two acidic anionogenic phosphonic acid groups and single enol –OH group in position 6 of purine moiety.

The type (ii) differs from the type (iii) by different strength of the basic group, resulting in different order of the dissociation of the protonized groups. In the type (ii) the proton from nitrogen 1 (N1) dissociates at pH lower than that from the phosphonic acid to the second dissociation degree, whereas in the type (iii) the proton from guanidinyl group dissociates at pH higher than that from the hydrogenphosphonate (−1) to phosphonate (−2). In both these types of analytes and in type (iv) (PMEG (**9**)) phosphonic acid is dissociated into the first and/or into the second dissociation degree within the whole applied pH range of BGEs.

3.1 (Amino)guanidino 9-alkylpurines and diisopropyl esters of their acyclic nucleoside phosphonates

The (amino)guanidino 9-alkylpurines (compounds **1–4**) and their acyclic nucleoside phosphonate diisopropyl esters (compounds **5** and **6**) are present in the form of single charged cations in acidic, neutral and weakly to medium alkaline solutions due to protonation of the strongly basic guanidinyl group and they are losing their charge in strongly alkaline solutions. The hydroxyl groups of phosphonic acid are blocked in (amino)guanidino 9-alkylpurine phosphonate diisopropyl esters (**5** and **6**) and they cannot participate in the acid–base equlibria. The dissociation equilibrium of (amino)guanidino 9-alkylpurines and their acyclic nucleoside phosphonate diisopropyl esters can be expressed as shown in Scheme 1 using 2-amino-6-guanidino-9-isopropyl-9*H*-purine (**2**) as an example.

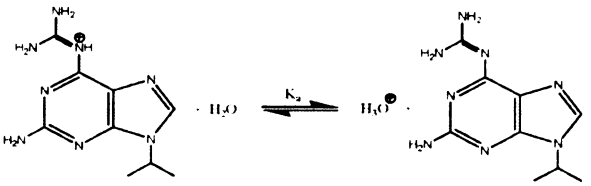

Scheme 1

This acid–base equilibrium is characterized by the thermodynamic dissociation constant, K_a, of the guanidinyl group:

$$K_a = \frac{a_{H_3O^+} a_B}{a_{BH^+}} = \frac{a_{H_3O^+} c_B \gamma_B}{c_{BH^+} \gamma_{BH^+}} \quad (2)$$

where $a_{H_3O^+}$ is the activity of the hydroxonium ions, and a_B and a_{BH^+} are the activities of the neutral and protonated forms of compound **2** (indicated as a general base B), respectively. In the second part of Eq. (2) the activities of the

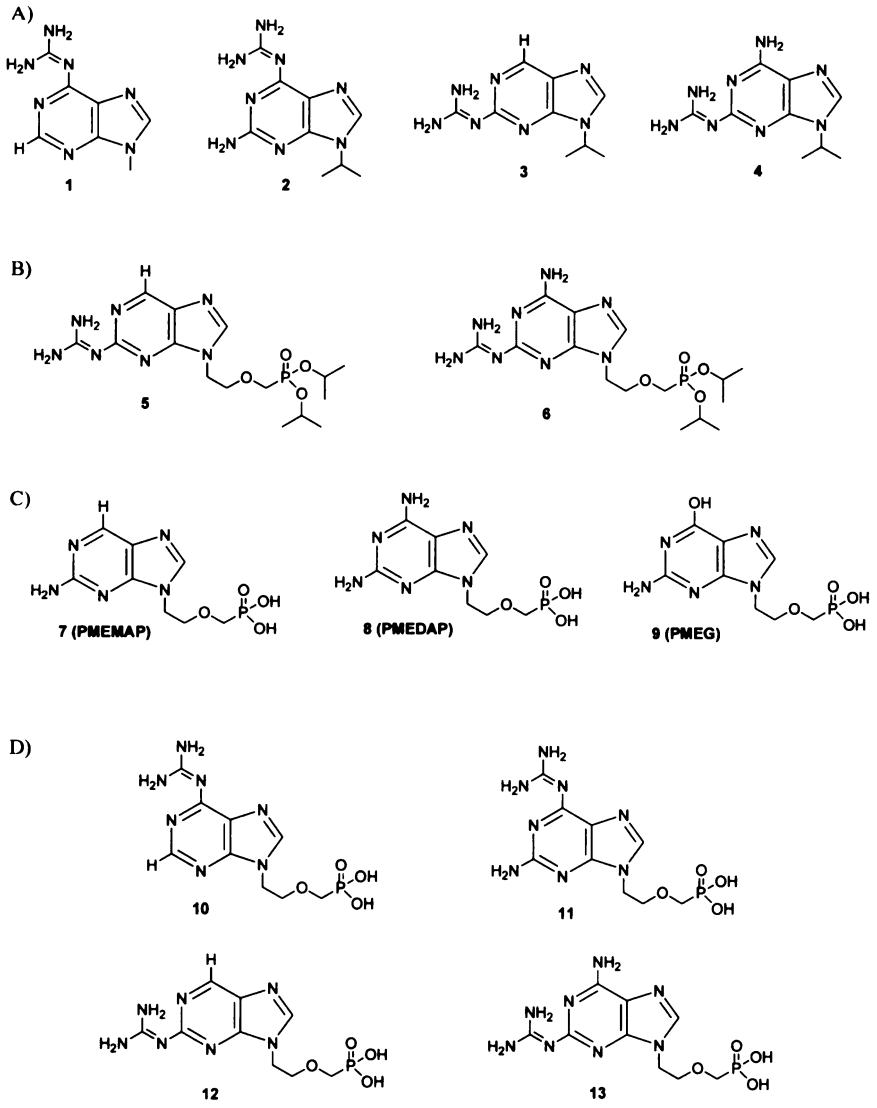

Figure 1. Molecular structures of analyzed compounds (A) guanidino 9-alkylpurines and amino-guanidino 9-alkylpurines; (B) acyclic nucleoside phosphonate diisopropyl esters of 2-guanidino-9-alkylpurines; (C) acyclic nucleoside phosphonates of amino 9-alkylpurines and PMEG; (D) acyclic nucleoside phosphonates of guanidino- and amino-guanidino 9-alkylpurines.

species B and BH^+, a_B and a_{BH^+}, are expressed as products of their molar concentrations, c_B and c_{BH^+}, and corresponding activity coefficients, γ_B and γ_{BH^+}, respectively. The activity coefficient γ_i of the charged species (ion *i*) in aqueous solution at 25°C can be calculated from the Debye–Hückel theory according to Eq. (3):

$$-\log\gamma_i = \frac{0.5085 z_i^2 \sqrt{I}}{1 + 3.281 a \sqrt{I}} \quad (3)$$

where z_i is the charge number and a is the effective diameter of the hydrated *i*th ion. The approximative average value of $a = 0.5$ nm was used in the calculations of the activity coefficients, since the exact diameters of hydrated ions are mostly unknown. The ionic strength of the solution (mol/dm^3), I, is defined by Eq. (4):

$$I = \frac{1}{2}\sum_i c_i z_i^2 \quad (4)$$

where c_i is molar concentration and z_i is the charge number of the *i*th ion in the solution.

The effective electrophoretic mobility m_{ef} of an analyte consisting of n ionic forms is defined by Eq. (5):

$$m_{ef} = \frac{\sum_{i=1}^{n} c_i m_i \mathrm{sign}(z_i)}{c} \quad (5)$$

where c_i, m_i, and z_i, are the molar concentration, actual ionic mobility and charge number of the *i*th ionic form, respectively, sign(z_i) is the sign of the charge number z_i and c is the total (analytical) concentration of the analyte. As follows from Eq. (5) effective mobility of the analyte as

a whole is equal to the sum of the products of molar fraction and ionic mobility of all ionic species of the analyte and it is related to molar concentrations of all ionic forms of the analyte and to the total (analytical) molar concentration of the analyte. On the other hand, the other experimentally measured parameter of CZE analyses, pH of the BGE, is related to the activity of the hydroxonium cations H_3O^+ (pH = $-\log(a_{H_3O^+})$). For that reason it is useful to introduce so-called "mixed" dissociation constant, K_a^{mix}, which is expressed by the activity of H_3O^+ cations and by molar concentrations of the ionic forms of the analyte; for the dissociation of the above protonated guanidinyl group of analyte 2 we can then obtain K_a^{mix} as

$$K_a^{mix} = \frac{a_{H_3O^+} c_B}{c_{BH^+}} \quad (6)$$

Since the activity coefficient of the electroneutral form of the base is supposed to be unity, the relationship between thermodynamic and mixed dissociation constants is

$$K_a = \frac{K_a^{mix}}{\gamma_{BH^+}} \quad (7)$$

or, after logarithmization and considering that $pk_a = -\log K_a$:

$$pK_a = pK_a^{mix} + \log\gamma_{BH^+} \quad (8)$$

As follows from Eq. (5) the effective mobility of the univalent base B, $m_{eff,B}$, is equal to

$$m_{eff,B} = m_{BH^+} \frac{c_{BH^+}}{c_{BH^+} + c_B} \quad (9)$$

where m_{BH^+} is actual ionic mobility of the protonated base, BH^+. The combination of Eqs. (6) and (9) provides the dependence of the effective mobility of base B, $m_{eff,B}$, on pH:

$$m_{eff,B} = \frac{m_{BH^+}}{1 + 10^{pH - pK_a^{mix}}} \quad (10)$$

Generally, the actual ionic mobility m_{BH^+} and mixed dissociation constant pK_a^{mix} are dependent on the ionic strength and temperature of the BGE, but if the CZE analyses are performed at constant ionic strength and temperature, then they can be considered as constant parameters of Eq. (10), and the effective mobility, $m_{eff,B}$, expressed by Eq. (10), can be considered as a function of pH only. This function can be then used as a regression function for fitting the pH dependence of the effective mobility obtained from CZE analyses of the investigated compounds in BGEs of different pH. The fitted parameters are the actual ionic mobility, m_{BH^+}, and the mixed dissociation constant, pK_a^{mix}, which can be subsequently corrected for the zero ionic strength, *i.e.*, to the thermodynamic dissociation constant pK_a (using Eq. 8) or to limiting (absolute) ionic mobilities (using one of the equations describing the concentration dependence of electrophoretic mobilities).

3.2 Acyclic nucleoside phosphonates of amino 9-alkylpurines

The acyclic nucleoside phosphonates of amino 9-alkylpurines (compounds **7** and **8**) behave as zwitterions with effective charge close to zero at strongly acidic BGEs due to the positive charge of protonated nitrogen in position 1 (N1) of purine moiety and the negative charge of hydrogenphosphonate (−1) group. With the increasing pH of the BGE these compounds are becoming negatively charged due to the deprotonation of N1 of purine and due to the dissociation of hydrogenphosphonate (−1) to phosphonate (−2). The dissociation equilibria of these type of compounds, using 2-amino-9-(2-(phosphonomethoxy)ethyl)-9*H*-purine (**7**, PMEMAP) as an example, are described as follows:

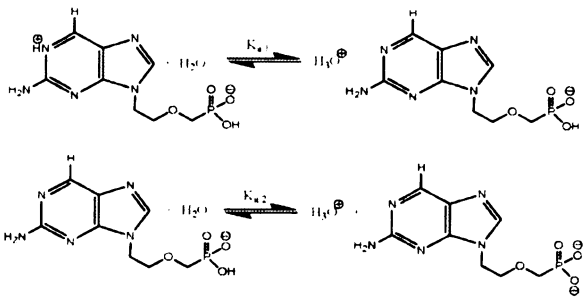

Scheme 2

Thermodynamic and mixed dissociation constants of the dissociation of protonated N1 in purine moiety, $K_{a,1}$ and $K_{a,1}^{mix}$, respectively, are given by

$$K_{a,1} = \frac{a_{H_3O^+} a_{HA^-B}}{a_{HA^-BH^+}} = \frac{a_{H_3O^+} c_{HA^-B} \gamma_{HA^-B}}{c_{HA^-BH^+} \gamma_{HA^-BH^+}} \quad (11)$$

$$K_{a,1}^{mix} = \frac{a_{H_3O^+} c_{HA^-B}}{c_{HA^-BH^+}} \quad (12)$$

where $a_{H_3O^+}$ is the activity of the hydroxonium ions, $a_{HA^-BH^+}$, ($c_{HA^-BH^+}$), and a_{HA^-B}, (c_{HA^-B}), are the activities (concentrations) of the zwitterionic and N1-deprotonated forms of acyclic nucleoside phosphonates of aminopurines, respectively.

The substitution of Eq. (12) in Eq. (11) and taking into account the unity value of activity coefficient of the zwitterionic form of the analyte result in the following relation between thermodynamic and mixed dissociation constants:

$$K_{a,1} = K_{a,1}^{mix} \gamma_{HA^-B} \quad (13)$$

or in the logarithmic form:

$$pK_{a,1} = pK_{a,1}^{mix} - \log\gamma_{HA^-B} \quad (14)$$

Thermodynamic and mixed dissociation constants of dissociation of phosphonic acid group to the second degree (−2), $K_{a,2}$ and $K_{a,2}^{mix}$, respectively, are given by the following equations:

$$K_{a,2} = \frac{a_{H_3O^+}a_{A^{2-}B}}{a_{HA^-B}} = \frac{a_{H_3O^+}c_{A^{2-}B}\gamma_{A^{2-}B}}{c_{HA^-B}\gamma_{HA^-B}} \quad (15)$$

$$K_{a,2}^{mix} = \frac{a_{H_3O^+}c_{A^{2-}B}}{c_{HA^-B}} \quad (16)$$

where a_{HA^-B}, (c_{HA^-B}), and $a_{A^{2-}B}$, ($c_{A^{2-}B}$), are the activities (concentrations) of the single and double negatively charged forms of acyclic nucleoside phosphonates of aminopurines, respectively.

Combination of Eqs. (15) and (16) provides the following relations between thermodynamic and mixed dissociation constants:

$$K_{a,2} = \frac{K_{a,2}^{mix}\gamma_{A^{2-}B}}{\gamma_{HA^-B}} \quad (17)$$

It is worth to mention that in this case the activity coefficients of two ionic species, HA^-B and $A^{2-}B$, have to be taken into account. After logarithmization of Eq. (17) and with respect to the relation $\log\gamma_{A^{2-}B} = 4\log\gamma_{HA^-B}$ (resulting from Eq. 3) the following relation is obtained for the thermodynamic and mixed dissociation constants:

$$pK_{a,2} = pK_{a,2}^{mix} - 3\log\gamma_{HA^-B} \quad (18)$$

For the dependence of the effective mobility of these types of analytes on pH the following equation can be derived:

$$m_{eff} = \frac{m_{HA^-B}10^{pK_{a,1}^{mix}-pH} - m_{A^{2-}B}10^{pH-pK_{a,2}^{mix}}}{1 + 10^{pK_{a,1}^{mix}-pH} + 10^{pH-pK_{a,2}^{mix}}} \quad (19)$$

where m_{HA^-B} and $m_{A^{2-}B}$ are the actual ionic mobilities of the ionic forms HA^-B and $A^{2-}B$, respectively.

3.3 Acyclic nucleoside phosphonates of (amino)guanidino 9-alkylpurines

The acyclic nucleoside phosphonates of (amino)guanidino 9-alkylpurines (compounds **10–13**) behave as zwitterions with effective charge close to zero in acidic BGEs, where the positive charge of the protonated guanidinyl group is compensated by the negative charge of hydrogenphosphonate. With the increasing pH of the BGE the effective charge of these compounds is becoming negative due to the dissociation of hydrogenphosphonate (−1) to phosphonate (−2) at around neutral pH and due the deprotonation of the guanidinyl group at alkaline pH. Using 6-guanidino-9-(2-(phosphonomethoxy)ethyl)-9*H*-purine (**10**) as a representative of these types of compounds, their dissociation equilibria can be described as shown in Scheme 3.

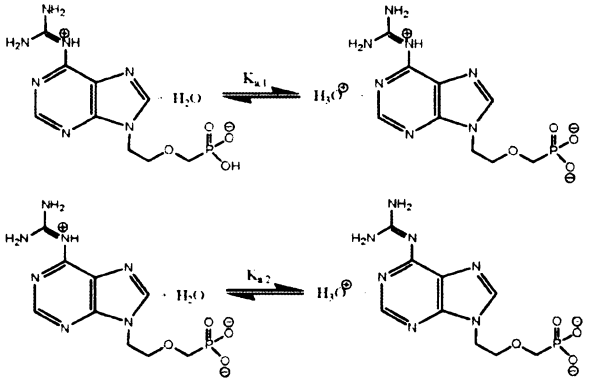

Scheme 3

The corresponding thermodynamic and mixed dissociation constants of phosphonic acid group to the second dissociation degree can be expressed as

$$K_{a,1} = \frac{a_{H_3O^+}a_{A^{2-}BH^+}}{a_{HA^-BH^+}} = \frac{a_{H_3O^+}c_{A^{2-}BH^+}\gamma_{A^{2-}BH^+}}{c_{HA^-BH^+}\gamma_{HA^-BH^+}} = K_{a,1}^{mix}\gamma_{A^{2-}BH^+} \quad (20)$$

where $a_{HA^-BH^+}$, ($c_{HA^-BH^+}$), and $a_{A^{2-}BH^+}$, ($c_{A^{2-}BH^+}$) are the activities (concentrations) of the zwitterionic and single charged anionic forms of this type of analytes, respectively, and the activity coefficient of the zwitterion, $\gamma_{HA^-BH^+}$, is supposed to be unity.

Similarly as in Section 3.2, the relation between thermodynamic and mixed dissociation constants can be expressed in the logarithmic form as

$$pK_{a,1} = pK_{a,1}^{mix} - \log\gamma_{A^{2-}BH^+} \quad (21)$$

Thermodynamic and mixed dissociation constants of the dissociation of the protonated guanidinyl group, $K_{a,2}$ and $K_{a,2}^{mix}$, respectively, are defined as

$$K_{a,2} = \frac{a_{H_3O^+}a_{A^{2-}B}}{a_{A^{2-}BH^+}} = \frac{a_{H_3O^+}c_{A^{2-}B}\gamma_{A^{2-}B}}{c_{A^{2-}BH^+}\gamma_{A^{2-}BH^+}} = \frac{K_{a,2}^{mix}\gamma_{A^{2-}B}}{\gamma_{A^{2-}BH^+}} \quad (22)$$

where $a_{A^{2-}BH^+}$, ($c_{A^{2-}BH^+}$), and $a_{A^{2-}B}$, ($c_{A^{2-}B}$) are the activities (concentrations) of the single charged and double charged anions of these type of analytes.

In the logarithmic form (and regarding the relationship $\log\gamma_{A^{2-}B} = 4\log\gamma_{A^{2-}BH^+}$) the relation between thermodynamic and mixed dissociation constants can be expressed as

$$pK_{a,2} = pK_{a,2}^{mix} - 3\log\gamma_{A^{2-}BH^+} \quad (23)$$

The dependence of the effective mobility of these types of analytes on pH is given by Eq. (24):

$$m_{eff} = \frac{m_{A^{2-}B} 10^{pK_{a,2}^{mix} - pH} - m_{A^{2-}BH^+} 10^{pH - pK_{a,1}^{mix}}}{1 + 10^{pH - pK_{a,1}^{mix}} + 10^{pK_{a,2}^{mix} - pH}} \quad (24)$$

where $m_{A^{2-}BH^+}$ and $m_{A^{2-}B}$ are the actual ionic mobilities of the ionic forms $A^{2-}BH^+$ and $A^{2-}B$, respectively.

3.4 9-(2-(Phosphonomethoxy)ethyl)guanine

PMEG (**9**) behaves as a trivalent acid owing to the presence of two acidic anionogenic hydroxyl groups of phosphonic acid and single enol −OH group in position 6 of purine moiety. The phosphonic acid is fully dissociated into the first degree below pH 3.5; thus, in the applied pH range (3.50–11.25), only the dissociation of hydrogen phosphonate (−1) to phosphonate (−2) and the dissociation of the enol −OH group can be monitored by CZE. These two acid-base equilibria of PMEG can be described as shown in Scheme 4.

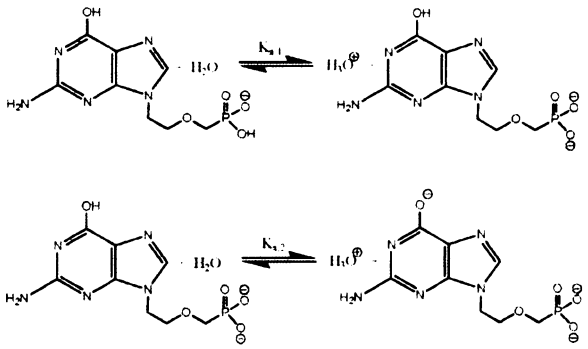

Scheme 4

The corresponding thermodynamic and mixed dissociation constants of phosphonic acid group to the second dissociation degree can be expressed as

$$K_{a,1} = \frac{a_{H_3O^+} a_{HA^{2-}}}{a_{H_2A^-}} = \frac{a_{H_3O^+} c_{HA^{2-}} \gamma_{HA^{2-}}}{c_{H_2A^-} \gamma_{H_2A^-}} = K_{a,1}^{mix} \frac{\gamma_{HA^{2-}}}{\gamma_{H_2A^-}} \quad (25)$$

where $a_{HA^{2-}}$, ($c_{HA^{2-}}$) and $a_{H_2A^-}$, ($c_{H_2A^-}$) are activities (concentrations) of double and single charged anions of **9** (PMEG), respectively.

Similarly as in the previous Sections 3.2 and 3.3 (regarding the relation $\log\gamma_{HA^{2-}} = 4\log\gamma_{H_2A^-}$) the relation between thermodynamic and mixed dissociation constants can be expressed as:

$$pK_{a,1} = pK_{a,1}^{mix} - 3\log\gamma_{H_2A^-} \quad (26)$$

Thermodynamic and mixed dissociation constants of the dissociation of the enol hydroxyl group at position 6 of purine, $K_{a,2}$ and $K_{a,2}^{mix}$, respectively, can be expressed as

$$K_{a,2} = \frac{a_{H_3O^+} a_{A^{3-}}}{a_{HA^{2-}}} = \frac{a_{H_3O^+} c_{A^{3-}} \gamma_{A^{3-}}}{c_{HA^{2-}} \gamma_{HA^{2-}}} = K_{a,2}^{mix} \frac{\gamma_{A^{3-}}}{\gamma_{HA^{2-}}} \quad (27)$$

where $a_{A^{3-}}$, ($c_{A^{3-}}$), and $a_{HA^{2-}}$, ($c_{HA^{2-}}$) are the activities (concentrations) of the triple charged and double charged anions of **9** (PMEG), respectively.

Following the above procedure and regarding the relationships $\log\gamma_{HA^{2-}} = 4\log\gamma_{H_2A^-}$ and $\log\gamma_{A^{3-}} = 9\log\gamma_{H_2A^-}$, the relation between thermodynamic and mixed dissociation constants can be expressed as

$$pK_{a,2} = pK_{a,2}^{mix} - 5\log\gamma_{H_2A^-} \quad (28)$$

The dependence of the effective mobility of this type of analyte on pH is given by Eq. (29):

$$m_{eff} = \frac{m_{HA^{2-}} 10^{pK_{a,1}^{mix} - pH} + m_{A^{3-}} 10^{pK_{a,2}^{mix} - pH}}{1 + 10^{pK_{a,1}^{mix} - pH} + 10^{pK_{a,2}^{mix} - pH}} \quad (29)$$

where $m_{A^{3-}}$ and $m_{HA^{2-}}$ are the actual ionic mobilities of the ionic forms A^{3-} and HA^{2-}, respectively.

4 Results and discussion

4.1 Selection of experimental conditions

For pK_a determination by CZE it is important to select experimental conditions in such a way that the measured effective mobilities are obtained as precisely and accurately as possible. As stated above, the actual ionic and effective mobilities depend on ionic strength and temperature. Consequently, the mobilities should be measured in the BGEs of constant ionic strength and at constant temperature. Measurements of effective mobilities in the pH range 3.50–11.25 allowed us to use the BGEs of constant ionic strength, 25 mM. The appropriate mixtures of the buffering anionic constituents with pK_a values close to pH of the BGE ($pH_{BGE} = pK_a \pm 0.7$) and strong cationic counterion (Tris for formic acid-based BGEs, pH 3.50–4.25, sodium for the other BGEs) were used for preparation of BGEs with this constant ionic strength and also with sufficient buffering capacity. The mobility measurement at constant temperature of 25°C was ensured by thermostating the outer polyimide capillary surface to constant temperature of 24°C and by setting the input power to the value of 0.66 W *per* meter of the capillary length, which causes 1°C temperature increase inside the capillary, resulting in the constant temperature of 25°C inside the capillary (see Section 2.4).

Another important factor is selection of the detection wavelength of the UV-absorption detector. With the photodiode array detector it was possible to detect the analytes in the broad wavelength range 190–300 nm. The detection wavelength of the analyzed compounds was set at their absorption maximum, at 225 nm, allowing their detection at low-concentration level below 0.1 mM, whereas the optimal detection wavelength for determination of migration time of the EOF marker (DMSO or isophorone) was 250 nm. The examples of CZE analyses of one of the investigated analytes, 2,6-diamino-9-(2-(phosphonomethoxy)ethyl)-9*H*-purine (compound **8**, PMEDAP) in three different BGEs are shown in Fig. 2. Figure 2A shows the analysis of this compound in the strongly acidic Tris-formate BGE, pH 3.75, in which PMEDAP is present mostly in its zwitterionic form with slightly negative effective charge resulting in counter EOF anionic migration with migration time close behind that of the EOF marker. In the weakly acidic sodium/MOPS BGE, pH 6.5, the effective charge of PMEDAP is close to -1 elementary charge due to the deprotonation of the N1 of purine resulting in the higher effective mobility and more distant position of the PMEDAP peak behind the EOF marker peak in Fig. 2B. CZE analysis of PMEDAP in alkaline sodium/CAPS BGE, pH 10.5 (see Fig. 2C) shows further increase of the relative migration time difference between PMEDAP and EOF marker peaks as a result of the increased PMEDAP effective charge and mobility due to the dissociation of the phosphonic acid group to the second degree. All these figures show the presence of small amounts of nonidentified admixtures (peaks X) in the synthetic PMEDAP preparation, which were not detected by HPLC analysis of this compound. This confirms complementarity of CZE and HPLC separation methods.

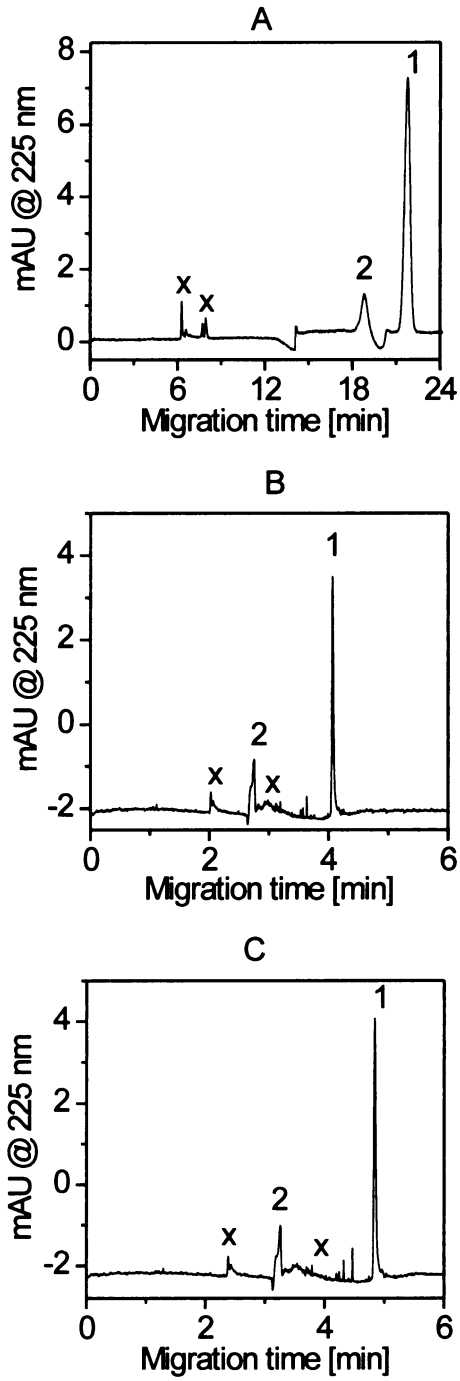

Figure 2. Selected records of CZE analysis of compound **8** (PMEDAP) in three different BGEs: (A) 47 mM HCOOH +25 mM Tris, pH 3.75; (B) 132 mM MOPS +25 mM NaOH, pH 6.50; (C) 41 mM CAPS +25 mM NaOH, pH 10.50. Capillary total/effective length 394/292 mm, ID/OD 75/360 μm; hydrodynamic sample injection 6.9–13.8 mbar for 5–10 s; UV-absorption detection at 225 nm; sample dissolved in deionized water in concentration 0.1 mM. 1, PMEDAP; 2, EOF marker; x, nonidentified admixtures.

4.2 Estimation of effective charge and effective electrophoretic mobility

In the applied pH range the effective charge of (amino)-guanidino 9-alkylpurines (**1–4**) and acyclic nucleoside phosphonate isopropyl diesters of (amino)-guanidinopurines (**5** and **6**) was changed from +1 elementary charge (e) at pH 3.50 to charge zero at pH 11.25 due to the deprotonation of the guanidinyl group. Effective mobility of the fully protonated cationic form of these compounds at pH 3.5 was in the range $(20.7–24.5) \times 10^{-9}$ $m^2V^{-1}s^{-1}$ for (amino)guanidino 9-isopropylpurines (**1–4**) and around the 16.3×10^{-9} $m^2V^{-1}s^{-1}$ value for acyclic nucleoside phosphonate diisopropyl esters (**5** and **6**), respectively. The lower mobility of **5** and **6** compared to the mobility of **1–4** reflects the lower charge to mass ratio of the former compounds due to their higher M_r at approximately the same charge as that of the latter compounds. The effec-

tive charge and the effective mobility of the acyclic nucleoside phosphonates of aminopurines (**7** and **8**) were close to zero at pH 3.5, resulting from their zwitterionic forms, in which the positive charge of protonated nitrogen in position 1 (N1) of purine moiety is compensated by the negative charge of the hydrogenphosphonate (−1) group. Effective charge of these compounds at alkaline pH 11.25 has changed to -2 e, and effective mobility was in the range (31.5–32.1) × 10^{-9} $m^2V^{-1}s^{-1}$.

Effective charge of **9** (PMEG) was negative in the whole applied pH range of BGEs being close to −1 e at pH 3.5 due to the dissociation of phosphonic acid group to the first degree and possessing increasing negative charge with increasing pH; at weakly alkaline BGEs the charge achieved a value of −2 e due to the dissociation of hydrogenphosphonate (−1) to phosphonate (−2), and at strongly alkaline pH 11.25 the charge was close to −3 e, since at this pH also the weakly acidic enol −OH group at position 6 of purine moiety has been almost fully dissociated. Consequently, the effective mobility of this analyte was also negative within the whole applied pH range achieving values of -17.9 × 10^{-9} $m^2V^{-1}s^{-1}$ for monovalent anion, −29.5 × 10^{-9} $m^2V^{-1}s^{-1}$ for divalent anion and −39.7 × 10^{-9} $m^2V^{-1}s^{-1}$ for trivalent anion.

The effective charge of acyclic nucleoside phosphonates of (amino)-guanidino purines with guanidinyl group in position 2 or 6 of purine moiety (compounds **10–13**) was close to zero at pH 3.5, resulting from their zwitterionic forms, in which the positive charge of protonated guanidinyl group is compensated by the negative charge of hydrogenphosphonate (−1) group. Effective charge of these compounds at weakly alkaline BGEs was close to −1 e with effective mobility in the range (−12.6 to −15.4) × 10^{-9} $m^2V^{-1}s^{-1}$ and at alkaline pH 11.25 the charge was close to -2 e, and effective mobility was in the range (−22.5 to -27.4) × 10^{-9} $m^2V^{-1}s^{-1}$. The values of effective charges and effective mobilities at 25°C in BGEs of 25 mM ionic strength and at pH 3.5 and 11.25 are summarized in Table 3.

Table 3. Effective electrophoretic mobilities, m_{eff}, and effective charges, q, at pH 3.5 and 11.25

Compound number	m_{eff}, 10^{-9} $m^2V^{-1}s^{-1}$ a)		q, (e) a)	
	pH 3.5	pH 11.25	pH 3.5	pH 11.25
1	24.5	0	+1.0	0
2	21.3	0	+1.0	0
3	21.7	0	+1.0	0
4	20.7	0	+1.0	0
5	16.9	0	+1.0	0
6	16.4	0	+1.0	0
7 (PMEMAP)	0	−31.4	0	−2
8 (PMEDAP)	0	−30.4	0	−2
9 (PMEG)	−17.9	−39.7	−1.0	−3
10	7	−26.9	0	−2
11	0	−26.7	0	−2
12	0	−28.0	0	−2
13	0	−23.1	0	−1.8

a) Related to standard temperature 25°C and ionic strength 25 mM.

4.3 Determination of thermodynamic dissociation constants

The calculation of mixed dissociation constants was accomplished by nonlinear fitting of the sets of experimentally determined effective electrophoretic mobilities within a broad pH range using the computer program Origin with appropriate regression functions, Eqs. (9), (19), (24), and (29). The courses of these functions for monovalent bases of (amino)guanidino 9-alkylpurines (**1–4**) and the acyclic nucleoside phosphonate diisopropyl esters (**5** and **6**) are depicted in Fig. 3, for the zwitterionic to divalent anionic acyclic nucleoside phosphonate of aminopurines (**7** and **8**) and for the trivalent anionic PMEG (**9**) in Fig. 4, and for the zwitterionic to divalent anionic acyclic nucleoside phosphonates of (amino)guanidino 9-alkylpurines (**10–13**) in Fig. 5. The values of correlation coefficient, mixed dissociation constants and actual cationic or anionic mobilities of the individual ionic species of the analyzed compounds are presented in the text parts of the figures. Thermodynamic dissociation constants, pK_a, were recalculated from mixed dissociation constants using Eq. (8) for dissociation of protonated guanidinyl group in amino-guanidino-9-alkylpurines (**1–4**) and the acyclic nucleoside phosphonate diisopropyl esters (**5** and **6**), Eqs. (14) and (18) for dissociation of protonated N1 of purine moiety and dissociation of phosphonic acid group to the second degree, respectively, in acyclic nucleoside phosphonates of aminopurines (**7** and **8**), Eqs. (21) and (23) for dissociation of phosphonic acid group to the second degree and dissociation of protonated guanidinyl group, respectively, in the acyclic nucleoside phosphonates of (amino)-guanidino 9-alkylpurines (**10–13**), and Eqs. (26) and (28) for dissociation of phosphonic acid group to the second degree and for dissociation of enol −OH group, respectively, in PMEG (**9**).

Thermodynamic pK_a of the protonated guanidinyl group was determined to be in the range 7.77–9.64 for (amino)-guanidino 9-alkylpurines (**1–4**), 9.85 and 9.26 for their acyclic nucleoside phosphonate diisopropyl esters (**5** and **6**) and 8.29–10.32 for their acyclic nucleoside phosphonates, pK_a of a phosphonic acid group to the second dissociation degree (−2) was found to be in the range

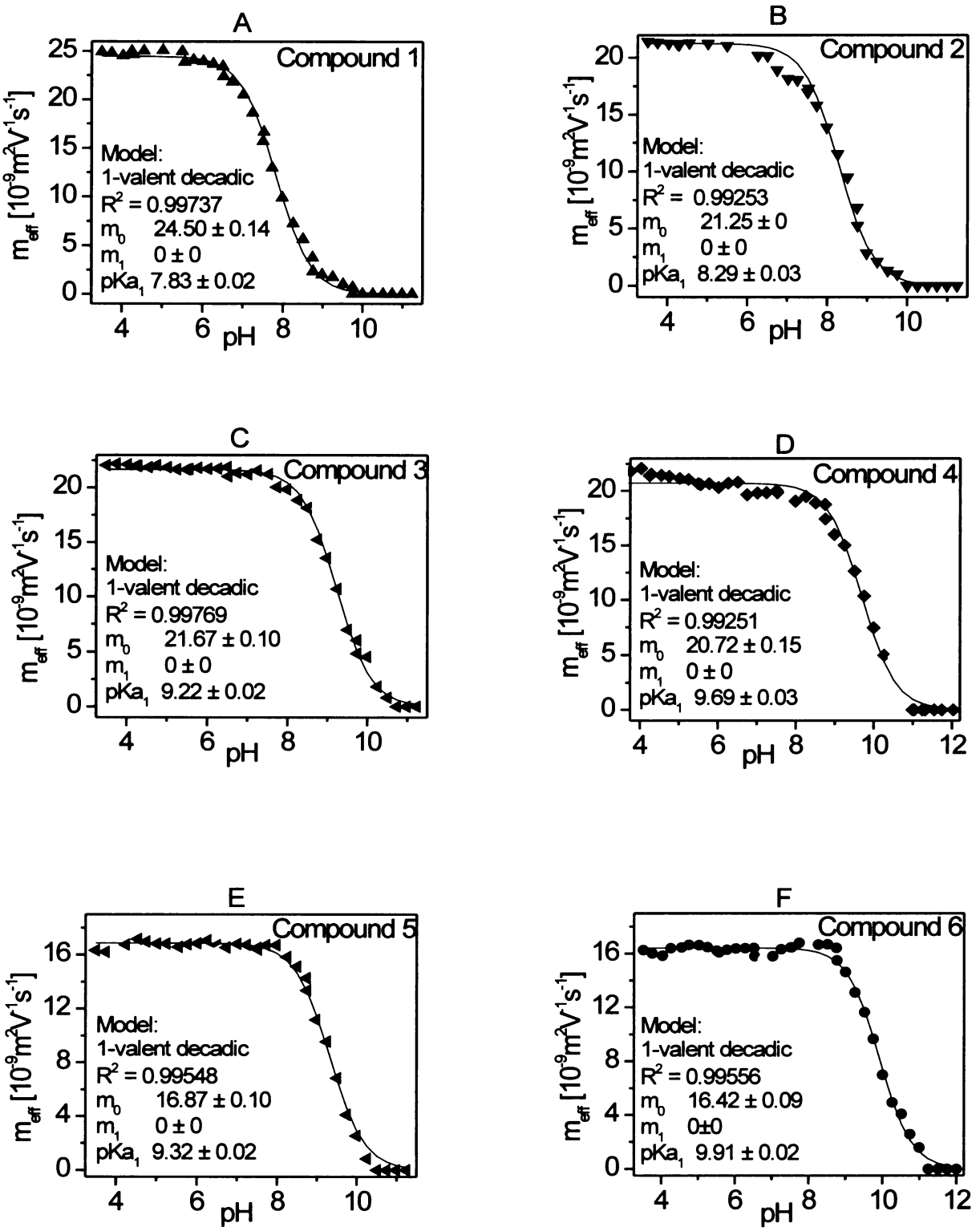

Figure 3. Dependencies of effective electrophoretic mobilities, m_{eff}, of (amino)guanidino 9-alkyl purines (**1–4**) and the acyclic nucleoside phosphonate diisopropyl esters (**5** and **6**) on pH. R, correlation coefficient; m, actual ionic mobility; pK_a, mixed dissociation constant.

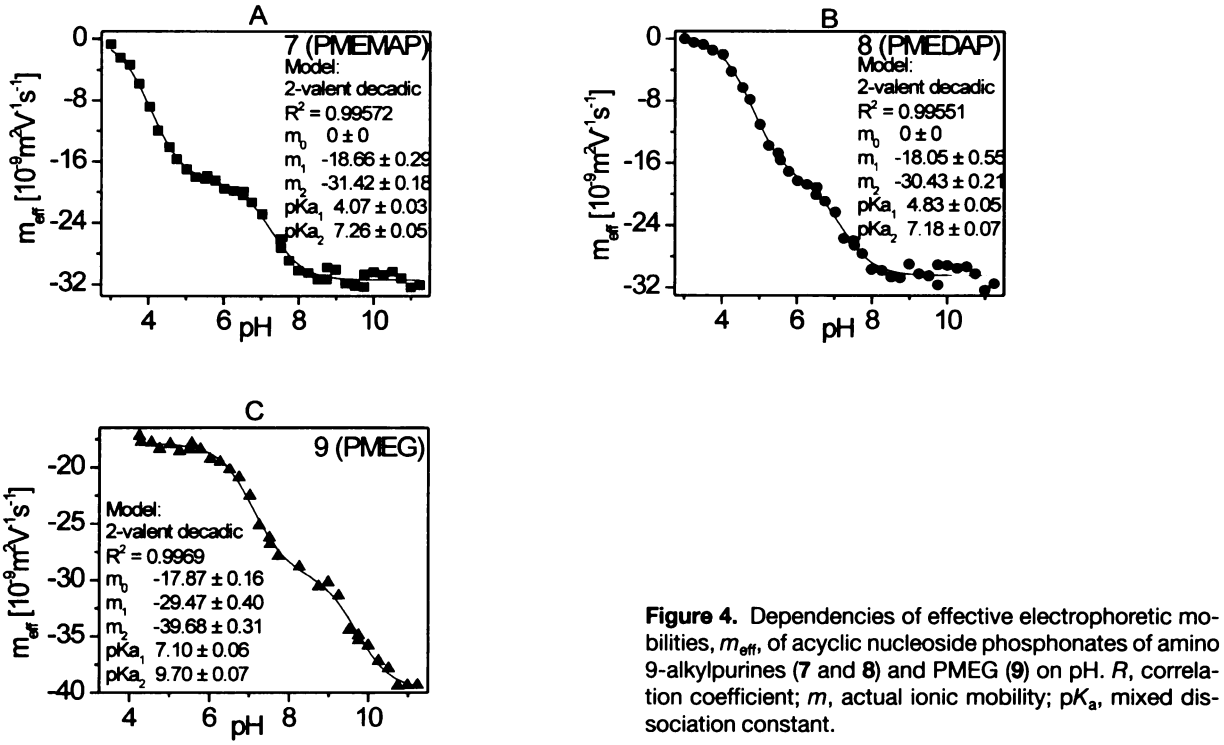

Figure 4. Dependencies of effective electrophoretic mobilities, m_{eff}, of acyclic nucleoside phosphonates of amino 9-alkylpurines (**7** and **8**) and PMEG (**9**) on pH. *R*, correlation coefficient; *m*, actual ionic mobility; pK_a, mixed dissociation constant.

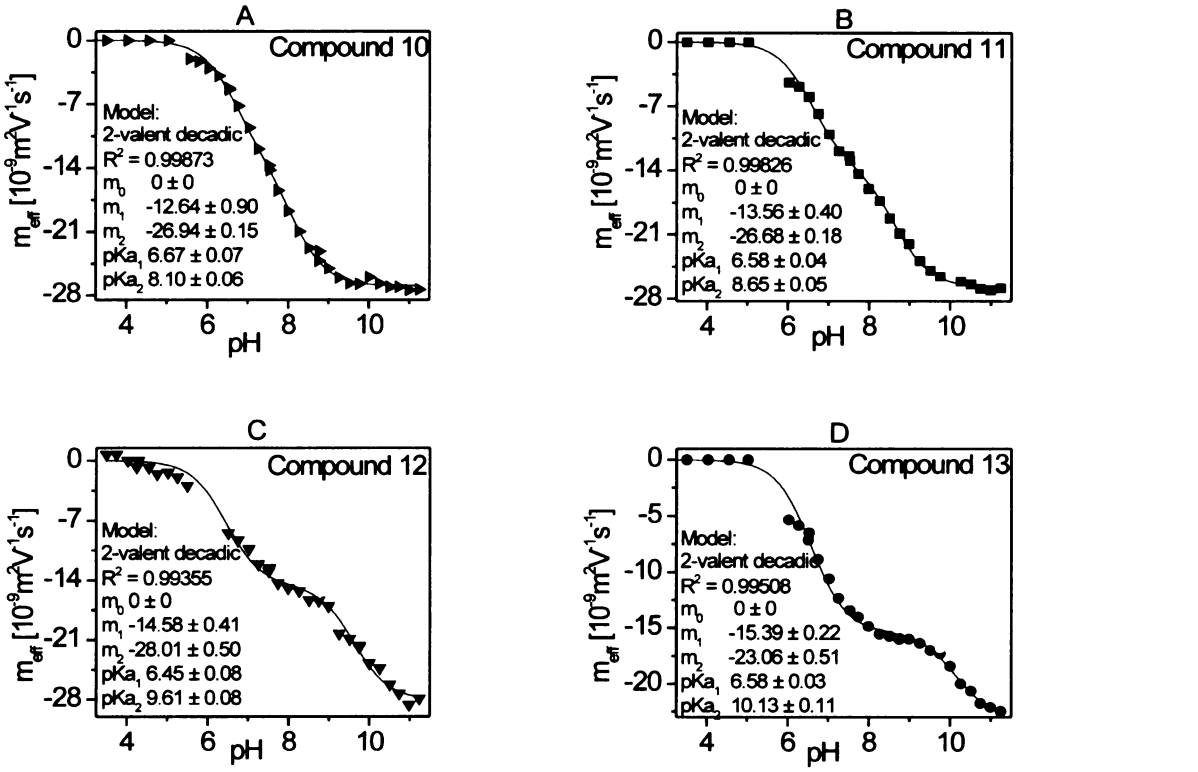

Figure 5. Dependencies of effective electrophoretic mobilities, m_{eff}, of acyclic nucleoside phosphonates of (amino)guanidino 9-alkylpurines (**10–13**) on pH. *R*, correlation coefficient; *m*, actual ionic mobility; pK_a, mixed dissociation constant.

Table 4. Thermodynamic pK_a values of ionogenic groups of analyzed compounds (at 25°C)

Compound number	pK_a		
	$(N1)H^+/(N1)$	$P(OH)O^-/P(O)_2^{2-}$	$(G)H^+/(G)$
1	n.d.	n.p.	7.77 ± 0.02
2	n.d.	n.p.	8.23 ± 0.03
3	n.d.	n.p.	9.16 ± 0.02
4	n.d.	n.p.	9.64 ± 0.03
5	n.d.	n.p.	9.26 ± 0.02
6	n.d.	n.p.	9.85 ± 0.03
7 (PMEMAP)	4.13 ± 0.04	7.46 ± 0.06	n.p.
8 (PMEDAP)	4.89 ± 0.05	7.37 ± 0.07	n.p.
9 (PMEG)	n.d.	7.29 ± 0.06	10.02 ± 0.07 (enol)[a]
10	n.d.	6.86 ± 0.06	8.29 ± 0.06
11	n.d.	6.77 ± 0.04	8.84 ± 0.05
12	n.d.	6.64 ± 0.08	9.80 ± 0.08
13	n.d.	6.77 ± 0.03	10.32 ± 0.11

a) The value belongs to the dissociation of the enol hydroxyl group of PMEG, guanidinyl group is not present in PMEG.

$(N1)H^+/(N1)$, dissociation of protonated N1 in purine moiety; $P(OH)O^-/P(O)_2^{2-}$, dissociation of phosphonic acid group to the second degree (−2); $(G)H^+/(G)$, dissociation of protonated guanidinyl group; n.d., not determined; n.p., not present.

6.64–6.86 for acyclic nucleoside phosphonates of (amino)-guanidinopurines (**10–13**) and in the range 7.29–7.46 for acyclic nucleoside phosphonates of aminopurines (**7** and **8**), pK_a of protonated nitrogen in position 1 (N1) of purine moiety was estimated to be 4.13 and 4.89 for acyclic nucleoside phosphonates of aminopurines (**7** and **8**). The values of thermodynamic pK_a with their SD are presented in Table 4.

From the comparison of these pK_a values the following conclusions can be drawn: Basicity of the guanidino derivatives (compounds **1–6** and **10–13**) with pK_a values in the range 7.77–10.32 is much higher (by three to six orders of magnitude) than that of the amino derivatives (**7** and **8**) with pK_a equal to 4.13 and 4.89, respectively. The stronger basicity of the guanidino derivatives compared to amino derivatives is reflected by the increased acidity of phosphonic acid in the former derivatives, see the pairs **12** (pK_a 6.64) *versus* **7** (pK_a 7.46), and **13** (pK_a 6.77) *versus* **8** (pK_a 7.37). Basicity of the derivatives with guanidinyl group in position 2 of purine is significantly larger (*ca.* by 1.5 unit difference in pK_a) than that of the compounds having guanidinyl group in position 6 of purine, see the pairs **3** (pK_a 9.16) *versus* **1** (pK_a 7.77), **4** (pK_a 9.64) *versus* **2** (pK_a 8.23), **12** (pK_a 9.80) *versus* **10** (8.29), and **13** (pK_a 10.32) *versus* **11** (pK_a 8.84). Basicity of the amino-guanidino derivatives is higher than that of the guanidino derivatives (*ca.* by the 0.5 unit difference in pK_a), see the pairs **2** (pK_a 8.23) *versus* **1** (pK_a 7.77), **4** (pK_a 9.64) *versus* **3** (pK_a 9.16), **6** (pK_a 9.85) *versus* **5** (pK_a 9.26), **11** (pK_a 8.84) *versus* **10** (pK_a 8.29), **13** (pK_a 10.32) *versus* **12** (pK_a 9.80). Similarly, the basicity of PMEDAP (**8**) (pK_a 4.89) with two amino groups in positions 2 and 6 of purine is higher than that of PMEMAP (**7**) (pK_a 4.13) with single amino group at position 2 of purine. As it was expected the basicity of the guanidinyl derivatives with free phoshonic acid group was found higher, *ca.* by 0.5–0.6 unit of pK_a, than that of 9-alkyl derivatives, see the pairs **10** (pK_a 8.29) *versus* **1** (pK_a 7.77), **11** (pK_a 8.84) *versus* **2** (pK_a 8.23), **12** (pK_a 9.80) *versus* **3** (pK_a 9.16), **13** (pK_a 10.32) *versus* **4** (pK_a 9.64). Approximately the same difference of basicity (0.5 unit of pK_a) was found in favor of the guanidinyl derivatives with free phosphonic acid when compared with their diisopropyl esters, see the pairs **12** (pK_a 9.80) *versus* **5** (pK_a 9.26), and **13** (pK_a 10.32) *versus* **6** (pK_a 9.85). In these last two cases apparently the basicity of the guanidinyl group is enlarged by the presence of anionogenic phosphonic acid group and by the potential of these compounds to form zwitterions. Basicity of the nonanionogenic diisopropyl esters of guanidino derivatives was only slightly higher (*ca.* 0.1–0.2 unit of pK_a) than that of the also nonanionogenic alkyl derivatives, see the pairs **5** (pK_a 9.26) *versus* **3** (pK_a 9.16), and **6** (pK_a 9.85) *versus* **4** (pK_a 9.64).

The determined pK_a values of the protonated nitrogen in position 1 of amino 9-alkylpurines, pK_a values of phosphonic acid to the second dissociation degree and pK_a values of enol hydroxyl group of PMEG were in a good agreement with pK_a values of these ionogenic groups in the related compounds determined by potentiometric pH titration [34].

In conclusion, CZE has proved to be a suitable and useful method for determination of dissociation constants (pK_a) of amino and (amino)guanidinopurine nucleotide analogs, such as acyclic nucleoside phosphonate, acyclic nucleoside phosphonate diesters and other related compounds, in a microscale, applying only few nanoliter sample volumes of 0.1 mM analyte solution *per* analysis. The determination of pK_a values of a series of the above related compounds allowed to quantify their basicity and to detect certain correlations between the basicity and the structure of these analytes.

This work was supported by the Grant Agency of the Czech Republic, Grants No. 203/03/0716, 203/04/0098, 203/05/2539, by the Research Project Z40550506 and Target Project 1QS400550501 of the Czech Academy of Sciences. It was performed within the frame of the pro-

jects of the Centre for New Antivirals and Antineoplastics ID 1M6138896301 of the Ministry of Education of the Czech Republic.

5 References

[1] Poole, S. K., Patel, S., Dehring, K., Workman, H., Poole, C. F., *J. Chromatogr. A* 2004, *1037*, 445–454.

[2] Česnek, M., Holý, A., Masojídková, M., *Tetrahedron* 2002, *58*, 2985–2996.

[3] Česnek, M., Holý, A., Masojídková, M., Zídek, Z., *Bioorg. Med. Chem.* 2005, *13*, 2917–2926.

[4] Ornskov, E., Linusson, A., Folestad, S., *J. Pharm. Biomed. Anal.* 2003, *33*, 379–391.

[5] Wan, H., Holmen, A. G., Wang, Y. D., Lindberg, W. *et al.*, *Rapid Commun. Mass Spectrom.* 2003, *17*, 2639–2648.

[6] Ishihama, Y., Nakamura, M., Miwa, T., Kajima, T., Asakawa, N., *J. Pharm. Sci.* 2002, *91*, 933–942.

[7] Caliaro, G. A., Herbots, C. A., *J. Pharm. Biomed. Anal.* 2001, *26*, 427–434.

[8] Kibbey, C. E., Poole, S. K., Robinson, B., Jackson, J. D., Durham, D., *J. Pharm. Sci.* 2001, *90*, 1164–1175.

[9] Wang, D. X., Yang, G. L., Song, X. R., *Electrophoresis* 2001, *22*, 464–469.

[10] Gong, S. X., Su, X. D., Bo, T., Zhang, X. *et al.*, *J. Sep. Sci.* 2003, *26*, 549–554.

[11] Herrero-Martinez, J. M., Sanmartin, M., Roses, M., Bosch, E., Rafols, C., *Electrophoresis* 2005, *26*, 1886–1895.

[12] Včeláková, K., Zusková, I., Kenndler, E., Gaš, B., *Electrophoresis* 2004, *25*, 309–317.

[13] Koval, D., Kašička, V., Jiráček, J., Collinsová, M., Garrow, T. A., *J. Chromatogr. B* 2002, *770*, 145–154.

[14] Sanz-Nebot, V., Toro, I., Benavente, F., Barbosa, J., *J. Chromatogr. A* 2002, *942*, 145–156.

[15] Psurek, A., Scriba, G. K. E., *Electrophoresis* 2003, *24*, 765–773.

[16] Dobos, Z., Lorand, T., Hollosy, F., Hallgas, B. *et al.*, *J. Chromatogr. B* 2004, *799*, 179–183.

[17] Barták, P., Bednář, P., Stránský, Z., Boček, P., Vespalec, R., *J. Chromatogr. A* 2000, *878*, 249–259.

[18] Foulon, C., Danel, C., Vaccher, C., Yous, S. *et al.*, *J. Chromatogr. A* 2004, *1035*, 131–136.

[19] Surmann, J. P., Warnke, U., *Pharmazie* 2001, *56*, 943–945.

[20] Wu, X. M., Gong, S. X., Bo, T., Liao, Y. P., Liu, H. W., *J. Chromatogr. A* 2004, *1061*, 217–223.

[21] Mofaddel, N., Bar, N., Villemin, D., Desbene, P. L., *Anal. Bioanal. Chem.* 2004, *380*, 664–668.

[22] Matoga, M., Laborde-Kummer, E., Langlois, M. H., Dallet, P. *et al.*, *J. Chromatogr. A* 2003, *984*, 253–260.

[23] Fang, X. M., Gong, F. Y., Ye, J. N., Fang, Y. Z., *Chromatographia* 1997, *46*, 137–140.

[24] Mendonsa, S. D., Hurtubise, R. J., *J. Chromatogr. A* 1999, *841*, 239–247.

[25] Cantu, M. D., Hillebrand, S., Carrilho, E., *J. Chromatogr. A* 2005, *1068*, 99–105.

[26] Porras, S. P., Jyske, P., Riekkola, M. L., Kenndler, E., *J. Microcol. Sep.* 2001, *13*, 149–155.

[27] Jimenez-Lozano, E., Marques, I., Barron, D., Beltran, J. L., Barbosa, J., *Anal. Chim. Acta* 2002, *464*, 37–45.

[28] Barbosa, J., Barron, D., Cano, J., Jimenez-Lozano, E. *et al.*, *J. Pharm. Biomed. Anal.* 2001, *24*, 1087–1098.

[29] Buckenmaier, S. M. C., McCalley, D. V., Euerby, M. R., *J. Chromatogr. A* 2004, *1026*, 251–259.

[30] Beckers, J. L., Everaerts, F. M., Ackermans, M. T., *J. Chromatogr.* 1991, *537*, 407–428.

[31] Cai, J., Smith, J. T., El Rassi, Z., *J. High Resolut. Chromatogr.* 1992, *15*, 30–32.

[32] Koval, D., Kašička, V., Jiráček, J., Collinsová, M., *Electrophoresis* 2003, *24*, 774–781.

[33] Hagberg, J., Duker, A., Karlsson, S., *Chromatographia* 2002, *56*, 641–644.

[34] Gomez-Coca, R. B., Kapinos, L. E., Holý, A., Vilaplana, R. A. *et al.*, *J. Chem. Soc., Dalton Trans.* 2000, *13*, 2077–2084.

VI

Veronika Šolínová
Václav Kašička

Institute of Organic Chemistry and Biochemistry, Academy of Sciences of the Czech Republic, Prague, Czech Republic

Review

Recent applications of conductivity detection in capillary and chip electrophoresis

The review provides a comprehensive survey of the recent applications of contact and contactless conductivity detection in capillary electrophoretic and chip electrophoretic analyses of a broad scale of compounds, from low-molecular-mass highly mobile small inorganic and organic ions, *via* medium-molecular-mass peptides and oligo- and polynucleotides up to high-molecular-mass biopolymers, proteins and nucleic acids fragments. The review presents also the recent developments in the construction of different types of conductivity detectors (detectors with galvanic contact of the sensing electrodes with the BGE and sample components, contactless conductivity detectors with capacitively coupled tubular and semitubular electrodes and combined conductivity/optical detectors) applied in the capillary electromigration methods performed in classical fused silica, polytetrafluorethylene, and polyetheretherketone capillaries or on glass and polymethylmethacrylate microchips. In addition, the principle and theoretical bases of conductivity detection in capillary electromigration techniques, zone electrophoresis, ITP, micellar EKC, and electrochromatography are briefly described.

Keywords: Capillary electrophoresis / Chip electrophoresis / Conductivity detection / Contactless conductivity detection

Received: April 25, 2006; revised: May 19, 2006; accepted: May 20, 2006

DOI 10.1002/jssc.200600167

1 Introduction

Contact conductivity detection and especially the contactless conductivity detection (CLCD) have become within the last years frequently used detection techniques in capillary electromigration methods [1–4]. The recent improvements in the construction of the capacitively coupled contactless conductivity detectors and their electronic circuitry have led to the higher sensitivity and robustness of these detectors, and also to their commercial utilization. In addition, due to their miniature dimensions and relatively simple construction, the conductivity detectors are also successfully integrated in the microfluidic chip electrophoresis devices. The increasing number of applications shows that conductivity detection is suitable not only for detection of chromophore- and fluorophore-free small inorganic and organic ions but also for other types of ionogenic compounds, including medium- and high-molecular-mass biomolecules, such as peptides, proteins, oligo- and polynucleotides, and nucleic acids fragments.

Conductivity detection in CE is performed in two modes either with or without direct contact of the sensing electrodes with the BGE and the sample components. The first conductivity detectors used in the CE methods had the electrodes in contact with the BGE. They were developed already in the 1970s for capillary ITP (CITP) [5, 6]. They have been much more sensitive than the previously used temperature detectors but their great disadvantage was that during the electromigration passage through the detector the BGE constituents and sample components interacted electrochemically or by a simple adsorp-

Correspondence: Dr. Václav Kašička, Institute of Organic Chemistry and Biochemistry, Academy of Sciences of the Czech Republic, Flemingovo 2, 166 10 Prague 6, Czech Republic.
E-mail: kasicka@uochb.cas.cz.
Fax: +420-220-183-592.

Abbreviations: **AA**, amino acid; **AC**, alternating current; **AcOH**, acetic acid; **AMP**, 2-amino-2-methyl-1-propanol; **AMPD**, 2-amino-2-methyl-1,3-propanediol; **BTP**, Bis-Tris propane; **18C6E**, 18-crown-6-ether; **18C6EH4**, 18-crown-6-ether-tetracarboxylic acid; **CLCD**, contactless conductivity detection; **CTAH**, cetyltrimethylammonium hydroxide; **DC**, direct current; **DMAA**, *N,N*-dimethylacetamide; **FI-CE**, flow injection-CE system; **FS**, fused silica; **HDB**, hexadimethrine bromide; **HEC**, hydroxyethylcellulose; **HF**, high frequency; **HIBA**, α-hydroxyisobutyric acid; **HP-β-CD**, hydroxypropyl-β-CD; **IE-CEC**, ion-exchange CEC; **MeOH**, methanol; **NACE**, nonaqueous CE; **PC**, propylene carbonate; **PMMA**, poly(methylmethacrylate); **p–p**, peak to peak; **TAPS**, *N*-tris(hydroxymethyl)-methyl-3-aminopropanesulfonic acid; **TE**, terminating electrolyte; **TRH**, thyrotropin releasing hormone; **TTAB**, tetradecyltrimethylammonium bromide; **Tween 20**, polyoxyethylene sorbitan monolaurate

tion with the surface of the electrodes, which caused defects and low reproducibility of the detection signal. These unfavorable phenomena are avoided in contactless conductivity detectors that have been first used also for CITP [7, 8] performed in PTFE (Teflon) capillaries. Later on, in 1998, using a new concept of capacitively coupled in-series placed two open tubular electrodes with detection cell between them, Zemann *et al.* [9] and da Silva and do Lago [10] have introduced the application of CLCD also for CZE performed in the fused-silica (FS) capillaries. In 2001, the contactless conductivity detector was first integrated on a chip electrophoresis device [11].

This review presents a short introduction to the principle and theoretical bases of conductivity detection in CE, describes the recent developments of the conductivity detectors and provides a comprehensive survey of applications of conductivity detection to monitor separations and analyses of different types of analytes by capillary electromigration methods performed in classical capillary format and in microchips.

2 Basic principles of conductivity detection in CE

In general, conductivity detection is based on the application of alternating current (AC) voltage of few kHz to few MHz frequency between two electrodes. The generated electric current (indirectly proportional to the resistance or directly proportional to conductance of the solution between the electrodes according to Ohm's law) is measured and yields the resistance or conductivity, respectively. Conductance of the BGE, G_{BGE}, containing all ionic species E^+, E^-, depends on their equivalent conductivities, λ_{E^+}, λ_{E^-}, their concentrations in the BGE, $c^C_{E^+}$, c^C_E, and on their degrees of dissociation, α_{E^+}, α_E

$$G_{BGE} = \frac{\lambda_{E^+} c^C_{E^+} \alpha_{E^+} + \lambda_E c^C_E \alpha_E}{10^{-3}K} \quad (1)$$

K is the constant of the detection cell, which depends on area and distance of the electrodes. Further, in order to simplify the presented equations, only the fully dissociated electrolytes are considered. The conductance of analyte zone, G_S, containing an anionic analyte A^- in the medium of the BGE solution, is determined by the concentration of the BGE ionic species E^+, c_{E^+}, and E^-, c_E, and concentration of the anionic analyte A^-, c^S_A, and their equivalent conductivities, λ_i

$$G_S = \frac{\lambda_{E^+} c^S_{E^+} + \lambda_E c^S_E + \lambda_A c^S_A}{10^{-3}K} \quad (2)$$

The counter cation A^+ of the analyte is not considered since in the applied electric field it migrates in a direction opposite to that of the anion and does not reach the detection cell. The concentrations of E^+ and E^- in the BGE and in the sample zone are related according to the following equations:

$$c^S_{E^+} = c^C_{E^+} + (1 - k_A)c^S_A \quad (3)$$

$$c^S_E = c^C_E - k_A c^S_A \quad (4)$$

where k_A is the transfer ratio of the analyte anion A^-, which is equal to the number of equivalents of the BGE co-ions displaced by an equivalent of the analyte ions. Consequently, the conductance of the sample zone can be expressed as

$$G_S = \frac{\lambda_{E^+}[c^C_{E^+} + (1 - k_A)c^S_A] + \lambda_E [c^C_E - c^S_A k_A] + \lambda_A c^S_A}{10^{-3}K} \quad (5)$$

The detector signal of the sample zone originates from the difference in conductance ΔG of sample zone and of the BGE

$$\Delta G = G_S - G_{BGE} = \frac{c^S_A [\lambda_{E^+}(1 - k_A) - \lambda_E k_A + \lambda_A]}{10^{-3}K} \quad (6)$$

From Eq. (6) it follows that the detector signal, which is directly proportional to ΔG, depends on the equivalent conductivities of the analyte anion A^-, of the BGE co-ion E^- and of the BGE counterion E^+. ΔG is also a function of the transfer ratio k_A, which is determined by the Kohlrausch regulating function, ω

$$\omega = \sum_i \frac{c_i z_i}{|m_i|} \quad (7)$$

where c_i, z_i, and m_i are molar concentrations, charge number and electrophoretic mobility of the i-th ion.

For the monovalent strong anions, the transfer ratio can be derived from the Kohlrausch's regulating function as

$$k_A = \frac{m_E (m_A + m_{E^+})}{m_A (m_E + m_{E^+})} \quad (8)$$

where m indicates electrophoretic mobilities of the respective ions. Taking into account the relation between conductivities and mobilities of species X, $\lambda_X = Fm_X$, where F is the Faraday constant, Eq. (6) can be rewritten as

$$\Delta G = G_S - G_{BGE} = \frac{c^S_A (m_A - m_E)(m_A + m_{E^+})}{m_A} \cdot \frac{F}{10^{-3}K} \quad (9)$$

Equation (9) clearly shows that the sensitivity of the conductivity detection is directly proportional to the difference in mobilities of the analyte and the BGE co-ion as well as the mobilities of the analyte and counterion. Hence, for maximal sensitivity of the conductivity detection, *i.e.*, for the highest S/N, theoretically it would be most suitable to use the BGE composed of co-ion and counterion the mobilities of which differ as much as pos-

sible from the mobilities of the sample ions. However, this counteracts the other conditions for high-efficient CE separations. The separation efficiency is maximized (electromigration dispersion is minimized) if the difference between analyte ion and BGE co-ion mobilities is minimized. With the increasing difference between sample ions and BGE co-ions, the peak symmetry as well as separation efficiency is falling down. If the BGE co-ion mobility is lower or higher than that of sample ion, the separation efficiency is reduced by peak fronting or peak tailing, respectively. The use of highly mobile BGE counterion is also problematic, since from one point of view it increases the detector signal but on the other hand it increases the conductivity of the BGE resulting in a limitation of using a high intensity of the electric field to prevent Joule heating effects (temperature increase and gradients) inside the capillary. Thus, in practical CE separations with conductivity detection, a compromise between detection sensitivity and separation efficiency has to be chosen for the BGE composition.

3 Conductivity detectors

3.1 Contact conductivity detectors

The first conductivity detectors used in the capillary electromigration methods had the electrodes in galvanic contact with the BGE. They were developed already in 1970s for CITP [5, 6], which was the first electromigration technique performed in the capillary format. The platinum microwire electrodes (od 0.05 mm) were sealed in the thin microholes, which were cut out in the walls of PTFE capillaries (id/od 0.45/0.7 mm). AC voltage of a few kHz frequency was applied on the electrodes and from the produced electric current the resistance or the conductivity of the migrating sample zones was measured. Alternatively, the direct current (DC) voltage (potential gradient) between the two microelectrodes placed in series (od 0.05 mm) with 0.1 mm distance was measured utilizing the DC driving current of ITP analysis to monitor the conductivity of ITP zones.

Contact conductivity detectors for modern high-performance capillary electromigration methods (HPCE) performed in the FS capillaries with internal diameter below 100 μm are implemented either in on-column or in the end-column mode. In the on-column mode, the two microelectrodes are fixed in the microholes drilled through the capillary wall whereas in the end-column mode one microelectrode is placed at the capillary outlet and the second electrode is placed close to the first electrode in the electrode vessel. The first on-column conductivity detector for CZE was designed by Zare and coworkers [12]. The platinum microwires were aligned and sealed in two diametrically positioned 40 μm holes made by drilling the FS capillary wall by a CO_2 laser. The conductivity changes of the BGE and sample zones were monitored by applying an AC voltage with oscillation frequency of 3.5 kHz between the electrodes. A transformator was used as a galvanic insulator between the sensing electrodes, which have a high DC potential to ground. Few years later in the same group the end-column conductometric detector was developed [13]. The sensing Pt microelectrode was centered at the capillary outlet and held by epoxy in the protective plastic jacket (1 cm long FS capillary), which was placed inside the outlet reservoir containing the grounding electrode. The conductivity measurement is made between the sensing microelectrode and the grounding electrode using an AC circuit, which was the same as that for the on-column detector. The end-column conductivity detection is technologically a simpler approach, since only a single metal microelectrode is placed, as close as possible to the capillary outlet. Conductivity changes are then measured between this sensing electrode and a second electrode, which is also positioned close to the capillary outlet but in fact already in the electrode vessel containing the BGE.

Another construction of the end-column conductivity detector was designed by Opekar and coworkers [14]. A Pt ring electrode was chemically deposited at the capillary end and at the other electrode, a Pt wire was immersed together with the capillary in the electrode vessel. This detector was further modified by the usage of a hydrophilic strip to ensure conductive contact between the BGE solution at the capillary outlet and the BGE in the electrode vessel as well as between the BGE at the capillary outlet and the sensing electrode [15, 16]. The cellophane strip was cemented to the end of a thin, tin-covered wire using a small drop of an electrically conductive silver epoxy resin. This drop served as one of the two conductometric electrodes. The wire with the cemented cellophane strip was fixed at the end of the separation capillary by thin PTFE tubing or by a PTFE ribbon. The free end of the cellophane strip was immersed in the BGE solution in the electrode vessel, where also the second Pt wire was placed. The conductivity was measured by a simple conductometer using an alternating voltage with an effective value of 1.0 V and a frequency of 1.0 kHz.

In the mid 1990s the contact conductivity detector has become commercially available for the postcolumn conductivity detection in CE devices. The applications of contact conductivity detectors in CE methods are summarized in Table 1.

3.2 Contactless conductivity detectors in capillaries

CLCD or more exactly capacitively coupled contactless conductivity detection (C^4D) is a particular type of electric conductivity measurement based detection where the electrodes are not in direct contact with the meas-

Table 1. Application of contact conductivity detectors in CE

Analyte (LOD or concentration range) /matrix[a)]	CE mode BGE composition	Capillary material and diameters (id/od)	Electrodes arrangement Frequency	References
K^+, Rb^+, Na^+, Li^+ (0.1 μM), Arg, His, tetramethylammonium, triethylamine/human serum	CZE 20 mM MES, 20 mM His, pH 6.1 5 mM potassium acetate, pH 5.4	FS: 50, 75/320 μm	On-column, Pt wires covered by epoxy resin f = 3.5 kHz	[12, 106, 107]
Ions of carboxylic acids: formate, acetate, propanoate, butanoate, pentanoate, hexanoate, heptanoate	10 mM MES, 10 mM His, pH 6.0, 0.5 mM TTAB 5 mM Cl^- adj. to pH 7.1 by Tris, 0.5 mM TTAB			
Fumarate, methylene succinate, malate, methyl malate	10 mM MES, 10 mM His, pH 6.0, 0.5 mM TTAB			
Tartarate, malate, succinate, citrate, acetate, lactate/wine				
α-ketoglutarate, malate	7 mM MES, 7 mM His, pH 6.0, 0.5 mM TTAB, 30% MeOH 5 mM Cl^- adj. to pH 7.1 by Tris, 0.4 mM TTAB 5 mM Cl^- adj. to pH 3.1 by Gly, 0.6 mM TTAB			
Carboxylate ions: formate, acetate, propanoate, butanoate, pentanoate, hexanoate	CZE 20 mM MES, 20 mM His, pH 6.0, 1 mM TTAB	FS: 80/355 μm	End-column, Pt wires covered by epoxy resin,f = 3.5 kHz	[13]
K^+ (3 nM)	CZE 20 mM sodium tetraborate	FS: 75/320 μm	Deposited Pt rings, AC current 5 μA f = 1 kHz	[14]
K^+ (26 μM), Na^+ (52 μM)/ mineral waters	CZE 30 mM MES, 15 mM LiOH, pH 6.1	FS: 75/375 μm	End-column: 1. Cellophane strip, on Sn-covered Cu wire covered by Ag epoxy resin, 2. Pt wire f = 1 kHz	[15, 16]

[a)] Matrix is specified for real world samples only, in the other cases model analyte mixtures are involved.

ured solution. The fundamentals as well as important factors influencing the characteristics of CLCD in capillary and microchip electrophoresis were recently reviewed by Geraldo *et al.* [17, 18].

The first prototype of CLCD was constructed in the early 1980s for CITP in the research group of Vacík and Gaš [7, 8, 19]. The detector consisted of a capacitive cell formed by four electrodes (copper enameled wires) arranged perpendicularly and equiplanar around the circumference of the PTFE capillary (id/od 0.45/0.70 mm). The input signal was produced by the high frequency (HF) generator (1 MHz) and led to the two emitting electrodes. The output signal was picked up by the other two electrodes and amplified by the receiver. This four-electrode arrangement of the high-frequency CLCD detector was used later with some modifications in the working group of Kaniansky not only for CITP but also for CZE performed both in the PTFE (id/od 300/500 μm) and FS capillaries (id/od 300/430 μm) [20–22]. A little bit higher sensitivity was achieved in FS than in the PTFE capillaries due to their thinner capillary walls and more suitable capacitance values.

In 1998, a new approach for CLCD in CE has been introduced Zemann *et al.* [9]. The detector consisted of two tubular electrodes for capacitive coupling, which were placed cylindrically around the outer surface of the FS capillary (see Fig. 1). The electrodes were of 30 mm length, cut from the syringe needles and they were separated with a detection gap of 2 mm. This design was further modified by the application the copper foil between the two electrodes, which had a shielding function [23]. The sensing electrodes were connected to an oscillator through a resistor. A high audio or low ultrasonic frequency for coupling of the AC voltage was used.

In the same year, almost simultaneously and independently, the same approach for CLCD detection in CZE was reported by da Silva and do Lago [10]. In their design, the sensing electrodes were painted directly on the outer capillary wall with the silver varnish. And the FS capillary was placed between poly(methylmethacrylate) (PMMA) bases and silicone septas. A ground plane was inserted between the two sensing electrodes. A function generator was connected with an electrode, which generated a HF sinusoidal signal, and the other one was connected to the input of a current-to-voltage converter. Few years later da Silva *et al.* [24] presented the improved detector, which was smaller and easier to operate. The detector could be placed both at the low- or high-voltage end of the capillary. Amplitude and frequency of the input signal should be optimized for each capillary diameter and BGE composition.

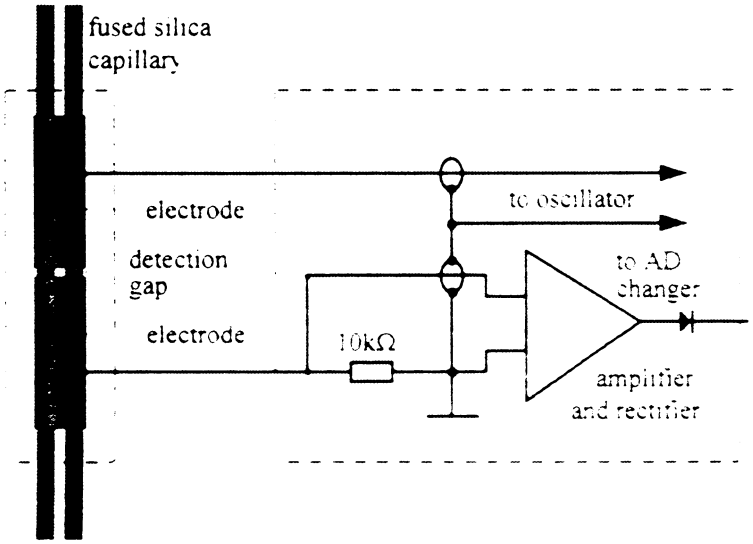

Figure 1. Schematic drawing of the capacitively coupled conductivity detector. Reprinted with permission from [9].

This approach with axial electrode arrangement was in the next years followed by several research groups and some other modifications, and refinements of both mechanic and electronic parts of the CLCD detector were reported.

Tůma *et al.* [25] developed a new prototype of CLCD using the strips of aluminum foil as electrode material. The foil strips formed semitubular shape electrodes between two PMMA blocks, where one of these two bases was movable. This construction allowed very easy exchange of the separation FS capillary. The qualitative and quantitative parameters of this detector with semitubular electrodes were found to be comparable with those achieved by the detector with tubular electrodes. After the studies testing the influence of geometry of the detection cell, especially width of electrodes and detection gap, on the sensitivity [26], the arrangement of the detection cell was further modified. The movable PMMA plate was divided into two parts, each containing a single electrode, which makes possible to change easily the gap between the two electrodes, *i.e.*, the length and volume of the detection cell. The effects of electrode geometry, planar, semitubular placed one beside the other, semitubular placed one against the other, tubular shape, on the detector characteristics were studied prior to finding the optimal arrangement [27].

Gaš and coworkers [28] have used two metal cylinders as tubular electrodes that surrounded the capillary in series for his new construction of CLCD. The input signal was provided by a HF voltage supply with a frequency of 625 kHz. A metal disk placed between the electrodes was connected to the ground. The detector has been further optimized and its construction has been improved in such a way that the two cylindrical brass electrodes were set to be 2.5 mm long, the detection gap between them was 1.5 mm and a copper disk with a hole for capillary placed between electrodes was used as a shielding. The output voltage of a HF generator was 50 V_{eff} [29]. The same parameters of the cell and electric circuit have been applied also for a double cell arrangement of the CLCD [30], which is suitable for investigation of dynamics of the electroseparation processes and for precise measurements of electrophoretic mobilities.

Zemann and coworkers [31] continued in the development and application of CLCD. A new prototype of CLCD with some small construction changes was used to detect fast separations of inorganic cations and anions, which were injected into the capillary from its both ends. The CLCD could be placed at various positions along the capillary length. The electrodes of this detector were 1 cm long, formed by stainless steel tubing, and placed at a distance of 1 mm from each other. Movable CLCD was miniaturized and built in commercial CE instrument [32]. The tubular electrodes were made of stainless steel with dimensions 0.4 mm wide, 8 mm long and were partly covered with heat-shrink tubing. The grounded copper plate was between electrodes. The rounded body of the cell was formed by epoxy resin covered by conductive nail assembled onto the capillary with dimensions 42 mm × 20 mm. The performance characteristics (noise, sensitivity, and peak width) were compared with a large cell and no significant differences were observed. In addition, these two miniaturized detectors placed on a single capillary were successfully tested for dual channel detection in CZE.

The original, full-size two-electrode CLCD was slightly modified (the detection gap was let 1 mm and the electrodes were cut down to 5 mm) and it was found suitable for detection of conductivity changes of the eluate in ion-exchange capillary chromatography [33].

Kubáň *et al.* [34, 35] have developed CLCD for simultaneous determination of inorganic or organic cations and anions, where samples were injected from both capillary ends. In the construction the authors followed the model of da Silva. The flexible detection cell comprised two 2 cm × 2 cm × 2.5 cm PMMA blocks. CLCD had two tubular silver electrodes, a thick leaf of copper foil was sandwiched between the electrodes, and the detection window was experimentally chosen as 2 mm long. The operating frequency of the detector was 290 kHz. LODs of inorganic cations and anions were simultaneously determined and found comparable with CZE, where samples were injected from one end of the capillary.

Hauser and coworkers [36] have constructed a modified CLCD, analogous to that developed by Zemann [9, 23]. Two 4 mm long electrodes were made of steel rings and placed 1 mm from each other around the easily exchangeable FS capillary. The detector operated up to a maximal frequency of 450 kHz and voltages of 25, 100, and 250 V_{p-p}. The usual working frequency was 190 kHz and voltage was 250 V_{p-p}. When the detector was placed in a Faraday cage the optimal frequency was changed to 100 kHz and the voltage was increased up to 300 V_{p-p}. A slightly modified detector [37] has been tested for CZE separation of inorganic ions in polyetheretherketon (PEEK) capillary. The detection window was enlarged to 2 mm and the detector operated at 100 kHz and 450 V_{p-p}.

Vuorinen *et al.* [38] developed CLCD following the model of da Silva *et al.* [24] and installed it in the commercial CE device. CLCD consisted of two silver covered copper coil electrodes, 7 mm long and with detection gap 0.4 mm. Detector operated at optimized frequency 291 kHz and voltage 20–25 V_{p-p}. Tan *et al.* [39] designed modified CLCD consisting of two 5 mm long stainless-steel tubes placed 2 mm apart from each other on the capillary. A thin grounded copper plane was placed between the electrodes to minimize the coupling capacitance between the electrodes in air. The electric circuitry was analogous to that described in [10], the detector was operated at the frequency of 200 kHz and with amplitude 220 V_{p-p}.

Baltussen *et al.* [40] presented two conductivity contactless cells. Both geometries consisted of electrodes placed cylindrically around the FS capillary. A simpler geometry configuration was based on two 2 cm long electrodes with detection gap of 2 mm. A slightly more complicated arrangement included a 0.25 mm thick shielding electrode, situated between two sensing electrodes. The electric circuitry was similar to that described in [9] with addition of lock-in amplifier. The detector operated at 100 kHz.

Wang and Fu [41] employed their CLCD in a miniaturized CE system with flow injection sample introduction (FI-CE device) [41]. The detection cell consisted of two 2 mm long tubular electrodes made from 100 μm thick Pt foil and positioned near the outlet of the separation capillary with 1 mm distance from each other. A 100 μm thick-grounded copper foil was sandwiched between the electrodes and the capillary passed through a 400 μm hole drilled through the foil. The detector operated at sine wave frequency 200 kHz and amplitude 10 V_{p-p}.

The applications of CLCD in CE methods are summarized in Table 2.

3.3 Combined contactless conductivity detectors in capillaries

Conductivity detection is in its principle a universal detection mode in CE methods. However, in spite of that, its combination with other detectors, is highly required, especially for analysis of complex samples containing both small fast inorganic and organic ions and large biopolymers, such as peptides, proteins and nucleic acids. Various combinations of CE detection techniques have been described, but almost always the detectors were placed in series. The special feature of the CLCD, particularly a gap between the two sensing electrodes, allows the measurement of the absorbance or fluorescence of the solution in the place of this gap, *i.e.*, in the same place where the conductivity of the solution is measured. This possibility has been utilized in some detector designs where CLCD was combined with photometric UV-absorption or fluorescent detection.

Chvojka *et al.* [42] designed a combined dual photometric-CLCD, in which both detection modes were independent and both static and dynamic properties were fully comparable with the characteristics of the individual detectors. Optical fibers were used to carry the photometric signal, whereas the conductivity signal is obtained from electrodes placed on the left- and right hand side of the fiber using AC voltage in the range 100–500 kHz. Later an improved dual photometric-CLCD has been developed [43, 44] where the CLCD was based on the previously developed semitubular electrodes [25, 26]. The optical part of the detector consisted of a single optical fiber fixed between the conductivity electrodes brought the light to the cell and a photodiode fixed close to the capillary, which recorded the light passing through the cell.

Tan *et al.* [45] presented another type of dual detector, which combined CLCD and fluorescent detection. The CLCD part of this detector was identical with that described in [39] with the exception that the window gap

Table 2. Application of contactless conductivity detectors in CE

Analyte (LOD or concentration range)/matrix[a)]	CE mode BGE composition	Capillary material and diameters (id/od)	Electrodes arrangement Frequency/excit. voltage	References
Cl^-, ClO_3^-, F^-, IO_3^-, glutamate	ITP Leading electrolyte (LE): 1 mM His, 1 mM His.HCl Terminating electrolyte (TE): 1 mM Glu	PTFE (teflon): 0.45/0.8 mm	Planar arrangement of four electrodes of capacitive pile, Cu enameling wire 0.2 mm, f = 1 MHz	[6–8, 19]
Rb^+, Ca^{2+}, Na^+, Mg^{2+}, Li^+ (4 ppb), Mn^{2+}, Br^-, Cl^-, NO_2^-, NO_3^-, SO_4^{2-}, F^- (13 ppb), $C_2O_4^{2-}$ (all 200 ppb), acetate, lactate, butyrate (all 50 ppb)	CZE 20 mM MES, 20 mM His, pH 6.0 (0.0001% hexadimethrine bromide (HDB)) 7.5 mM sorbic acid, 15 mM Arg, 0.0007% HDOH, pH 8.9	FS: 50/375 μm, tested id 5–100 μm	Cylindrical Ag rings or synergic needles, 30 (15–50) mm long, detection gap 2–5 mm, f = 40–100 kHz, amplitude 7–10 V_{p-p}	[9, 23]
K^+ (5 μM)	20 mM MES, 20 mM His, 1 mM 18C6E, pH 6.1			
Ba^{2+}, K^+ (17 ppb), Ca^{2+} (15 ppb), Na^+ (9.4 ppb), Mg^{2+} (24 ppb), Li^+ (1.5 μM)	CZE 10 mM MES/His, pH 6.0 (0.2 mM CTAB) 20 mM His/lactate, pH 4.9	FS: 75/360 μm	Tubular 2 mm long Ag rings painted around capillary, detection gap 1 (0.7) mm, grounding between electrodes, f = 0.6 or 1.1 MHz, amplitude 20 V_{p-p}	[10, 24, 68, 80, 81, 85, 87, 88, 105]
Tetramethyl(ethyl, butyl)-ammonium, (4.2–10.4 μM)	5 mM potassium acetate, pH 5.2			
$HCOO^-$, Cl^- (48 ppb), NO_3^- (96 ppb), CH_3COO^-, SO_4^{2-} (115 ppb), NH_4^+ (10 ppb), K^+, Ca^{2+}, Na^+, Mg^{2+}/rain water	20 mM MES, 20 mM His, pH 6.2 (2.5 mM 18C6E, 0.2 mM CTAB)			
Cl^- (2.5 μM), SO_4^{2-} (1.25 μM), PO_4^{3-} (5.26 μM), malate (0.97 μM), ascorbate (1.2 μM), K^+ (0.05 μM), Ca^{2+} (0.12 μM), Na^+ (0.17 μM), Mg^{2+} (0.08 μM)/coconut water	20 mM MES, 20 mM His, pH 6.0, 0.2 mM CTAB 7.5 mM His, 30 mM lactic acid, 0.3 mM CTAH, pH 3.7 20 mM His, 20 mM lactic acid, 2.5 mM, pH 4.9			
Mono- and di-saccharides: fructose (16 μM), fructose (30 μM), glucose (41 μM), sucrose (26 μM), galactose (18 μM)/coconut water, soft drinks, juices	10 mM NaOH, 4.5 mM Na_2HPO_4, 0.2 mM CTAB			
Aliphatic alcohols: propanol (1.0 mM), 2-methyl-propanol (0.8 mM), butanol (1.0 mM), pentanol (1.5 mM), hexanol (3.6 mM)/fuel	MEKC 20 mM MES, 20 mM His, pH 6.2, 0.2 mM CTAH 20 mM His/lactate, pH 4.9, 2.5 mM 18C6E			
Cl^- (0.99 μM), F^- (0.89 μM), I^- (0.97 μM), NO_2^- (1.11 μM), NO_3^- (0.87 μM), SO_4^{2-} (0.46 μM), PO_4^{3-} (1.40 μM)/milk	CZE 10 mM PEG-DC, 4.11 mM BTP, pH 3.5 7 mM succinate, 0.5 mM BTP, 0.2% methylhydroxyethylcullulose (MHEC), pH 3.55, (+75 mM β-CD)	PTFE: 300/500 μm FS	Four electrodes, HF generator (4 MHz) according to [7, 8]	[20–22]
K^+ (0.5 μM), Ba^{2+}, Ca^{2+}, Na^+, Mg^{2+}, Li^+ model mixture	CZE 20 mM MES, 20 mM His, pH 6.0	FS: 75/375 μm	Semitubular from Al foil, 2 strips around capillary, 2 mm long, detection gap 1 mm, f = 200 kHz, amplitude ± 10 V_{p-p}	[25, 27, 78]
Ca^{2+} (4.1 mg/L), Na^+, Mg^{2+} (9.4 mg/L), K^+/mineral water	20 mM MES, 20 mM His, 0.1 mM TTAB, pH 6.0			
K^+ (10–100 μM), Cs^+ (10–100 μM)	CZE 20 mM citric acid, 10 mM LiOH, 1% HEC, pH 3.1	FS: 75/375 μm	Semitubular from Al foil, 2 strips around capillary, 2–10 mm long, detection gap 1, 2, 3, 5.5 mm f = 460, 230, 115, 58 kHz, amplitude ± 10 V_{p-p}	[26]
Aliphatic amines and ammonium ions: tetrapropylammonium, *N*-methylcyclohexylammonium, *N,N*-dimethyldodecylammonium, tetramethylammonium, propylammonium, dipropylammonium, tetrabutylammonium, dodecylammonium	CZE-NACE 10 mM AcOH, 10 mM Tris acetate, pH 4.75 10 mM 2,6-dihydroxybenzoic acid, 10 mM tetraethylammonium 2,6-dihydroxy-benzoate in DMF, DMAA, PC as solvent CZE-NACE 25 mM perchloric acid in PC 50 mM butylamine, 25 mM perchloric acid,PC	FS: 75/360 μm	Axial arrangement of two brass cylinders with shielding (grounding) Cu disk between them, f = 625 kHz, amplitude ± 50 V_{p-p}	[28–30, 73, 89, 91–94, 99, 101–104]

Table 2. Continued ...

Analyte (LOD or concentration range)/matrix[a)]	CE mode BGE composition	Capillary material and diameters (id/od)	Electrodes arrangement Frequency/excit. voltage	References
Amitriptylin, doxepin, nortryptylin	25 mM tetraethylammonium acetate, 250 (2.5) mM AcOH in PC			
I^-	EACA/HCl in MeOH and water tetrapropylammonium perchlorate in ACN			
K^+, Cs^+, Ca^{2+}, Na^+	CZE 10 mM AcOH, 5 mM LiOH, pH 4.7			
Chlorobromoacetic acids: mono-, di-, tri-chloroacetic, mono-, di-, tri-bromoacetic, mono-, di-bromo-chloroacetic, bromo-dichloroacetic (all 0.1 ppm)/water	6.25 mM NaH_2PO_4, 6.25 mM Na_2H-PO_4, 5 mM diethylenetriamine (DETA), pH 9.4 50 mM citric acid, 10–70 mM LiOH, 5 ppm HDB, pH 2.63–4.61 100 mM boric acid, 80 mM Tris, 3 mM DETA, pH 8.62			
AAs (9.1–29 μM)/Budvar beer, pangamin, yeast, human urine, saliva, extract from herbs	70–14.2 mM chloracetic acid, 0–9.3 mM LiOH, pH 2.0–3.2 2.3 M AcOH, 0.1% HEC, pH 2.1			
AAs: 18 proteinogenic, Orn, Cit, methyl-histidine (Me-His) (all 4.3–42.9 μM), creatinine/human plasma	1.7 M AcOH, 0.1% HEC pH 2.2 40 mM chloracetic acid, 0.1% HEC, pH 2.2			
AAs: Lys, His, Gly, Ala, Ser, Val, Ile, Leu, Asn, Thr, Glu, Phe, Tyr, Pro, OH-Pro/digests of collagen, egg white, milk casein, linseed oil-stand oil, gum arabic, animal glues (binding media)	51.9 mM chloracetic acid adj. with LiOH, pH 2.26			
Long-chain fatty acids: palmitic, stearic, linolic, linolenic, oleic, dicarboxylic acids: pimelic 7di, suberic 8di, azelaic 9di, sebaic 10di/drying oils used as binding media	CZE-NACE 5 mM phosphate buffer, pH 6.86, 4 mM sodium dodecylbenzensulfonate, 10 mM Brij, 2% (v/v) 1-octanol, 45% (v/v) ACN 10 mM salicylic acid, 20 mM His, pH 5.85, 0.2 mM CTAB			
Fosfomycin (0.6–2 μg/mL)/plasma, microdialysis samples	25 mM benzoic acid, 0.5 mM CTAB, adj. with 1 M Tris, pH 6.95, 8.05			
Cl^- (11 μg/L), F^- (6 μg/L), I^- (64 μg/L), Br^- (160 μg/L), NO_2^- (92 μg/L), NO_3^- (21 μg/L), SO_4^{2-} (29 μg/L), PO_4^{3-} (95 μg/L)	Ion-exchange CEC (IE-CEC) 10 mM *p*-toluenesulfonic acid, 20 mM His, pH 8.05	FS: 75/360 μm	Length 5 mm, detection gap 1 mm f = 2–200 kHz amplitude 25 V_{p-p}	[33]
Inorganic ions: NH_4^+, K^+, Na^+, Mg^{2+}, Li^+ (70 ppb, 200–100 ppb)	CZE 50 mM MES, 50 mM His, 1 mM 18C6E, pH 6.1	FS: 50/375 μm	10 mm long cylinders stainless steel, detection gap 1 mm f = 100 kHz	[31]
Br^-, NO_2^-, NO_3^-, SO_4^{2-}, $C_2O_4^{2-}$, Cl^- (70 ppb, 200–100 ppb)/mineral water	50 mM MES, 50 mM His, 0.001% sodium polyanetholsulfonate (SPAS), pH 6.1			
K^+, Na^+, Li^+, NO_3^-, BrO_3^-, Br^-	CZE: 50 mM MES, 50 mM His, pH 6.0	FS: 50/360 μm	Two tubular stainless steel electrodes, 0.4 mm × 8 mm, partly covered with heat-shrink tubing, grounded Cu plate	[32]
Cl^-, NO_2^-, NO_3^-, SO_4^{2-}, PO_4^{3-}, COO^-, Br^-, K^+, Mg^{2+}, Na^+, NH_4^+, Ca^{2+}, Mn^{2+}, Li^+, Co^{2+}, Zn^{2+} (all 7.5–65 μg/L), Cd^{2+}, F^- (all 125 μg/L), Ba^{2+} (90 μg/L), Cr^{3+}, Cr^{6+}/drainage, tap, rinse, rain, surface, lysimetric water, plant exudates and extracts, ore leachates	CZE-DOI 20 mM MES, 20 mM His, 1.5 mM 18C6E, 20 μM CTAB, pH 6.0 8 mM His, 2.8 mM HIBA, 0.32 mM 18C6E, pH 4.25 9 mM His, 4.6 mM lactic acid, 0.38 mM 18C6E, pH 4.25 5 mM His, 5 mM HIBA, adj. by AcOH, pH 3.75 4.5 mM His, adj. with AcOH, pH 3.75		Two tubular Ag electrodes, 20 (5–30) mm long, shielding Cu foil, detection gap 2 (0.6–5.1) mm, f = 290 kHz, amplitude 2–20 V_{p-p}	[34, 35, 71, 77, 79, 82–84]
Se^{4+} (190 μg/L), Se^{6+} (7.5 μg/L)/soil sample	FI-CE 8.75 mM His, adj. with AcOH, pH 4.0			
Tetramethylammonium, benzyl ammonium, tetrabutylammonium	CZE 6 mM ammonium acetate, pH 6.8			
Phenolic acids: benzoic, 4-hydroxybenzoic, ferulic, siringic, cinnamic, sinapic, vanillic, 2,4-dihydroxybenzoic, p-coumaric acids (2.3–3.3 μM, after sample stacking 0.12–0.17 μM)	CZE 150 mM AMP, pH 11.6 30 mM MES, 30 mM His, 30 μM CTAB, 10% MeOH, pH 6.0			

Table 2. Continued ...

Analyte (LOD or concentration range)/matrix[a)]	CE mode BGE composition	Capillary material and diameters (id/od)	Electrodes arrangement Frequency/excit. voltage	References
Cr^{3+} (10 μg/L), Cr^{6+} (39 μg/L), NH_4^+ (1 μg/L), K^+ (4 μg/L), Ca^{2+} (3 μg/L), Mg^{2+} (1.5 μg/L), Na^+ (4 μg/L), Cl^- (6 μg/L), NO_3 (10 μg/L), $SO_4$2− (6 μg/L), Se^{4+} (190 μg/L), Se^{6+} (7.5 μg/L), $HPO_4$2− (200 μg/L), NO2− (150 μg/L)/mineral, tap, drainage, surface, rain waters	FI-CE 12 mM His, 0.5 mM HIBA, 1 mM 18C6E, adj. with 10% v/v AcOH, pH 4.05 7.5 mM His, 1 mM HIBA, 1 mM 18C6E, adj. with AcOH, pH 2.8 12 mM His, adj. with AcOH, pH 4.00	FS: 50, 75/360 μm	Two tubular steel electrodes, 4 mm long, detection gap 1 mm, f = 100 or 190 kHz, (tested to 450 kHz), amplitude 250, 300, 450 V_{p-p}, (tested 25, 100, 200, 300, 400 V_{p-p})	[36, 60, 60–62, 64, 69, 75, 76, 86, 90, 96–98]
K^+, Mg^{2+}, Na^+, Li^+, NO_3^-, SO_4^{2-}, PO_4^{3-}, Br^-, Ba^{2+}, Ca^{2+}, Mn^{2+}, Rb^+, Co^{2+}, Cd^{2+}, Zn^{2+}, Fe^{3+}, Cs^+, Sr^{2+}, Pb^{2+}, NH_4^+, Cu^{2+}, Ni^{2+} (all 0.089–0.27 μM, 1–200 μM, heavy metal ions 1–5 μM)/river water	CZE 0 (20) mM MES/His, 0.00015% HDB, pH 6.0 20 mM MES/His, 1 mM 18C6E, pH 6.1 10 mM His, adj. with AcOH, pH 2.75 10 mM CAPS/Arg			
Citrate, malate, acetate (0.5 mg/L), lactate (0.5 mg/L), benzoate (0.5 mg/L), sorbate (0.5 mg/L), ascorbate (3 mg/L)/vitamin C tablete, soft drink	CZE 0.135 mM tartaric acid, 10 mM His, pH 6.5, (0.1 mM CTAB and 0.025% HP-β-CD)			
Amines: (0.52 μM), ephedrine, pindolol (0.06 μM), atenolol (0.48 μM), metoprolol, lebetalol (0.96 μM), acebutolol, adrenaline, noradrenaline, isoprotorenol, doxylamine, octopamine/pharmaceuticals: ternormin, sanalepsi, vick medi-nite	CZE 10 (20) mM MES/His, pH 6.2, (6.1) 10 mM citric acid, pH 3.0 20 mM lactic acid, pH 2.83 100 mM lactic acid, 5 mM His, pH 2.75 100 (250) mM AcOH, pH 2.91, 2.71 100 mM AcOH, 1 mM His			
Human IgM (0.15 ng/mL), L,D-doxylamine, L,D-adrenaline (0.28 μM), L,D-isoprotorenol (0.42 μM), L,D-noradrenaline (0.44 μM), L,D-propranolol, 1S,2S-(+)-,1R,2R-(−)-pseudoephedrine (0.3 μM)	CZE 20 mM TAPS, 20 mM AMPD, pH 8.7, 0.01% Tween 20 100 mM lactic acid, 5 mM His, 40 mM HP-β-CD, pH 2.75 100 mM lactic acid, 5 mM His, 30 mM HP-β-CD, pH 2.75			
NH_4^+, K^+, Na^+, Ca^{2+}, Mg^{2+}, Cl^-, NO_3^-, SO_4^{2-}/human blood serum, urine	60 mM lactic acid, 7.5 mM His, 10 mM HP-β-CD, pH 3.06 20 mM lactic acid, 20 mM HP-β-CD, pH 2.45			
AAs: L,D-Arg, L,D-Ser, L,D-Thr, L,D-Met, L,D-Trp, L,D-Tyr, L,D-Asp, L,D-Val (all 2.5–20 μM)	CZE 6.5 (13) mM maleic acid, 7.5 (15) mM Arg, 1.5 mM 18C6E, pH 5.5			
(R/S)-1-cyclohexyl ethylamine, (R/S)-1-phenylethylamine (0.5 μM)	10 mM 18C6EH4, 10 mM citrate/Tris, pH 2.2 25 mM citric acid, 5 mM DM-β-CD, 5 mM 18C6E, pH 2.4			
Chlorhexidine digluconate (0.4 μg/mL), polyhexamethylene biguanide (4 μg/mL)/eye drops	CZE 2.3 M AcOH, pH 2.1, 0.05% Tween 20 15 mM Arg, 10 mM AcOH, pH 8.3			
Amines (all 1–2 μM): short-chained aliphatic primary, secondary, tertiary amines, branched aliphatic amines, diamines, hydroxyl-substituted amines	CZE 10 mM MES/His, pH 6.0 50 mM AcOH, 10 mM Bis-Tris, pH 4.0 25 mM AcOH, pH 3.0 0.5 M AcOH, pH 2.5 0.5 M AcOH, pH 2.5, 50 mM 18C6E, pH 2.5			
Carbohydrates: D-sucrose, D-galactose, D-glucose, D-fructose	10 mM NaOH, 4.5 mM Na_2HPO_4, 0.00015% HDB, pH > 12			
AAs: Thr, Met, Leu (all 1 μM)	10 mM NaOH, 4.5 mM Na_2HPO_4, 1 mM CTAB, pH < 12			
NH_4^+, K^+, Mg^{2+}, Na^+, Li^+, NO_3^-, Cl^-, Br^-, SO_4^{2-}, oxalate, tartate, citrate (all around 10 μM)/red wine, tap water	CE with dual opposite injection (CE-DOI) 10 mM MES, 10 mM His, 1 mM 18C6E, pH 6.0	FS, PEEK: 50, 75/360 μm	Two tubular steel, 4 mm long, detection gap 2 mm, f = 100 kHz, amplitude 450 V_{p-p}	[37, 74]
Underivatized AAs: (50–100 mM), Arg (20 μM), Lys (30 μM), His (40 μM)/urine, beer	CZE 6 mM lactic acid, pH 2.4 50 mM AMP(AMPD), pH 10.8 50 mM AMP, 5 (10) mM CAPS, pH 11.1 (10.8)			

Table 2. Continued ...

Analyte (LOD or concentration range)/matrix[a]	CE mode BGE composition	Capillary material and diameters (id/od)	Electrodes arrangement Frequency/excit. voltage	References
K^+ (0.24 mg/L), Ba^{2+} (2.14 mg/L), Ca^{2+} (0.15 mg/L), Na^+ (0.12 mg/L), Mg^{2+} (0.18 mg/L), Mn^{2+} (0.34 mg/L), Li^+ (0.22 mg/L)	CZE 20 mM MES, 20 mM His, pH 6.0	FS: 50/150 μm	Two Cu wire coil electrodes covered by Ag, 7 mm long, detection gap 0.4 mm, f = 291 – 300 kHz, amplitude 20 – 25 V_{p-p}.	[38]
Catecholamines: 4-hydroxy-3-methoxybenzylamine hydrochloride, (9.0 mg/L), dopamine (11.2 mg/L), D,L-normetanephrine (11.2 mg/L), D,L-metanephrine (10.1 mg/L)	CZE 10 mM ammonium acetate, pH 4.0			
Zn^{2+} (5 nM), Co^{2+} (10 nM), Cu^{2+} (30 nM), Ni^{2+} (15 nM), Na^+, K^+, Mg^{2+}, Ca^{2+}/tap water	FASI-CE 0 – 10 mM MES, 0 – 10 mM His, adj. with AcOH, pH 4.9 10 mM MES, 10 mM His, 15% ACN, pH 4.9	FS: 50/375 μm	Two stainless-steel tubes, 5 mm long, gap 1 mm, thin-grounded Cu plane, f = 200 kHz, amplitude ± 220 V_{p-p}	[39]
K^+, Li^+ (both 0.3 μM)	CZE 20 mM sodium borate, pH 7.5	FS: id 50 μm	Two cylindrical, 2 cm long, 0.25 mm thick, detection gap 2 mm, f = 250 kHz	[40]
Peptides: bradykinin, angiotensin II, α-melanocyte stimulating hormone, luteinizing hormone releasing hormone, TRH, [Leu]enkephalin, bombesin, oxytocin, [Met]enkephalin (2 – 0.5 μM)	CZE 100 mM phosphate buffer, pH 2.5			
NH_4^+ (2.6 μM), Na^+ (2.7 μM), Mg^{2+} (3.5 μM), K^+ (2.5 μM), Ca^{2+} (2.8 μM)/surface water	Miniaturized FI-CE 20 mM MES, 20 mM His, 1.5 mM 18C6E, pH 6.0	FS: 25/375 μm	2 mm long tubular from Pt foil, detection gap 1 mm, 100 μm thin grounded Cu foil between electrodes with 400 μm hole for capillary, f = 200 kHz, amplitude 10 V_{p-p}	[41]

[a] Matrix is specified for real world samples only, in the other cases model analyte mixtures are involved.

Table 3. Application of contactless conductivity detectors combined with optical detectors in CE

Analyte (LOD or concentration range)/matrix[a]	CE mode BGE composition	Detection type Capillary material: (id/od) Detection wavelength	Electrodes arrangement Frequency/excit. voltage	References
K^+ (10 μM), Na^+, salicylate (0.7 μM), acetylsalicylate, benzoate, picrate, benzenosulfonate, brombenzoate, Cl^-, SO_4^{2-}, Ca^{2+}, Mg^{2+}, procaine, tyramine, ephedrine, codeine/infusion solution	CZE 20 mM boric acid, 10 mM LiOH, pH 9.20 20 mM citric acid, 10 mM LiOH, pH 2.95	Photometric-contactless FS: 75/375 μm λ = 200 nm	Tightly winding a Cu wire around capillary connected with all coils together, 3 mm long, detection gap 2 mm, f = 200 kHz, amplitude ± 10 V_{p-p}	[42]
K^+ (10 μM), Na^+, Ca^{2+}, Mg^{2+}, tyramine, His, pyridoxine, sorbic, butyric acid, gallic acid, Ca pantothenate, ascorbic acid, citric acid/multivitamin preparation	CZE 20 mM AcOH, 10 mM LiOH, pH 4.5 20 mM boric acid, 10 mM LiOH, pH 9.20	Photometric-contactless FS: 75/375 μm λ = 210 nm	Semitubular from Al foil, 2 strips around capillary fixed to block, 3 mm long, detection gap 2 mm, f = 200 kHz, amplitude ± 10 V_{p-p}	[43, 44]
Li^+, Na^+, K^+, Mg^{2+}, Ba^{+2}, Ca^{2+} (0.2 – 3 μM)	CZE 10 mM MES, 10 mM His, pH 6.0	Fluorescent-contactless FS: 75/375 μm	Two stainless-steel tubes, thin-grounded Cu plane, 5 mm long, detection gap 2 mm	[45]
FITC-labeled AAs: Phe, Gly, Trp, Lys (0.4 – 2.5 μM)	10 mM Tris, 5 mM MES, pH 8.2	λ_{exc} = 470 nm, λ_{em} = 530 nm		
FITC-labeled peptides: Pro-Met, Gly-Tyr, Gly-Thr (0.4 – 0.6 μg/mL)	10 mM Tris, 5 mM MES, pH 8.2			

[a] Matrix is specified for real world samples only, in the other cases model analyte mixtures are involved.

was prolonged to 2 mm. A thin-grounded copper plane was placed between the electrodes to minimize the coupling capacitance between the electrodes in the air. For fluorescent detection the light emitting diode (λ = 470 nm) was used as the excitation source. An optical fiber was fixed perpendicularly against the window by a methacrylate plate with T-shape groove to collect the emitting fluorescence, passing through two pieces of interference filters (λ = 530 nm).

The applications of CLCD combined with optical detectors in CE methods are summarized in Table 3.

3.4 Contactless conductivity detectors in chip-based systems

In 2001 Laugere *et al.* [11] developed the first CLCD with two- and four-electrode arrangement for microchip CE. After several experimental optimizations, a two-electrode detector was found unsuitable for miniaturization, so a four-electrode detector was chosen for further experiments in microchip CE. The silver electrodes with sizes 10 mm × 0.5 mm were covered by silicon nitride on the glass chip and the basic physical characteristics, such as impedance, frequency, potential and current of the detector have been determined [46–50].

Another four-electrode CLCD for microchip CE was suggested by Lichtenberg *et al.* [51]. The detector was integrated inside the chip. All the four platinum electrodes were 100 μm long, two inner 30 μm and two outer 20 μm wide. Operating electrodes were placed 400 μm from each other, positioned perpendicular to the channel. The amplitude was 15 V_{p-p}, and the operating frequency was 10–100 kHz.

New types of CLCDs for microchip CE were developed by Wang and coworkers [52, 53]. Electrodes have rectangular shape made of aluminum foil and were placed 1.3 mm from each other. Their arrangement was antiparallel. The operating frequency was set at 200 kHz and the amplitude at 5 V_{p-p}. The electric circuit was designed according to da Silva [24]. In another design, the CLCD was integrated into the microchip in combination with the amperometric detector [54]. Do Lago *et al.* [55] have also adapted his original CLCD design for application in a microchip. The electrodes were made of copper strips, detector operated at frequency 530 kHz and amplitude 10 V_{p-p}. A new movable CLCD for microchip CE was introduced by Wang *et al.* [56], the detector could be placed at different points along the separation channel due to the electrodes holder. It was tested on CE separations of low explosive ionic compounds. The same authors designed a microchip with dual-opposite injection for simultaneous measurement of cations and anions with movable CLCD [57]. Similar construction of movable CLCD with small difference in electrode length was designed by Chen *et al.* [58].

Hauser and coworkers [59, 60] integrated the CLCD into a commercially available chip. The detector consisted of two silver parallel electrodes placed 1 mm from each other. They were 0.5 mm wide and 5 mm long. The amplitude was 500 V_{p-p} and the operating frequency 100 kHz. Special papers were dedicated to studies of the cell geometry and frequency behavior of the CLCD [61] and to the investigation of the analytical performance of the detector, mainly with regard to the S/N ratio, as well as investigation of the effects of a Faraday shielding between the electrodes and of different internal diameters of electrodes on the S/N ratio [62] for better understanding of the characteristics of the axial contactless conductivity cell. On the chip, the electrodes consisted of two parallel selfadhesive copper strips of 1 mm width and 5 mm length and separated by a gap of 1 mm.

More detailed investigations of the effects of the cell geometry (orientation, length, width, distance from the channel of the electrodes, gap between them), and operating parameters (stray capacitance, excitation voltage, and feedback resistor) on the performance of the CLCD detector were reported by Kubáň and Hauser [63]. In this group two thin antiparallel adhesive copper strips were tested as electrodes with different width (0.5–3 mm) and length (13.2–20 mm), detection gap (0.5–3 mm), feedback resistor (0.22–2.2 MO) frequency (100–800 kHz), and amplitude (25–100 V_{p-p}) on the PMMA microchip. The optimal parameters of this construction (1.4 mm length, 1.0 mm width of the electrodes, detection gap 0.5 mm, frequency 600 kHz, and excitation voltage 20 V_{p-p}) were used for detection of different types of analytes [64–66].

The applications of CLCD in chip CE are summarized in Table 4.

4 Applications of conductivity detectors

4.1 Model mixtures

It is natural that at the early days of the application of conductivity detection in CE methods, when the new detector designs were under development, mostly only model mixtures of the most suitable analytes, highly mobile small inorganic and organic ions, have been analyzed. The aim of the experiments was not only to separate and analyze these mixtures but also to test the characteristics of the newly developed detectors. Some representative analyses of model mixtures are described below, the others are presented in the Tables 1–4.

Many separations of small inorganic and/or organic cations [9, 23, 25, 32, 34, 36, 38, 45, 48–53, 55–57, 59, 67–69] and anions [9, 32, 36, 52, 53, 56, 57, 70] have been carried out by CZE in the BGEs composed of MES and histidine (His) at different concentrations and at pH around 6.0; sometimes the selectivity of cationic separations has been improved by the addition of a complexing agent, 18-crown-6-ether (18C6E), and the EOF has been reversed by the addition of CTAB for simultaneous [31, 34, 37] or divided [63, 70] separations of inorganic cations and anions. Examples of simultaneous determination of inorganic cations and anions in 20 mM MES/His with addition of 1.5 mM 18C6E and 10 (20) mM CTAB (pH 6.0) by CZE with dual injection from both capillary ends [34], are shown in Fig. 2. Other commonly used BGEs for determination of cations have been lactic acid (pH 4.9) [9], lactic

Table 4. Application of contactless conductivity detectors in chip CE

Analyte (LOD or concentration range)/matrix[a)]	CE mode BGE composition	Microchip material Channel dimensiones	Electrodes arrangement Frequency/excit. voltage	References
K^+, Li^+, Na^+ (5 μM)	CZE	Glass	Two or four electrodes, Al	[8, 46–50]
Peptides: Lys-Pro-His-Gly-Glu-Ala-Asp-Ser-Lys, Glu-Lys-Phe-Glu-Lys-Ser-Ala-Asn-Val-Asp-Gly (both 0.2 mM)	20 mM MES, 20 mM His, pH 6.0 50 mM phosphate buffer, 2 mM SDS, pH 2.5	width/depth 150,70/20 μm	foil, covered by silicon nitride or SiC, two outer electrodes 106 × 25 μm, two inner electrodes 106 × 35 μm (test device 10 mm × 0.5 mm), f = 10 kHz – 1 MHz	
Ions of organic acids: fumaric, citric, succinic, acetic, pyruvic and lactic (all 100 μM)	20 mM MES, 20 mM His, 0.2 mM TTAB, pH 6.0			
Li^+, Na^+, K^+ (18 μM)	CZE 10 mM MES, 10 mM His, pH 6.0	Glass width/depth 50/12 μm	4 Pt electrodes, long 100 μm, two inner 30 μm wide, 2 outer 20 μm wide, detection gap 400 μm, f = 10 – 100 kHz, amplitude 15 V_{p-p}	[51]
K^+ (2.8 μM), Ba^{+2}, Na^+ (5.8 μM), Li^+, Ac^-, SO_4^{2-} (5.1 μM), Cl^- (6.4 μM), PO_4^{3-}, NO_3^- (7.2 μM), F^-, NH_4^+ (3.2 μM), perchlorate (6.2 μM), methylammonium (5.8 μM, 400 – 1600 μM)	CZE 20 mM MES, 20 mM His, pH 6.1	Glass PMMA width/depth 50/50 μm (squared cross section)	Rectangular-shaped from Ag foil strip, 0.8 mm × 10 mm, 4 mm wide, placed in antiparallel arrangement 1 mm from each other, f = 50 – 1000 kHz, amplitude ± 5 V_{p-p}	[52, 53, 67, 100]
Alkyl derivatives methyl-phosphate acid (MPA): ethyl-, pinacolyl-, isopropyl-MPA, (48 – 86 μg/L, 0.3 – 100 mg/L)/river water	5 (20) mM MES, 5 (20) mM His, pH 6.1 20 mM Tris, adj. 20 mM boric acid, pH 6.1 20 mM borate, adj. 20 mM boric acid, pH 6.1			
Aliphatic amines: tetramethylammonium, *N,N*-dimethyldodecylamine, tetrapropylammonium ion, tetrabutylammonium ion	CZE-NACE 5 mM 2,6-dihydroxybenzoic acid, 5 mM tetraethylammonium 2,6-dihydroxy-benzoate in DMF, DMAA, DMSO, PC			
Na^+, NH_4^+, methylammonium (all 2 mM)	CZE 20 mM MES, 20 mM His, 15 mM lithium dodecylsulfate (LiDS), pH 6.1	Glass Combined CLCD and amperometric detection	Rectangular shaped from Ag foil, 0.8 mm × 10 mm, 4 mm wide, antiparallel orientation 1.3 mm gap, f = 200 kHz, amplitude ± 5 V_{p-p}	[54]
Amperometric: trinitrotoluen (85 ppm), di-, trinitrobenzene (2.4 ppm), trinitrobenzene, *o*-,*m*-,*p*-aminophenol (0.3 – 0.9 mM)	20 mM sodium acetate, 20 mM AcOH, 7:3, pH 5.0			
K^+, Na^+, Li^+	CZE 30 mM MES, 30 mM His, pH 6.1	Laminated polyester chip width/depth 150/15 μm	Two adhesive Cu strips, antiparaller orientation, gap 1 mm, width 1 mm, length 5 mm, f = 600 kHz, amplitude ± 20 V_{p-p}	[55]
Methylammonium, NH_4^+ (80 μM), Na^+ (70 μM), K^+, Cl^- (150 μM), NO_3^-, perchlorate (130 μM), methyl phosphonic acid (MPA), pinacolyl-, isopropyl-MPA	CE-DOI 20 mM MES, 20 mM His, pH 6.1	PMMA chip width/depth 50/50 μm	Rectangular shaped from Ag foil, 0.8 mm × 24 mm, electrodes fixed to detection holder moved along channel, antiparallel orientation, gap 0.8 mm, f = 200 kHz, amplitude ± 5 V_{p-p}	[56, 57, 95]
Methyl parathion (3 mg/L), parathion, paraoxon (5 mg/L)	CZE 5 mM MES, 5 mM His, pH 6.1			
Na^+, K^+, Li^+/sea water	CZE 20 mM boric acid, 20 mM Tris, pH 8.0	PMMA chip width/depth 50/40 μm	Rectangular-shaped Al electrodes, antiparaller orientation, shielding, width 0.8 mm, length 15 mm, gap 0.8 mm, f = 200 kHz, amplitude ± 5 V_{p-p}	[58]
NH_4^+, Na^+ (0.41 μM), Mg^{2+} (0.35 μM), K^+ (0.49 μM), Sr^{2+} (1.4 μM), Mn^{2+} (2.1 μM), Zn^{2+} (2.8 μM), Cr^{3+} (6.8 μM)	CZE 10 mM MES, 10 mM His, 2 mM 18C6E, pH 6.0 5 mM MES, 3 mM HIBA, pH 4.5	Glass chip width/depth 50/20 μm	Two Ag electrodes, 0.5 mm × 5 mm, detection gap 1 mm, f = 100 kHz, amplitude 500 V_{p-p}	[60, 70, 72, 90]
Citrate (2.3 μM), lactate (5.5 μM) 4-acetamidophenol, ibuprofen, salicylic acid (5 – 10 μM)	10 mM CHES, 6 mM Arg, pH 9.0 10 mM CAPS, 10 mM Arg, pH 10			
Na^+, K^+, Li^+, Rb^+ (1.5 μM), Fe^{3+} (3.5 μM), Cd^{2+} (8 μM), Co^{2+} (2 μM), Cl^- (2.5 μM), NO_3^- (3 μM), ClO_4^- (2 μM)	CZE 10 mM MES, 10 mM His, 4 mM 18C6E, pH 6.0 5 mM His, 3 mM HIBA, pH 4.5	PMMA chip width/depth 50/50 μm Glass chip	Two thin parallel selfadhesive Cu strips of 1 (2) mm width and 5 (4) mm length placed in 90°angle across channel, detection gap 1 (2.5) mm, shielding, f = 100 kHz, amplitude 400 (300, 500) V_{p-p}	[59]
Oxalate (4.4 μM), tartrate (7 μM), succinate (10 μM), acetate (25 μM), lactate (30 μM)	10 mM MES, 10 mM His, pH 6.0 10 mM MES, 10 mM His, 0.2 mM CTAB, pH 6.0			

Table 4. Continued ...

Analyte (LOD or concentration range)/matrix[a]	CE mode BGE composition	Microchip material Channel dimensiones	Electrodes arrangement Frequency/excit. voltage	References
4-acetamidophenol, ibuprofen, salicylic acid (5–10 μM), alkyl sulfonates (6 μM): ethane sulfonate, heptane sulfonate	CZE 25 mM MOPSO, 15 mM Arg, 0.1 mM CTAB, pH 7.0			
Carboxylic acids: methanoic (3.3 μM), ethanoic (5 μM), butanoic (10 μM), hexanoic (30 μM), ethanedioic (1.5 μM), malic (2.7 μM), hexanedioic (12 μM), hydroxybutanedioic, octanedioic	20 mM MES, 20 mM His, 0.2 mM CTAB, pH 6.020 mM MES, 20 mM His, 0.1 mM CTAB, pH 6.0			
AAs: Trp, Glu, Asp, Phe, Thr, Tyr	CZE 50 mM AMP, 10 mM CAPS, pH 10.8			
Artificial sweeteners (9 μM): acesulfame-K, cyclamate	20 mM MES, 20 mM His, 0.1 mM CTAB, pH 6.0			
Sugars: sucrose (10 μM), fructose (30 μM)	10 mM NaOH, pH 12.0 100 mM triethylamine, pH 12.0			
Drugs: dopamine, ephedrine, methanephrine	10 mM MES, 0.2% HEC			
Human immunoglobulin M (IgM) (34 ng/mL), antihuman IgM	20 mM TAPS, 20 mM AMPD, pH 8.7, 0.01% Tween 20			
Amines: octopamine, adrenaline, noradrenaline, isoprotorenol, doxylamine, pindolol, atenolol, acebutolol	100 mM AcOH, 1 mM His 10 mM citric acid, pH 3.0			
NH_4^+ (150 μg/L), Na^+ (150 μg/L), Mg^{2+} (90 μg/L), K^+ (200 μg/L), Ca^{2+} (150 μg/L), Li^+ (150 μg/L)/rain, tap, mineral waters; red, white wines; fruit juice, beer, milk	CZE 10.5 mM His, 50 mM AcOH, 2 mM 18C6E, pH 4.1 30 mM MES, 30 mM His, 2.5 mM 18C6E, pH 6.0	PMMA chip Cross injection configuration width/depth 50/50 μm (squared cross section)	Two thin antiparallel adhesive Cu strips of 1 (0.5–3) mm width and 14 (13.2–20) mm length, detection gap 0.5 (0.5–3) mm, f = 600 (tested 100–800) kHz, amplitude 20 (25–100) V_{p-p}	[63–66]
Cl^- (125 μg/L), NO_3^- (250 μg/L), SO_4^{2-} (200 μg/L)/Tap, mineral waters; red, white wines	20 mM MES, 20 mM His, pH 6.0			
Oxalate, tartrate, malate, citrate, succinate, acetate, lactate, formate, pyruvate, pyroglutamate/ red, white wines; fruit juice, beer, milk	10 mM His, 7 mM Glu, pH 5.75			
Citrate, malate, acetate (3 mg/L), lactate (3 mg/L), benzoate (3 mg/L), sorbate (3 mg/L), ascorbate (10 mg/L)/vitamin C tablete, soft drink	Tartaric acid, His, pH 6.5, 0.06% HP-β-CD, 0.125 mM CTAB			
AAs: Lys, Arg, Gly, Ala, Val, Ile, Ser, Thr, Met, Gln, Phe, Pro (all 50–12 μM) Peptides: [Leu]enkephalin (5.2 μM), bradykinin (11.7 μM), oxytocin (6.0 μM), angiotensin II (11.0 μM), TRH (11.0 μM) Proteins: cytochrome c (6.0 μM), HSA (0.6 μM), myoglobin (1.4 μM), immunoglobulin G DNA fragment	2.3 M AcOH, pH 2.1, 0.05% Tween 20			

[a] Matrix is specified for real world samples only, in the other cases model analyte mixtures are involved.

acid/His (pH 4.9) [24, 68], citric acid (pH 2.95) [26, 42], and acetic acid (AcOH)/LiOH (pH 4.7) [29]. An alkaline sorbate/Arg (pH 8.9) [9] or borate buffer (pH 7.5) [14, 40] has been used as alternative BGEs for separation of anions or cations. Inorganic anions were also separated in succinate/1,3-bis[tris(hydroxymethyl)-methylamino]propane (Bis-Tris propane, BTP) (pH 3.55) and polyethylenglycol dicarboxylic acid (PEG-DC)/BTP (pH 3.5) [20]. Potassium acetate BGE proved to be suitable for detection of alkylammonium cations [10] and ammonium acetate BGE for separation of catecholamines [38]. Simultaneous determination of organic and alkali and alkaline earth ions was performed in His/α-hydroxyisobutyric (HIBA)/18C6E BGE (pH 6.0) and His/lactic acid/18C6E (pH 4.25) [35]. In that study the effect of the properties of BGEs (pH, concentration of BGE, and concentration of the complexation additive 18C6E in BGE) was examined. Selected BGE, His/HIBA/18C6E BGE (pH 6.0) was used for simultaneous

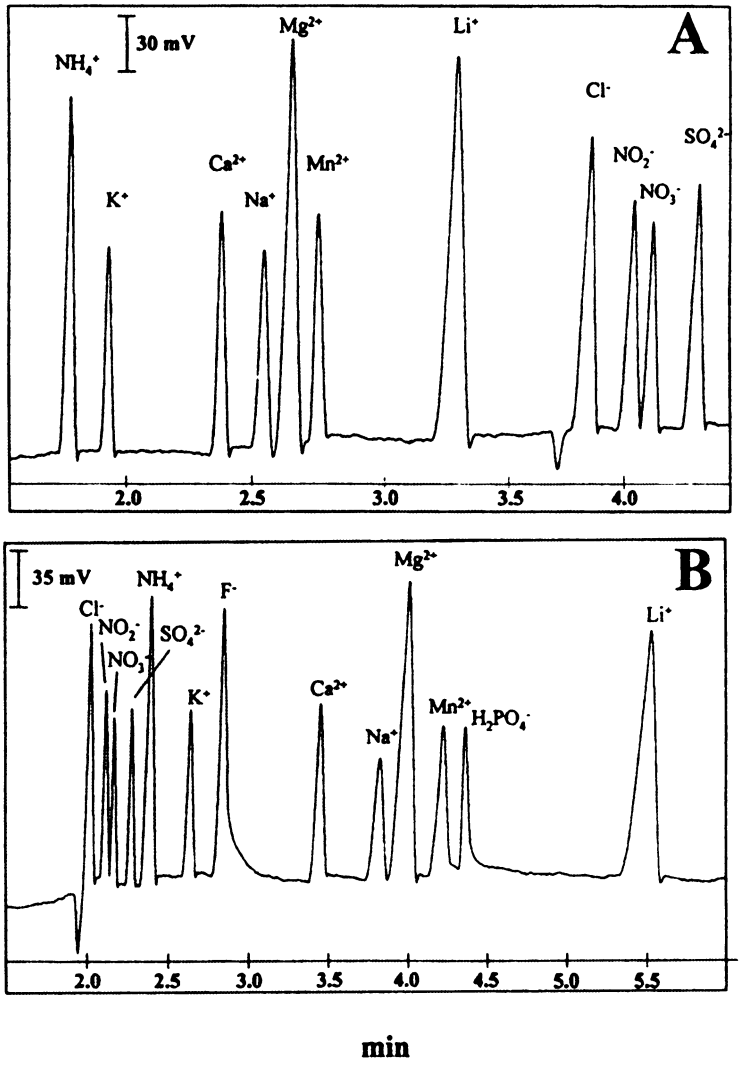

Figure 2. Simultaneous determination of inorganic cations and anions in a standard solution containing 1 mg/L of each ion (except for F^- 2 mg/L and $H_2PO_4^-$ 3 mg/L). Experimental conditions: (A) BGE: 20 mM MES/His, 1.5 mM 18-crown-6-ether, 10 μM CTAB, pH 6.0; T = 23°C, separation voltage −20 kV, hydrodynamic injection with capillary ends elevated to a height of 30 cm for 30 s (cathodic end) and 10 cm for 30 s (anodic end), time between injection 35 s, effective capillary length (anions) 46 cm and (cations) 21 cm (total length 67 cm); (B) BGE: 20 mM MES, 20 mM His, 1.5 mM 18-crown-6-ether, 20 μM CTAB, pH 6.0; T = 23°C, voltage −22.5 kV, hydrodynamic injection with capillary ends elevated to a height of 30 cm for 20 s (cathodic end) and 20 cm for 30 s (anodic end), time between injections 35 s, effective capillary length (anions) 41 cm and (cations) 26 cm (total length 67 cm). Reprinted with permission from [34].

determination of inorganic ions by flow injection-CE system (FI-CE) with dual opposite end injection [71]. His/HIBA BGE without any additives was utilized for separation of heavy metal cations determined by microchip CE [59]. Separation and CLCD detection of inorganic or carboxylic acids and artificial sweeteners were also performed in MES/His BGE on a chip [72]. Alkyl methylphosphonic acids (breakdown products of nerve agents) were separated in MES/His (pH 6.0) with high sensitivity, fast response, high precision, and good linearity [67]. Separation of 20 underivatized amino acids (AAs) was carried out in acetate buffer in 35 min [73]. Later 12 underivatized AAs were separated in three acidic BGEs, composed of glycolic acid, HIBA and lactic acid, and in two basic BGEs, containing 2-amino-2-methyl-1-propanol (AMP) or 2-amino-2-methyl-1,3-propanediol (AMPD and Ammediol) (pH 10.8) and the best separation was achieved in lactic acid [74]. AAs (Trp, Phe, Thr, Tyr, Glu, and Asp) were

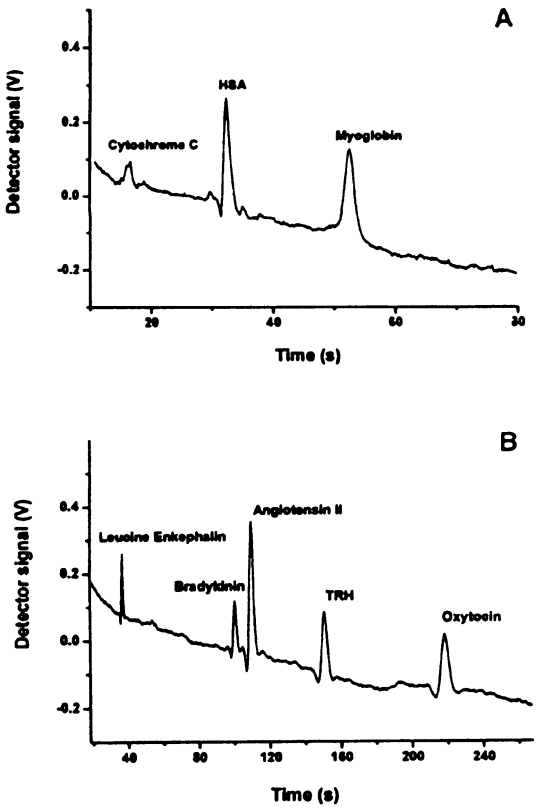

Figure 3. Electrophoretic separation of (A) proteins, cytochrome *c* (40 μM), HSA (15 μM), and myoglobin (30 μM), and (B) peptides, Leu-enkephalin (1000 μM), bradykinin (190 μM), angiotensin II (640 μM), thyrotropin releasing hormone (TRH) (1186 μM), and oxytocin (109 μM), on microchip CE. Experimental conditions: BGE: 2.3 M AcOH, 0.05% Tween, pH 2.1; $T = 24 \pm 1°C$, separation voltage 6 kV (A) and 4 kV (B), total/effective length of the separation channel 75/85 mm. Reprinted with permission from [66].

separated in alkaline BGE 3-(cyclohexylamino)-1-propansulfonic acid (CAPS) and AMP (pH 10.8) [36, 72] and another separation of a set of 12 AAs (Lys, Arg, Gly, Ala, Val, Ile, Ser, Thr, Met, Gln, Phe, and Pro) was carried out in AcOH (pH 2.1) containing 0.05% polyoxyethylene sorbitan monolaurate (Tween 20) [66]. A mixture of four FITC-labeled AAs (Phe, Gly, Trp, and Lys) and a mixture of three FITC-labeled peptides (Pro-Met, Gly-Tyr, and Gly-Thr) were separated in Tris/MES (pH 8.2) using the combined CLCD and fluorescent detection [45]. A mixture of four carbohydrates and three AAs was successfully analyzed in BGE composed of $NaOH/Na_2HPO_4$/CTAB mixture (pH > 12) [75]. Human immunoglobulin (IgM) without labeling was determined as a model analyte of large molecules in *N*-tris(hydroxymethyl)-methyl-3-aminopropanesulfonic acid (TAPS)/AMPD in capillaries as well as on chips [60] and similarly monoclonal immunoglobulin G (IgG) in 2.3 M AcOH containing 0.05% Tween 20 on a chip [66]. The same BGE has been employed also for CLCD detection of CE separation of other medium- and high-molecular-mass compounds, such as DNA-fragment (1652 bp), proteins (cytochrome *c*, HSA, and myoglobin), and peptides (Leu-enkephalin, bradykinin, angiotensin II, thyrotropin releasing hormone, and oxytocin) as demonstrated in Fig. 3 [66]. The model mixture of low mobility anions lactate and citrate and another model mixture of pharmaceutically relevant compounds were successfully analyzed in Good's buffers containing CHES/Arg (pH 9.0) and CAPS/Arg (pH 10) [59]. Sulfonates were analyzed in neutral BGE composed of 3-morpholino-2-hydroxypropane sulfonic acid (MOPSO)/Arg [72]. Highly alkaline BGEs, composed of NaOH and triethylamine, were used for the separation of sucrose and fructose [72]. A set of nine peptides were separated in conventional phosphate buffer (pH 2.5) [11, 40]. The successful separations of different UV-light nonabsorbing organic amines, such as short-chained aliphatic primary, secondary and tertiary amines, branched aliphatic amines, diamines, and hydroxyl-substituted amines were achieved in five different BGEs: Arg/AcOH (pH 8.3), MES/His (pH 6.0), AcOH/Bis-Tris (pH 4.0), 25 mM AcOH (pH 3.0) and 0.5 M AcOH (pH 2.5) [76]. Complete separation of *cis*- and *trans*-1,2-diaminocyclohexane was achieved in 0.5 M AcOH (pH 2.5) with 18C6E as a modifier. Nine phenolic acids, derivatives of benzoic, and cinnamic acids, were separated in 150 mM AMP-based BGE (pH 11.6) and CLCD was compared with UV-absorption detection [77]. After sample stacking procedure, CLCD was found to be more sensitive than UV detection.

4.2 Real samples

As the sensitivity and reproducibility of the conductivity detectors in CE methods have been improved they have started being employed in the CE analysis of the real world samples of various origins. Some representative examples are described in this section, the others are presented in the Tables 1–4.

Very frequent applications concern determination of inorganic and organic ions in water samples of different sources, such as, *e.g.*, in mineral waters [15, 31, 65, 71, 78], sea water [58], tap water [39, 63, 65, 71], surface water [41], rinse water [79], rain water collected in Sao Paulo [80, 81], and many different types of water samples collected in different areas of the Czech Republic [34, 82]. The example of determination of inorganic cations in mineral water Mattoni by CE with CLCD in His/MES/tetradecyltrimethylammonium bromide (TTAB) BGE [78] is shown in Fig. 4. Different samples of drainage water were quantitatively analyzed by miniaturized and traditional FI-CE systems with flow injection sample introduction in MES/His/18C6E [41]; inorganic anions in these

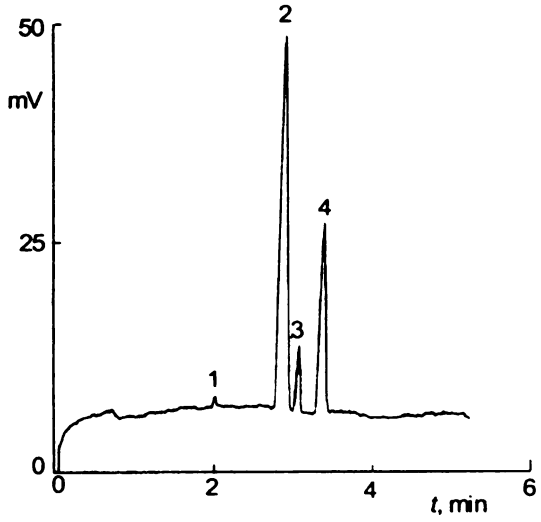

Figure 4. Electrophoregram of determination of inorganic cations in mineral water Mattoni. Experimental conditions: BGE: 20 mM His, 20 mM MES, 0.1 mM TTAB, pH 6.0; $T = 30°C$, separation voltage 20 kV, effective/total capillary length 45/60 cm, id/od 75/375 μm, hydrodynamic injection at 20 mbar for 6 s. Peak identification: 1, K^+; 2, Ca^{2+}; 3, Na^+; 4, Mg^{2+}. Reprinted with permission from [78].

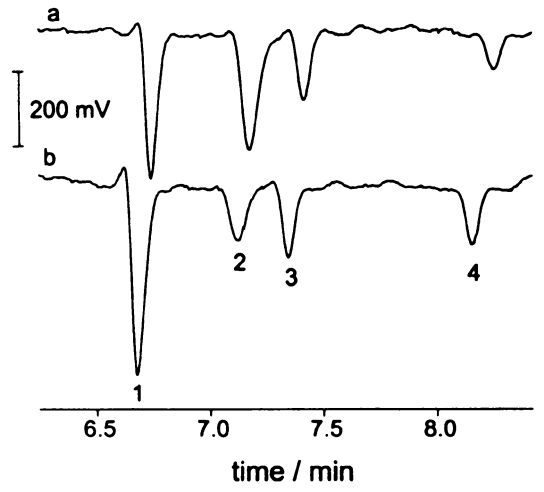

Figure 5. Electrophoretic separation of fructose, glucose and sucrose using galactose as internal standard in unprocessed (a) and processed (b) coconut water. Experimental conditions: BGE, 10 mM NaOH, 4.5 mM Na_2HPO_4, 0.2 mM CTAH, pH 11.5; voltage, 15 kV; effective/total capillary length 41/50 cm, id 50 μm, gravity injection at 100 mm for 10 s. Peak identification: 1, fructose; 2, glucose; 3, galactose; 4, sucrose. Reprinted with permission from [87].

waters were determined in His/AcOH (pH 4.0) [71] or in His/HIBA/18C6E/AcOH (pH 2.8) [83]. This method with the same BGE was used for the fast and sensitive speciation of Se^{4+} and Se^{6+} in soil samples [84]. CZE with field-amplified sample injection (FASI) in BGE composed of MES/His (pH 4.9) in hydro-organic water/ACN solvent (85/45 v/v) has been used for the analysis of heavy metal ions (Zn^{2+}, Co^{2+}, Cu^{2+}, and Ni^{2+}) and for the determination of Mg^{2+} ions in tap water [39]. Another rapid method was used for quantification of inorganic cations and anions in ethanol fuel [85] using MES/His/cetyltrimethylammonium hydroxide (CTAH) for separation of anions and His/lactic acid (pH 4.9) for separation of cations. Determination of metal cations (I.A and II.A groups) in biological matrices with high sodium concentration, was carried out utilizing the reduction of mobilities of Mg^{2+} and Ca^{2+} by addition of methanol (MeOH) and lactate in His/MES BGE [68]. The content of inorganic cations and anions was determined in human blood serum and urine in maleic acid/Arg (pH 5.5) with addition of 18-crown-6-ether for separation of cations [86]. Successful separation of inorganic cations in red and white wines, fruit juice, beer, and milk was obtained by microchip CE in His/AcOH/18C6E (pH 4.1), the inorganic anions in red and white wines were analyzed in MES/His (pH 6.0), and both inorganic and small organic anions in red and white wines, fruit juices, beer, and milk were determined in His/Glu (pH 5.75) [65]. The content of small organic and inorganic anions in vitamin C tablets and soft drinks was found by conventional CE as well as by chip CE [64]. Inorganic and small organic cations and sugars, such as fructose, glucose, and sucrose were also determined in five different samples of coconut water in MES/His/CTAB running buffer [87]. The separation of fructose, glucose, sucrose, and galactose as an internal standard in unprocessed and processed coconut water is shown in Fig. 5. Common mono- and disaccharides in soft drinks were separated and determined in high pH BGEs by CZE [88]. Inorganic anions present in milk were separated in BTP/succinate by a method based on complexation with α-CDs [22]. Simultaneous determination of Cr^{3+} and Cr^{6+} in rinse water from the galvanic industry was presented as an alternative method to standard validated methods [79]. The antibiotic fosfomycin in biological fluids was successfully determined in BGE consisting of benzoic acid/CTAB/Tris (pH 6.95) in human plasma and at pH 8.05 in microdialysis samples [89]. β-Blockers such as pindolol, propranolol, atenolol, metoprolol, labetalol, and acebutolol were separated in lactic acid and AcOH (pH 2.7) [90]. Optimized experimental conditions of model separation of AAs were applied for the determination of AAs content in budvar beer, human urine and saliva, pangamin yeast, and extracts from herbs [73]. CZE separation of 18 proteinogenic AAs, three nonproteinogenic AAs (citrulline, ornithine, and methylhistidine) and creatinine in human plasma was carried out in 1.7 M AcOH with 0.1% m/v hydroxyethylcellulose (HEC) (pH 2.2) [91]. Advantageous usage of CLCD instead of UV-absorption

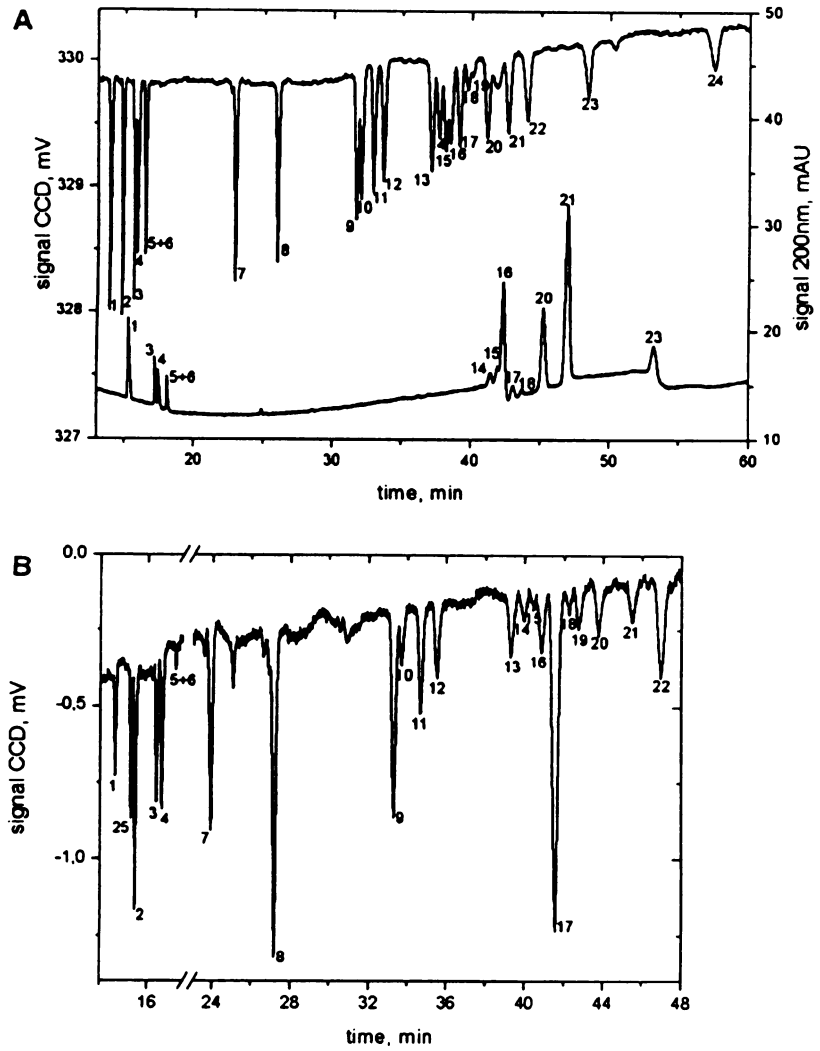

Figure 6. CZE separation of (A) a model mixture of AAs containing 24 mg/L of each (except for 1-methylhistidine, 12 mg/L, and 3-methylhistidine, 12 mg/L) with CLCD and diode array detection and (B) AAs in a human plasma with CLCD detection. Experimental conditions: BGE: 1.7 M AcOH, 0.1% HEC, pH 2.2; separation voltage 20 kV, electric current 20 μA, $T = 25°C$, effective capillary length 67 cm for CLCD and 72 cm for DAD, total capillary length 80 cm, id/od 50/375 μm, hydrodynamic injection 300 mbar s. Peak identification: 1, Creatinine; 2, Lys; 3, Arg; 4, His; 5, 1-MeHis; 6, 3-MeHis; 7, Gly; 8, Ala; 9, Val; 10, Ile; 11, Leu; 12, Ser; 13, Thr; 14, Asn; 15, Met; 16, Trp; 17, Gln; 18, citrullin; 19, Glu; 20, Phe; 21, Tyr; 22, Pro; 23, Cys; 24, Asp; 25, Orn. Reprinted with permission from [91].

detection for these compounds is demonstrated on the CZE separation of a model mixture in Fig. 6A, and on the CZE separation of AAs in plasma in Fig. 6B. The CE method for identifying different species of proteinaceous binders – collagen, egg white, gum arabic, linseed oil-stand oil, and milk casein, on the basis of their AAs composition was developed by Kenndler and coworkers [92, 93], underivatized AAs were separated in chlor roacetic acid/LiOH (pH 2.26). This method was used in the analysis of historic and artistic objects and it provided useful data for their restoration and conservation. For similar purposes, long-chain fatty acids and dicarboxylic acids were identified in drying oils used as binding media for objects of art by CE with indirect UV and CLCD in two weakly acidic BGEs at pH 6.86 and 5.85, respectively [94]. On-chip separation of the phosphonic acid products of organophosphate nerve agent, paraoxon, and methyl parathion, in His/MES (pH 6.1) was presented as an enzymatic assay for screening organophosphate nerve agents, based on precolumn conversion by organophosphorus hydrolase [95]. Chemically similar alkyl methylphosphonic acids acting as warfare agent degradation products

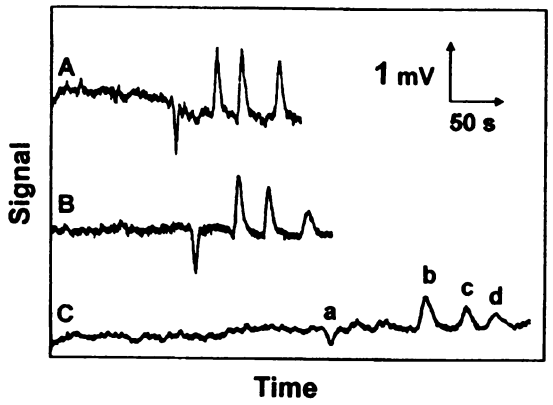

Figure 7. NACE separation of alkylamines in organic solvents, DMF (A), DMAA (B), and DMSO (C), analytes: tetramethylammonium (a), tetrapropylammonium (b), tetrabutylammonium (c), and *N,N*-dimethyldodecylamine (d), concentration of each 500 μM. Experimental conditions: BGE: 5 mM 2,6-dihydroxybenzoic acid, 5 mM tetraethylammonium, 5 mM 2,6-dihydroxy benzoate, separation voltage 1.5 kV, effective/total length of chip separation channel 73/80 mm, injection 1.5 kV for 1 s (A, B) and 2 s (C). Reprinted with permission from [100].

were sensitively monitored by microchip electrophoresis in river water [67]. The antiseptics, chlorhexidine digluconate, and polyhexamethylene biguanide, were determined with high sensitivity in eye drops, using 2.3 M AcOH (pH 2.1) as BGE [96]. Pharmaceutical drug substances such as ephedrine, dopamine, metanephrine, octapamine, noradrenaline, adrenaline, isoproterenol, and doxylamine were analyzed in citric acid (pH 3.0) [72], MES/His (pH 6.2) [72, 75], and lactic acid (pH 2.83), BGE [90], then the content of real pharmaceutical preparation Ternormin, Sanalepsi N and Vick Medi-Nite were determined. L- and D-enantiomers of six of these lipophilic drug substances and pseudoephedrin were also separated in lactic acid/His BGE (pH 2.7–3.1) with chiral selector hydroxypropyl-β-CD (HP-β-CD) [97]. CLCD was also employed to monitor enantiomeric separation of AAs (Arg, Ser, Thr, Met, Trp, Asn, Val, Phe, and Tyr) in citric acid (pH 2.1) and/or citrate/Tris (pH 2.2) with 10 mM (+)-(18-crown-6-ether)-2,3,11,12-tetracarboxylic acid (18C6EH4) as chiral selector [97]. Another example of enantioseparation in citric acid (pH 2.4) was demonstrated on (*R/S*)-1-phenylethylamine and (*R/S*)-1-cyclohexyl ethylamine with high resolution 2.3 and 3.3. Combination of dimethyl-β-CD (DM-β-CD) and nonchiral crown ether 18C6EH4 was chosen as a chiral selector [98].

4.3 Other applications

In addition to analytical CE applications CLCD has been utilized also in CE separation used for the determination of physico-chemical characteristics of compounds. Their examples are also included in the Tables 1–4. The haloacetic acids were separated in phosphate, citrate, and borate buffers [99] to compare their simulated separation predicted by the computer simulation program PeakMaster with real separation results. Another application concerns the determination of thermodynamic pK_a values of the carboxylic groups and limiting mobilities of cationic forms of underivatized AAs from the CZE measurement of the pH dependence of their effective electrophoretic mobilities; the pK_a values of carboxylic groups of AAs were found to be in the range 1.70–3.43 and the cationic mobilities were in the range 24.7×10^{-9} to 39.5×10^{-9} $m^2V^{-1}s^{-1}$ [30]. Migration behavior of aliphatic amines in organic solvents was studied by nonaqueous CE (NACE) on a chip [100]. Effect of three different organic solvents upon the separation and detection of alkylamines is shown in Fig. 7. A series of papers from the Kenndler's group deal with the usage of organic solvents, such as formamide (FA) [101], propylene carbonate (PC) [102], and nitromethane [103] in NACE with CLCD to test the applicability of these solvents in CZE. Strongly UV-absorbing organic solvents, such as DMF, *N,N*-dimethylacetamide (DMAA), and PC were described and characterized as alternative mediums to aqueous BGEs in CZE with CLCD [28]; suitability of CLCD for NACE was demonstrated on separation of aliphatic amines and/or their ammonium ions and on the determination of their actual mobilities and pK_a values. A special study was focused on relationships between mobility and diffusion coefficient as a function of ionic strength in different organic solvents in NACE [104].

CLCD was capable of detecting even the zones of noncharged aliphatic alcohols separated by MEKC with a micellar pseudophase formed by sodium dodecylsulfate and the mobile phase composed of phosphate buffer with and without methanol added as a modifier of the mobile phase [105].

5 Conclusions

CLCD has proved to be a suitable detection technique for capillary and microchip electrophoresis. The mechanical constructions and electric circuitry of CLCD have been recently significantly improved, better characteristics such as sensitivity and reproducibility were obtained and the detectors started becoming commercially available. CLCD is becoming widely used for detection of inorganic ions and non-UV-absorbing as well as for UV-absorbing small organic ions and it is a promising method for the determination of biomolecules since successful application of CLCD for CE separations of AAs, peptides and proteins and for enzymatic assays and immunoassays on chip have been already demonstrated.

The work was supported by the Grant Agency of the Czech Republic, grants nos., 203/04/0098, 203/05/2539, 203/06/1044, and by the Research Project Z40550506. Dr. P. Sázelová and Ms V. Lišková are thanked for their help in manuscript preparation.

6 References

[1] Zemann, A. J., *Trends Anal. Chem.* 2001, *20*, 346–354.

[2] Zemann, A. J., *Electrophoresis* 2003, *24*, 2125–2137.

[3] Tanyanyiwa, J., Leuthardt, S., Hauser, P. C., *Electrophoresis* 2002, *23*, 3659–3666.

[4] Kubáň, P., Hauser, P. C., *Electroanalysis* 2004, *16*, 2009–2021.

[5] Verheggen, T. P. E. M., van Ballegooijen, E. C., Massen, C. H., Everaerts, F. M., *J. Chromatogr.* 1972, *64*, 185–189.

[6] Vacík, J., Zuska, J., Everaerts, F. M., Verheggen, T. P. E. M., *Chem. Listy.* 1972, *66*, 647–652.

[7] Gaš, B., Vacík, J., *Chem. Listy* 1980, *74*, 652–658.

[8] Gaš, B., Demjanenko, M., Vacík, J., *J. Chromatogr.* 1980, *192*, 253–257.

[9] Zemann, A. J., Schnell, E., Volgger, D., Bonn, G. K., *Anal. Chem.* 1998, *70*, 563–567.

[10] da Silva, J. A. F., do Lago, C. L., *Anal. Chem.* 1998, *70*, 4339–4343.

[11] Laugere, F., Lubking, G. W., Berthold, A., Bastemeijer, J., Vellekoop, M. J., *Sensor. Actuat. A-Phys.* 2001, *92*, 109–114.

[12] Huang, X., Pang, T. K. J., Gordon, M. J., Zare, R. N., *Anal. Chem.* 1987, *59*, 2747–2749.

[13] Huang, X. H., Zare, R. N., Sloss, S., Ewing, A. G., *Anal. Chem.* 1991, *63*, 189–192.

[14] Muller, D., Jelínek, I., Opekar, F., Štulík, K., *Electroanalysis* 1996, *8*, 722–725.

[15] Tůma, P., Opekar, F., Jelínek, I., *Chem. Listy* 1999, *93*, 533–535.

[16] Tůma, P., Opekar, F., Jelínek, I., Štulík, K., *Electroanalysis* 1999, *11*, 1022–1026.

[17] Geraldo, J., Brito-Neto, A., da Silva, J. A. F., Blanes, L., do Lago, C. L., *Electroanalysis* 2005, *17*, 1198–1206.

[18] Geraldo, J., Brito-Neto, A., da Silva, J. A. F., Blanes, L., do Lago, C. L., *Electroanalysis* 2005, *17*, 1207–1214.

[19] Vacík, J., Zuska, J., Muselasová, I., *J. Chromatogr.* 1985, *320*, 233–240.

[20] Kaniansky, D., Zelenská, V., Masár, M., Iványi, F., Gazdíková, S., *J. Chromatogr. A* 1999, *844*, 349–359.

[21] Kaniansky, D., Masár, M., Marak, J., Bodor, R., *J. Chromatogr. A* 1999, *834*, 133–178.

[22] Masár, M., Bodor, R., Kaniansky, D., *J. Chromatogr. A* 1999, *834*, 179–188.

[23] Mayrhofer, K., Zemann, A. J., Schnell, E., Bonn, G. K., *Anal. Chem.* 1999, *71*, 3828–3833.

[24] da Silva, J. A. F., Guzman, N., do Lago, C. L., *J. Chromatogr. A* 2002, *942*, 249–258.

[25] Tůma, P., Opekar, F., Jelínek, I., *Electroanalysis* 2001, *13*, 989–992.

[26] Tůma, P., Opekar, F., Štulík, K., *Electrophoresis* 2002, *23*, 3718–3724.

[27] Novotný, M., Opekar, F., Štulík, K., *Electroanalysis* 2005, *17*, 1181–1186.

[28] Muzikář, J., van de Goor, T., Gaš, B., Kenndler, E., *J. Chromatogr. A* 2001, *924*, 147–154.

[29] Gaš, B., Zuska, J., Coufal, P., van de Goor, T., *Electrophoresis* 2002, *23*, 3520–3527.

[30] Včeláková, K., Zusková, I., Kenndler, E., Gaš, B., *Electrophoresis* 2004, *25*, 309–317.

[31] Unterholzner, V., Macka, M., Haddad, P. R., Zemann, A., *Analyst* 2002, *127*, 715–718.

[32] Macka, M., Hutchinson, J., Zemann, A., Zhang, S. S., Haddad, P. R., *Electrophoresis* 2003, *24*, 2144–2149.

[33] Hilder, E. F., Zemann, A. J., Macka, M., Haddad, P. R., *Electrophoresis* 2001, *22*, 1273–1281.

[34] Kubáň, P., Karlberg, B., Kubán, P., Kubán, V., *J. Chromatogr. A* 2002, *964*, 227–241.

[35] Kubáň, P., Kubáň, P., Kubáň, V., *Electrophoresis* 2002, *23*, 3725–3734.

[36] Tanyanyiwa, J., Galliker, B., Schwarz, M. A., Hauser, P. C., *Analyst* 2002, *127*, 214–218.

[37] Tanyanyiwa, J., Leuthardt, S., Hauser, P. C., *J. Chromatogr. A* 2002, *978*, 205–211.

[38] Vuorinen, P. S., Jussila, M., Siren, H., Palonen, S., Riekkola, M. L., *J. Chromatogr. A* 2003, *990*, 45–52.

[39] Tan, F., Yang, B. C., Guan, Y. F., *Anal. Sci.* 2005, *21*, 955–958.

[40] Baltussen, E., Guijt, R. M., van der Steen, G., Laugere, F. *et al.*, *Electrophoresis* 2002, *23*, 2888–2893.

[41] Wang, L. X., Fu, C. G., *Instrum. Sci. Technol.* 2004, *32*, 303–309.

[42] Chvojka, T., Jelínek, I., Opekar, F., Štulík, K., *Anal. Chim. Acta* 2001, *433*, 13–21.

[43] Novotný, M., Opekar, F., Jelínek, I., Štulík, K., *Anal. Chim. Acta* 2004, *525*, 17–21.

[44] Novotný, M., Opekar, F., Jelínek, I., *Chem. Listy* 2005, *99*, 132–136.

[45] Tan, F., Yang, B. C., Guan, Y. F., *Anal. Sci.* 2005, *21*, 583–585.

[46] Bastemeijer, J., Lubking, W., Laugere, F., Vellekoop, M., *Sensor. Actuat. B-Chem.* 2002, *83*, 98–103.

[47] Laugere, F., Lubking, G. W., Bastemeijer, J., Vellekoop, M. J., *Sensor. Actuat. B-Chem.* 2002, *83*, 104–108.

[48] Guijt, R. M., Baltussen, E., van der Steen, G., Frank, H. *et al.*, *Electrophoresis* 2001, *22*, 2537–2541.

[49] Berthold, A., Laugere, F., Schellevis, H., de Boer, C. R. *et al.*, *Electrophoresis* 2002, *23*, 3511–3519.

[50] Laugere, F., Guijt, R. M., Bastemeijer, J., van der Steen, G. *et al.*, *Anal. Chem.* 2003, *75*, 306–312.

[51] Lichtenberg, J., de Rooij, N. F., Verpoorte, E., *Electrophoresis* 2002, *23*, 3769–3780.

[52] Wang, J., Pumera, M., Collins, G., Opekar, F., Jelinek, I., *Analyst* 2002, *127*, 719–723.

[53] Pumera, M., Wang, J., Opekar, F., Jelínek, I. *et al.*, *Anal. Chem.* 2002, *74*, 1968–1971.

[54] Wang, J., Pumera, M., *Anal. Chem.* 2002, *74*, 5919–5923.

[55] do Lago, C. L., da Silva, H. D. T., Neves, C. A., Brito-Neto, J. G. A., da Silva, J. A. F., *Anal. Chem.* 2003, *75*, 3853–3858.

[56] Wang, J., Chen, G., Muck, A., *Anal. Chem.* 2003, *75*, 4475–4479.

[57] Wang, J., Chen, G., Muck, A., Collins, G. E., *Electrophoresis* 2003, *24*, 3728–3734.

[58] Chen, Y., Yang, P. Y., Li, J. H., Chen, D., Chen, G., *Anal. Bioanal. Chem.* 2006, *384*, 683–691.

[59] Tanyanyiwa, J., Hauser, P. C., *Anal. Chem.* 2002, *74*, 6378–6382.

[60] Abad-Villar, E. M., Tanyanyiwa, J., Fernandez-Abedul, M. T., Costa-Garcia, A., Hauser, P. C., *Anal. Chem.* 2004, *76*, 1282–1288.

[61] Kubáň, P., Hauser, P. C., *Electrophoresis* 2004, *25*, 3387–3397.

[62] Kubáň, P., Hauser, P. C., *Electrophoresis* 2004, *25*, 3398–3405.

[63] Kubáň, P., Hauser, P. C., *Lab Chip* 2005, *5*, 407–415.

[64] Law, W. S., Kubáň, P., Zha, J. H., Li, S. F. Y., Hauser, P. C., *Electrophoresis* 2005, *26*, 4648–4655.

[65] Kubáň, P., Hauser, P. C., *Electrophoresis* 2005, *26*, 3169–3178.

[66] Abad-Villar, E. M., Kubáň, P., Hauser, P. C., *Electrophoresis* 2005, *26*, 3609–3614.

[67] Wang, J., Pumera, M., Collins, G. E., Mulchandani, A., *Anal. Chem.* 2002, *74*, 6121–6125.

[68] da Silva, J. A. F., Ricelli, N. L., Carvalho, A. Z., do Lago, C. L., *J. Brazil. Chem. Soc.* 2003, *14*, 265–268.

[69] Tanyanyiwa, J., Hauser, P. C., *Electrophoresis* 2002, *23*, 3781–3786.

[70] Tanyanyiwa, J., Abad-Villar, E. M., Fernandez-Abedul, M. T., Costa-Garcia, A. *et al.*, *Analyst* 2003, *128*, 1019–1022.

[71] Kubáň, P., Kubáň, P., Hauser, P. C., Kubáň, V., *Electrophoresis* 2004, *25*, 35–42.

[72] Tanyanyiwa, J., Abad-Villar, E. M., Hauser, P. C., *Electrophoresis* 2004, *25*, 903–908.

[73] Coufal, P., Zuska, J., van de Goor, T., Smith, V., Gaš, B., *Electrophoresis* 2003, *24*, 671–677.

[74] Tanyanyiwa, J., Schweizer, K., Hauser, P. C., *Electrophoresis* 2003, *24*, 2119–2124.

[75] Rainelli, A., Hauser, P. C., *Anal. Bioanal. Chem.* 2005, *382*, 789–794.

[76] Gong, X. Y., Hauser, P. C., *Electrophoresis* 2006, *27*, 468–473.

[77] Kubáň, P., Štěrbová, D., Kubáň, V., *Electrophoresis* 2006, *27*, 1368–1375.

[78] Šolínová, V., Jelínek, I., Opekar, F., Kašička, V., *Chem. Listy* 2004, *98*, 191–196.

[79] Kubáň, P., Kubáň, P., Kubáň, V., *Electrophoresis* 2003, *24*, 1397–1403.

[80] Rocha, F. R., da Silva, J. A. F., Lago, C. L., Fornaro, A., Gutz, I. G. R., *Atmos. Environ.* 2003, *37*, 105–115.

[81] Fornaro, A., Gutz, I. G. R., *Atmos. Environ.* 2003, *37*, 117–128.

[82] Kubáň, P., Kubáň, P., Kubáň, V., *Electrophoresis* 2003, *24*, 1935–1943.

[83] Kubáň, P., Reinhardt, M., Muller, B., Hauser, P. C., *J. Environ. Monitor.* 2004, *6*, 169–174.

[84] Kubáň, P., Kubáň, P., Kubáň, V., *Anal. Bioanal. Chem.* 2004, *378*, 378–382.

[85] Munoz, R. A. A., Richter, E. M., de Jesus, D. P., do Lago, C. L., Angnes, L., *J. Brazil. Chem. Soc.* 2004, *15*, 523–526.

[86] Wan, Q. J., Kubáň, P., Tanyanyiwa, J., Rainelli, A., Hauser, P. C., *Anal. Chim. Acta* 2004, *525*, 11–16.

[87] Richter, E. M., de Jesus, D. P., Munoz, R. A. A., do Lago, C. L., Angnes, L., *J. Brazil. Chem. Soc.* 2005, *16*, 1134–1139.

[88] Carvalho, A. Z., da Silva, J. A. F., do Lago, C. L., *Electrophoresis* 2003, *24*, 2138–2143.

[89] Petsch, M., Mayer-Helm, B. X., Sauermann, R., Joukhadar, C., Kenndler, E., *Electrophoresis* 2004, *25*, 2292–2298.

[90] Tanyanyiwa, J., Hauser, P. C., *Electrophoresis* 2004, *25*, 3010–3016.

[91] Samcová, E., Tůma, P., *Electroanalysis* 2006, *18*, 152–157.

[92] Kaml, I., Včeláková, K., Kenndler, E., *J. Sep. Sci.* 2004, *27*, 161–166.

[93] Harrison, S. M., Kaml, I., Prokoratová, V., Mazánek, M., Kenndler, E., *Anal. Bioanal. Chem.* 2005, *382*, 1520–1526.

[94] Surowiec, I., Kaml, I., Kenndler, E., *J. Chromatogr. A* 2004, *1024*, 245–254.

[95] Wang, J., Chen, G., Muck, A., Chatrathi, M. P. *et al.*, *Anal. Chim. Acta* 2004, *505*, 183–187.

[96] Abad-Villar, E. M., Etter, S. F., Thiel, M. A., Hauser, P. C., *Anal. Chim. Acta* 2006, *561*, 133–137.

[97] Gong, X. Y., Kubáň, P., Tanyanyiwa, J., Hauser, P. C., *J. Chromatogr. A* 2005, *1082*, 230–234.

[98] Gong, X. Y., Hauser, P. C., *J. Chromatogr. A* 2005, *1094*, 196–199.

[99] Lopez-Avila, V., van de Goor, T., Gaš, B., Coufal, P., *J. Chromatogr. A* 2003, *993*, 143–152.

[100] Wang, J., Pumera, M., *Anal. Chem.* 2003, *75*, 341–345.

[101] Porras, S. P., Kenndler, E., *Electrophoresis* 2004, *25*, 2946–2958.

[102] Muzikář, J., van de Goor, T., Gaš, B., Kenndler, E., *Anal. Chem.* 2002, *74*, 428–433.

[103] Subirats, X., Porras, S. P., Roses, M., Kenndler, E., *J. Chromatogr. A* 2005, *1079*, 246–253.

[104] Muzikář, J., van de Goor, T., Kenndler, E., *Anal. Chem.* 2002, *74*, 434–439.

[105] da Silva, J. A. F., do Lago, C. L., *Electrophoresis* 2000, *21*, 1405–1408.

[106] Huang, X. H., Luckey, J. A., Gordon, M. J., Zare, R. N., *Anal. Chem.* 1989, *61*, 766–770.

[107] Gordon, M. J., Huang, X., Pentoney, Jr., S. L., Zare, R. N., *Science* 1988, *242*, 224–228.

